Shadows of galactic centers and circular photon orbits

Alexander F. Zakharov

Alikhanov ITEP – NRC Kurchatov Institute

Bogoliubov Laboratory for Theoretical Physics, JINR, Dubna

«The prize is the pleasure of finding the thing out, the kick in the discovery, the observation that other people use it [my work]–those are the real things»
R. P. Feynman

TWENTY-SECOND LOMONOSOV
CONFERENCE August, 21-27, 2025
ON ELEMENTARY PARTICLE PHYSICS
MOSCOW STATE UNIVERSITY

References

1. AFZ, Galactic Center Shadows: Beyond the Standard Model, *Physics of Atomic Nuclei* **88***,* 154–170, (2025), https://doi.org/10.1134/S106377882570019X

2. AFZ, Shadow in the Galactic Center: Theoretical Concept -- Prediction -- Realization, *Natural Science Review* **3**, (2025), arxiv:2506.16927, https://nsr-jinr.ru/article/52

Our recent publications on the subject

AFZ, Phys. Part. Nucl. Lett. (2023)

AFZ, Universe (2022)

AFZ, Astron. Astrophys. Trans. (2022)

P. Jovanovic, D. Borka, V. Borka Jovanovic, AFZ, JCAP (2023)

AFZ, Phys. Part. Nucl. (2023)

AFZ, IJMPD (2023)

AFZ, arxiv:2305.15446

P. Jovanovic, D. Borka, V. Borka Jovanovic, AFZ, PRD (2024)

P. Jovanovic, D. Borka, V. Borka Jovanovic, AFZ, Symmetry (2024)

About citations

L. B. Okun said to young colleagues: “You have to prove that your studies are known in the world. Let me know a number of citations at your papers”.

A few year ago at ITEP seminar, a ITEP researcher informed people that a Nobel prize winner quoted his paper (and it was like a small sensation that Nobel prize winners knew papers from researchers of our Institute), and I decided to take a look how many Nobel prize winners quoted our paper and recognized that V. L. Ginzburg, S. Weinberg, G. Smoot, A. Ghez and her co-authors, R. Genzel and his co-authors. In particular, V. L. Ginzburg quoted my book and our paper on gravitational microlensing in his last reviews on the most interesting problems of physics and astrophysics.

I counted more than 30 citations on our papers from A. Ghez and R. Genzel groups in their papers on trajectories of bright stars near the GC.

Astron Astrophys Rev (2024)32:3
https://doi.org/10.1007/s00159-024-00154-z

REVIEW ARTICLE

Experimental studies of black holes: status and future prospects

Reinhard Genzel[1,2,3] · Frank Eisenhauer[1,4] · Stefan Gillessen[1]

Received: 27 February 2024 / Accepted: 21 March 2024

Abstract
More than a century ago, Albert Einstein presented his general theory of gravitation (GR) to the Prussian Academy of Sciences. One of the predictions of the theory is that not only particles and objects with mass, but also the quanta of light, photons, are tied to the curvature of space-time, and thus to gravity. There must be a critical compactness, above which photons cannot escape. These are black holes (henceforth BH). It took 50 years after the theory was announced before possible candidate objects were identified by observational astronomy. And another 50 years have passed, until we finally have in hand detailed and credible experimental evidence that BHs of 10 to 10^{10} times the mass of the Sun exist in the Universe. Three very different experimental techniques, but all based on Michelson interferometry or Fourier-inversion spatial interferometry have enabled the critical experimental breakthroughs. It has now become possible to investigate the space-time structure in the vicinity of the event horizons of BHs. We briefly summarize these interferometric techniques, and discuss the spectacular recent improvements achieved with all three techniques. Finally, we sketch where the path of exploration and inquiry may go on in the next decades.

Keywords Black holes · Galactic center · Interferometry · GRAVITY

Contents

Extended author information available on the last page of the article

Published online: 25 April 2024

References at Russian authors

Dexter J, Tchekhovskoy A (2020)

Babak S… (2017)

Shakura NI, Sunyaev RA (1973)

Jovanovic P, Jovanovic Borka V., Borka D., Zakharov A. (2024)

Zakharov A. et al. (2007)

A&A, 692, A242 (2024)
https://doi.org/10.1051/0004-6361/202452274

Astronomy & Astrophysics

Improving constraints on the extended mass distribution in the Galactic center with stellar orbits

GRAVITY Collaboration*: K. Abd El Dayem[1], R. Abuter[4], N. Aimar[1,7], P. Amaro Seoane[14,2,20,15], A. Amorim[8,7], J. Beck[2], J. P. Berger[3,4], H. Bonnet[4], G. Bourdarot[2], W. Brandner[5], V. Cardoso[7,17], R. Capuzzo Dolcetta[21], Y. Clénet[1], R. Davies[2], P. T. de Zeeuw, A. Drescher[2], A. Eckart[6,13], F. Eisenhauer[2,19], H. Feuchtgruber[2], G. Finger[2], N. M. Förster Schreiber[2], A. Foschi[1], F. Gao[13], P. Garcia[10,7], E. Gendron[1], R. Genzel[2,11], S. Gillessen[2], M. Hartl[2], X. Haubois[9], F. Haussmann[2], G. Heißel[16,1], T. Henning[5], S. Hippler[5], M. Horrobin[6], L. Jochum[9], L. Jocou[3], A. Kaufer[9], P. Kervella[1], S. Lacour[1,4], V. Lapeyrère[1], J.-B. Le Bouquin[3], P. Léna[1], D. Lutz[2], F. Mang[2], N. More[2], T. Ott[2], T. Paumard[1], K. Perraut[3], G. Perrin[1], O. Pfuhl[4,2], S. Rabien[2], D. C. Ribeiro[2], M. Sadun Bordoni[2,**], S. Scheithauer[5], J. Shangguan[2], T. Shimizu[2], J. Stadler[12,2], O. Straub[2,18], C. Straubmeier[6], E. Sturm[2], L. J. Tacconi[2], I. Urso[1], F. Vincent[1], S. D. von Fellenberg[13,2], F. Widmann[2], E. Wieprecht[2], J. Woillez[4], and F. Zhang[22,23,24]

(Affiliations can be found after the references)

Received 17 September 2024 / Accepted 12 November 2024

ABSTRACT

Studying the orbital motion of stars around Sagittarius A* in the Galactic center provides a unique opportunity to probe the gravitational potential near the supermassive black hole at the heart of our Galaxy. Interferometric data obtained with the GRAVITY instrument at the Very Large Telescope Interferometer (VLTI) since 2016 has allowed us to achieve unprecedented precision in tracking the orbits of these stars. GRAVITY data have been key to detecting the in-plane, prograde Schwarzschild precession of the orbit of the star S2 that is predicted by general relativity. By combining astrometric and spectroscopic data from multiple stars, including S2, S29, S38, and S55 – for which we have data around their time of pericenter passage with GRAVITY – we can now strengthen the significance of this detection to an approximately 10σ confidence level. The prograde precession of S2's orbit provides valuable insights into the potential presence of an extended mass distribution surrounding Sagittarius A*, which could consist of a dynamically relaxed stellar cusp comprising old stars and stellar remnants, along with a possible dark matter spike. Our analysis, based on two plausible density profiles – a power-law and a Plummer profile – constrains the enclosed mass within the orbit of S2 to be consistent with zero, establishing an upper limit of approximately $1200\,M_\odot$ with a 1σ confidence level. This significantly improves our constraints on the mass distribution in the Galactic center. Our upper limit is very close to the expected value from numerical simulations for a stellar cusp in the Galactic center, leaving little room for a significant enhancement of dark matter density near Sagittarius A*.

Key words. black hole physics – gravitation – instrumentation: interferometers – Galaxy: center

1. Introduction

Since 2016, the GRAVITY interferometer at ESO's Very Large Telescope (GRAVITY Collaboration 2017) has allowed us to obtain astrometric data with unprecedented accuracy (reaching in the best cases a 1σ uncertainty of 30 μas) of the S-stars orbiting around Sagittarius A* (Sgr A*) in the Galactic center (GC). This has turned them into a powerful tool to investigate the gravitational potential near the supermassive black hole (SMBH) at the center of our Galaxy, reaching distances from Sgr A* down to about a thousand times its Schwarzschild radius (R_S). Furthermore, astrometric and polarimetric observations of flares from Sgr A* with GRAVITY have revealed that the mass inside the flares' radius of a few R_S is consistent with the black hole mass measured from stellar orbits (GRAVITY Collaboration 2018b, 2023a). This, together with the radio-VLBI image of Sgr A* (Event Horizon Telescope Collaboration 2022), confirms that Sgr A* is a SMBH beyond any reasonable doubt.

For the S2 star, due to its short orbital period of 16 years and its brightness ($m_K \approx 14$), astrometric data are available for two complete orbital revolutions around Sgr A*, while spectroscopic data cover one and a half revolutions (Schödel et al. 2002; Ghez et al. 2003, 2008; Gillessen et al. 2017). At the pericenter, S2 reaches a distance of $\sim 1400\,R_S$ from the SMBH with a speed of $7700\,\mathrm{km\,s^{-1}} \simeq 0.026\,c$. Monitoring the star's motion on the sky and radial velocity with GRAVITY and SINFONI around the time of the pericenter passage in 2018, crucial data were obtained in order to detect the first-order effects in the post-Newtonian (PN) expansion of general relativity (GR) on its orbital motion. The first one is the gravitational redshift of spectral lines, which was detected together with the transverse Doppler effect, predicted by special relativity, with a $\approx 10\sigma$ significance in GRAVITY Collaboration (2018a) and a $\approx 5\sigma$ significance in Do et al. (2019). GRAVITY Collaboration (2019) improved the significance of the detection to $\approx 20\sigma$. The other effect is the prograde, in-plane precession of the orbit's pericenter angle; namely, the Schwarzschild precession (SP). It

* GRAVITY is developed in collaboration by MPE, LESIA of Paris Observatory/CNRS/Sorbonne Université/Univ. Paris Diderot, and IPAG of Université Grenoble Alpes/CNRS, MPIA, Univ. of Cologne, CENTRA – Centro de Astrofisica e Gravitação, and ESO.

** Corresponding author; mbordoni@mpe.mpg.de

corresponds to an advance of $\delta\varphi_{Schw} = \frac{3\pi R_S}{a(1-e^2)}$ per orbit, which for S2 is equal to 12.1 arcmin per orbit in the prograde direction. In GRAVITY Collaboration (2020), this effect was detected at the 5σ level, and improved in GRAVITY Collaboration (2022) to $\approx 7\sigma$ by combining the data of S2 with data of the stars S29, S38, and S55, which could be observed with GRAVITY around the time of their pericenter passage and whose pericenter distances are comparable to that of S2.

The Lense-Thirring effect, caused by the spin of the central SMBH, appears at a 1.5PN order and gives both an additional contribution to the in-plane precession and a precession of the orbital plane (Merritt et al. 2010). We define $A_{LT} = 4\pi\chi\left(\frac{R_S}{2a(1-e^2)}\right)^{3/2}$, which for S2 is equal to 0.11 arcminutes. Consequently, the in-plane precession per orbit becomes $\delta\varphi_{Kerr} = \delta\varphi_{Schw} - 2A_{LT}\cos(i)$, while the precession per orbit of the orbital plane is given by $\delta\Phi_{Kerr} = A_{LT}$, where χ is the dimensionless spin of the SMBH (with $0 \le \chi \le 1$) and i is the angle between the direction of the SMBH spin and that of the stellar orbital angular momentum. The effect is thus at least 50 times smaller than the SP, assuming a SMBH with maximum spin, and is out of reach for current measurements. In order to measure the spin of Sgr A*, we would need to observe a star with a pericenter distance that is at least three times smaller than that of S2, given the astrometric accuracy achievable with GRAVITY (Waisberg et al. 2018; Capuzzo-Dolcetta & Sadun-Bordoni 2023).

Any extended mass distribution around Sgr A*, following a spherically symmetric density profile, would add a retrograde precession of the stellar orbits, counteracting the prograde SP (GRAVITY Collaboration 2020, 2022). This mass distribution is expected to be composed mainly of a dynamically relaxed cusp of old stars and stellar remnants. Peebles (1972); Frank & Rees (1976); Bahcall & Wolf (1976) first addressed the problem of the distribution of stars around a central massive BH. Bahcall & Wolf (1976) found that a single-mass stellar population around a central massive BH reaches a stationary density distribution over the two-body relaxation timescale, which is a power law, $\rho(r) \propto r^s$, with slope $s = -1.75$. In the GC, the old stellar population can be approximately represented by light stars with masses around $1\,M_\odot$ and heavier stellar black holes with masses around $10\,M_\odot$ (Alexander 2017). For such a population, mass segregation occurs, where heavier objects tend to concentrate toward the center due to dynamical interactions with lighter objects. The mass-segregation solution for the steady-state distribution of stars around a massive BH is derived in Alexander & Hopman (2009). It has two branches, weak and strong segregation, based on the dominance of heavier or lighter objects in the scattering interactions. In the weak segregation branch, the heavy objects settle into a power-law distribution with a slope of -1.75, while the lighter objects exhibit a shallower profile with a slope of -1.5, as was already heuristically derived in Bahcall & Wolf (1977). Conversely, the strong segregation branch results in steeper slopes and a larger difference between the light and heavy masses. The heavy masses settle into a much steeper cusp with $-2.75 \lesssim s \lesssim -2$, while the light masses settle into a cusp with $-1.75 \lesssim s \lesssim -1.5$. Preto & Amaro-Seoane (2010) provided a clear realization through N-body simulations of the strong mass segregation solution, showing also that the stellar cusp can develop on timescales that are much shorter than the relaxation time, which is shorter than the Hubble time for the GC (Alexander & Hopman 2009; Genzel et al. 2010). In Linial & Sari (2022), it is argued that weak segregation must exist interior to a certain break radius, r_B, where the massive population dominates the scattering, while for radii larger than r_B the light objects dominate the scattering and strong segregation occurs.

The existence of such a stellar cusp in the GC is also validated by the observational results of Gallego-Cano et al. (2018) and Schödel et al. (2018) for the distribution of giant, subgiant, and main-sequence stars within the central few parsecs. They find that the density distribution of the light objects is shallower than $s = -1.5$, being compatible with a power-law with slope between -1.4 and -1.15. This is impossible in the steady state, Bahcall & Wolf framework in order to maintain an equilibrium distribution, but could be explained by a number of factors, such as stellar collisions (Rose & MacLeod 2024), taking into account the complex star formation history of the nuclear star cluster (Baumgardt et al. 2018), or by diffusion in angular momentum leading to tidal disruptions; namely, diffusion into the loss cone (Zhang & Amaro-Seoane 2024). Red giant stars, instead, do not show a cusp but a distribution that appears to flatten toward the central ~0.3 pc (Buchholz et al. 2009; Do et al. 2009; Bartko et al. 2010; Gallego-Cano et al. 2018), possibly due to the stripping of red giant envelopes due to the interaction with a star-forming disk (Amaro-Seoane & Chen 2014).

In addition to the stellar cusp, an intermediate-mass black hole (IMBH) companion of Sgr A* could be present in the GC. It has been shown that an IMBH enclosed within the orbit of S2 can only have a mass of $<10^3\,M_\odot$ (GRAVITY Collaboration 2023b; Will et al. 2023). Moreover, it was predicted by Gondolo & Silk (1999) that dark matter particles could be accreted by the SMBH to form a dense spike, increasing the dark matter density in the GC by up to ten orders of magnitude with respect to the expected density in the case of a Navarro–Frenk–White (NFW) profile. In this scenario, the spike could contribute to the extended mass distribution around Sgr A*, while in the absence of such a spike, the contribution of dark matter within the radial range of the S-stars' orbits would be negligible under an NFW profile. The dark matter spike would also follow a power-law distribution, $\rho(r) \propto r^s$, with slope $-2.5 < s < -2.25$ in the case of a generalized NFW profile (Gondolo & Silk 1999; Shen et al. 2024). Another possibility that has been investigated is that dark matter could exist in the form of an ultralight scalar field or a massive vector field cloud that clusters around Sgr A* (Foschi et al. 2023; GRAVITY Collaboration 2024), or as a compact fermion ball supported by degeneracy pressure (Viollier et al. 1993; Argüelles et al. 2019; Becerra-Vergara et al. 2020).

Additionally, a deviation from general relativity, such as the one introduced by massive gravity theories or $f(R)$-gravity, could modify the gravitational potential through a Yukawa-like correction in the Newtonian limit, adding an additional precession of the stellar orbits to the prograde SP and the retrograde precession induced by an extended mass distribution (Hees et al. 2017; De Martino et al. 2021; Tan & Lu 2024; Jovanović et al. 2024a,b). For the specific case of massive gravity, the additional precession would be prograde and equal to $\delta\varphi_Y = \pi\sqrt{1-e^2}\frac{a^2}{\lambda^2}$ (Jovanović et al. 2024a), where $\lambda = \frac{\hbar}{m_g c}$ is the Compton wavelength of the massive graviton, m_g the mass of the graviton, and $\hbar$ the reduced Planck constant. From the observed precession of the S2 star, it is thus possible to derive a lower limit on λ and an upper limit on m_g, as is done in Hees et al. (2017); Jovanović et al. (2024a,b).

In GRAVITY Collaboration (2022), the 1σ upper limit on any extended mass distributed within the orbit of S2 is found to be $\approx 3000\,M_\odot$, assuming a Plummer density profile (Plummer 1911). In this paper, we use S-star data, including one more year orbit is consistently compatible with zero. We set a strong upper limit of approximately $1200\,M_\odot$ with a 1σ confidence level, significantly improving upon the limits established in GRAVITY Collaboration (2022). Our findings align with theoretical predictions for a dynamically relaxed stellar cusp in the GC, composed of stars, brown dwarfs, white dwarfs, neutron stars, and stellar black holes, according to numerical simulations using an updated version of the code developed in Zhang & Amaro-Seoane (2024). This analysis predicts an enclosed mass of approximately $1210\,M_\odot$ within S2's orbit. Given that our upper limit is very close to this predicted value, we conclude that we find no evidence for a significant dark matter spike in the GC.

S2 is currently moving toward the apocenter of its orbit, which it will reach in 2026. We expect that GRAVITY data collected in the coming years, combined with ERIS spectroscopy, will further refine our constraints on the extended mass distribution in the GC, as the mass distribution primarily influences stellar orbits in the apocenter half (Heißel et al. 2022). This will allow us to refine the comparison with the theoretical predictions for the stellar cusp, which is of fundamental importance in order to understand the distribution of the faint, old main-sequence stars and subgiants in the GC. These stars are too faint to be currently detected with GRAVITY, but their detection could be in reach of future observations with the GRAVITY+ upgrade at the VLTI (GRAVITY+ Collaboration 2022) and the MICADO instrument at the ELT (Davies et al. 2018). These stars could potentially be in tighter orbits around Sgr A* and could allow us to measure its spin and quadrupole moment. Furthermore, the comparison between our observational constraints and theoretical predictions is also important to better understand the distribution of compact objects in the GC and in galactic nuclei in general. This could offer precious insights in view of the future LISA mission (Amaro-Seoane et al. 2017), which will be able to detect the inspirals of compact objects into SMBHs (EMRIs) (Amaro-Seoane et al. 2007). In fact, the rate of EMRIs depends strongly on the density distribution of compact remnants within ~10 mpc of the central SMBH (Preto & Amaro-Seoane 2010), which corresponds to the apocenter distance of S2 for the GC.

Acknowledgements. We are very grateful to our funding agencies (MPG, ERC, CNRS [PNCG, PNGRAM], DFG, BMBF, Paris Observatory [CS, PhyFOG], Observatoire des Sciences de l'Univers de Grenoble, and the Fundação para a Ciência e Tecnologia), to ESO and the Paranal staff, and to the many scientific and technical staff members in our institutions, who helped to make NACO, SINFONI, and GRAVITY a reality. JS is supported by the Deutsche Forschungsgemeinschaft (DFG, German Research Foundation) under Germany's Excellence Strategy – EXC-2094 – 390783311. A.A., A.F., P.G. and V.C. were supported by Fundação para a Ciência e a Tecnologia, with grants reference SFRH/BSAB/142940/2018, UIDB/00099/2020 and PTDC/FIS-AST/7002/2020. F.W. has received funding from the European Union's Horizon 2020 research and innovation programme under grant agreement No 101004719. Based on observations collected at the European Southern Observatory under the ESO programme IDs 109.22ZA.005, 109.22ZA.002, 105.20B2.004, 0103.B-0032(C), 0101.B-0576(E), 0101.B-0576(C).

References

Alexander, T. 2017, ARA&A, 55, 17
Alexander, T., & Hopman, C. 2009, ApJ, 697, 1861
Amaro-Seoane, P., & Chen, X. 2014, ApJ, 781, L18
Amaro-Seoane, P., Gair, J. R., Freitag, M., et al. 2007, Class. Quant. Grav., 24, R113
Amaro-Seoane, P., Audley, H., Babak, S., et al. 2017, Laser Interferometer Space Antenna (ESA PUBLICATIONS DIVISION C/O ESTEC), submitted to ESA on January 13th in response to the call for missions for the L3 slot in the Cosmic Vision Programme
Angélil, R., & Saha, P. 2014, MNRAS, 444, 3780
Argüelles, C. R., Krut, A., Rueda, J. A., & Ruffini, R. 2019, Int. J. Mod. Phys. D, 28, 1943003
Bahcall, J. N., & Wolf, R. A. 1976, ApJ, 209, 214
Bahcall, J. N., & Wolf, R. A. 1977, ApJ, 216, 883
Bartko, H., Martins, F., Trippe, S., et al. 2010, ApJ, 708, 834
Baumgardt, H., Amaro-Seoane, P., & Schödel, R. 2018, A&A, 609, A28
Becerra-Vergara, E. A., Argüelles, C. R., Krut, A., Rueda, J. A., & Ruffini, R. 2020, A&A, 641, A34
Buchholz, R. M., Schödel, R., & Eckart, A. 2009, A&A, 499, 483
Capuzzo-Dolcetta, R., & Sadun-Bordoni, M. 2023, MNRAS, 522, 5828
Chatzopoulos, S., Fritz, T. K., Gerhard, O., et al. 2014, MNRAS, 447, 948
Davies, R., Alves, J., Clénet, Y., et al. 2018, SPIE Conf. Ser., 10702, 107021S
Davies, R., Absil, O., Agapito, G., et al. 2023, A&A, 674, A207
Dehnen, W. 1993, MNRAS, 265, 250
De Martino, I., della Monica, R., & De Laurentis, M. 2021, Phys. Rev. D, 104, L101502
Do, T., Ghez, A. M., Morris, M. R., et al. 2009, ApJ, 703, 1323
Do, T., Hees, A., Ghez, A., et al. 2019, Science, 365, 664
Eisenhauer, F., Genzel, R., Alexander, T., et al. 2005, ApJ, 628, 246
Event Horizon Telescope Collaboration 2022, ApJ, 930, L12
Feldmeier-Krause, A., Zhu, L., Neumayer, N., et al. 2016, MNRAS, 466, 4040
Foschi, A., Abuter, R., Aimar, N., et al. 2023, MNRAS, 524, 1075
Frank, J., & Rees, M. J. 1976, MNRAS, 176, 633
Gallego-Cano, E., Schödel, R., Dong, H., et al. 2018, A&A, 609, A26
Genzel, R., Eisenhauer, F., & Gillessen, S. 2010, Rev. Mod. Phys., 82, 3121
Ghez, A. M., Duchêne, G., Matthews, K., et al. 2003, ApJ, 586, L127
Ghez, A. M., Salim, S., Weinberg, N. N., et al. 2008, ApJ, 689, 1044
Gillessen, S., Plewa, P. M., Eisenhauer, F., et al. 2017, ApJ, 837, 30
Gondolo, P., & Silk, J. 1999, Phys. Rev. Lett., 83, 1719
GRAVITY Collaboration (Abuter, R., et al.) 2017, A&A, 602, A94
GRAVITY Collaboration (Abuter, R., et al.) 2018a, A&A, 615, L15
GRAVITY Collaboration (Abuter, R., et al.) 2018b, A&A, 618, L10
GRAVITY Collaboration (Abuter, R., et al.) 2019, A&A, 625, L10
GRAVITY Collaboration (Abuter, R., et al.) 2020, A&A, 636, L5
GRAVITY Collaboration (Abuter, R., et al.) 2022, A&A, 657, L12
GRAVITY Collaboration (Abuter, R., et al.) 2023a, A&A, 677, L10
GRAVITY Collaboration (Straub, O., et al.) 2023b, A&A, 672, A63
GRAVITY Collaboration 2024, MNRAS, 530, 3740
GRAVITY+ Collaboration (Abuter, R., et al.) 2022, The Messenger, 189, 17
Habibi, M., Gillessen, S., Martins, F., et al. 2017, ApJ, 847, 120
Hees, A., Do, T., Ghez, A. M., et al. 2017, Phys. Rev. Lett., 118, 211101
Heiel, G., Paumard, T., Perrin, G., & Vincent, F. 2022, A&A, 660, A13
Jovanović, P., Borka Jovanović, V., Borka, D., & Zakharov, A. F. 2024a, Symmetry, 16, 397
Jovanović, P., Borka Jovanović, V., Borka, D., & Zakharov, A. F. 2024b, Phys. Rev. D, 109, 064046
Linial, I., & Sari, R. 2022, ApJ, 940, 101
Merritt, D. 2013, Dynamics and Evolution of Galactic Nuclei (Princeton: Princeton University Press)
Merritt, D., Alexander, T., Mikkola, S., & Will, C. M. 2010, Phys. Rev. D, 81, 062002
Peebles, P. J. E. 1972, ApJ, 178, 371
Plewa, P. M., Gillessen, S., Eisenhauer, F., et al. 2015, MNRAS, 453, 3234
Plummer, H. C. 1911, MNRAS, 71, 460
Preto, M., & Amaro-Seoane, P. 2010, ApJ, 708, L42
Rose, S. C., & MacLeod, M. 2024, ApJ, 963, L17
Schödel, R., Ott, T., Genzel, R., et al. 2002, Nature, 419, 694
Schödel, R., Gallego-Cano, E., Dong, H., et al. 2018, A&A, 609, A27
Shen, Z.-Q., Yuan, G.-W., Jiang, C.-Z., et al. 2024, MNRAS, 527, 3196
Tan, Y., & Lu, Y. 2024, Phys. Rev. D, 109, 044047
Viollier, R., Trautmann, D., & Tupper, G. 1993, Phys. Lett. B, 306, 79
Waisberg, I., Dexter, J., Gillessen, S., et al. 2018, MNRAS, 476, 3600
Will, C. M. 1993, Theory and Experiment in Gravitational Physics (Cambridge University Press)
Will, C. M., Naoz, S., Hees, A., et al. 2023, ApJ, 959, 58
Zhang, F., & Amaro-Seoane, P. 2024, ApJ, 961, 232

[1] LESIA, Observatoire de Paris, Université PSL, CNRS, Sorbonne Université, Université de Paris, 5 place Jules Janssen, 92195 Meudon, France

[2] Max Planck Institute for Extraterrestrial Physics, Giessenbachstraße 1, 85748 Garching, Germany

[3] Univ. Grenoble Alpes, CNRS, IPAG, 38000 Grenoble, France

[4] European Southern Observatory, Karl-Schwarzschild-Straße 2, 85748 Garching, Germany

Black hole types

- Black holes with stellar masses 10 -- 10^2 M_{Sun}

- Massive black holes 10^2 -- 10^5 M_{Sun}
- Supermassive black holes 10^5 – 10^{10} M_{sun}

How to probe a black hole

Albert Einstein's theory of gravity, general relativity, predicts that the collapse of enough mass can leave a self-sustaining gravitational field so strong that, inside a distance called the event horizon, nothing can escape, not even light. But are black holes exactly the inscrutable things general relativity predicts? Observers may now have the tools to find out.

1. Trace the stars

Tracking the orbits of stars around the black hole in our Galaxy's center can reveal whether the black hole warps space and time exactly as general relativity predicts.

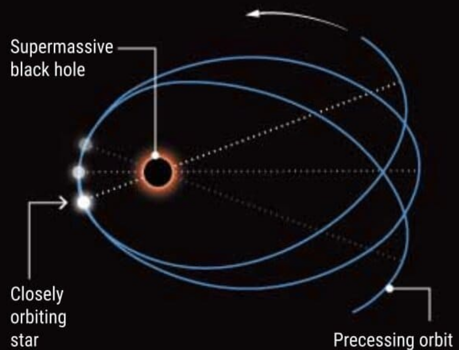

2. Take a picture

An image of a supermassive black hole holds clues to whether, as general relativity predicts, it has an event horizon rather than a surface, and mass and spin are its sole properties.

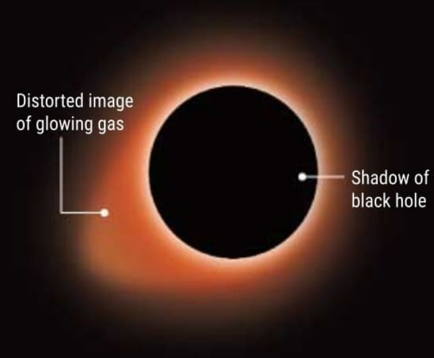

3. Catch the waves

When two small black holes spiral together, they radiate gravitational waves, which could reveal whether the supposed black holes are instead material objects. The final black hole reverberates at frequencies and overtones that provide another test of whether its only properties are mass and spin.

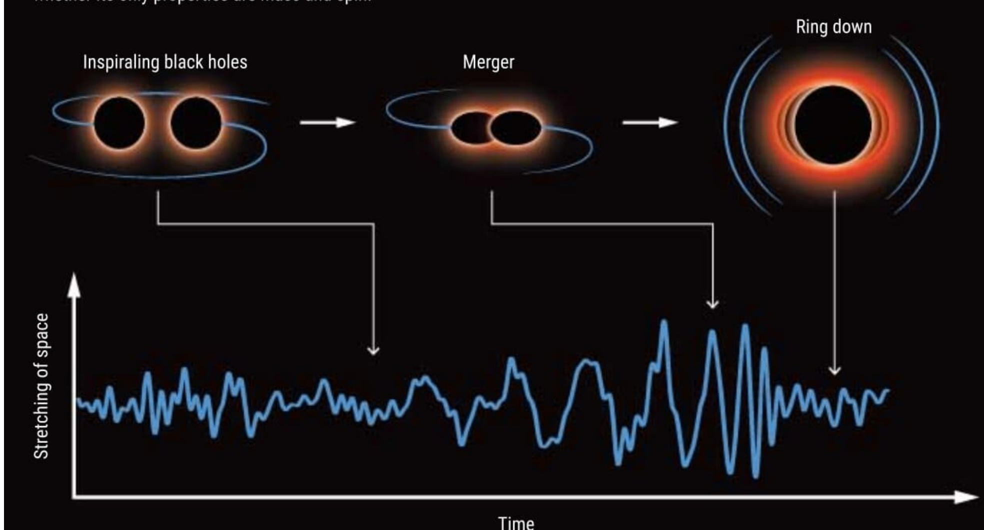

Great success of relativistic astrophysics

Three Nobel prizes in last years (2017, 2019, 2020)

LIGO-Virgo: BBHs, BNS (kilonova) GW 170817;

GRAVITY, Keck and new tests of GR (gravitational redshift for S2 near its periapsis passage)

The confirmation of relativistic precession for S2 (GRAVITY)

Shadow reconstructions in M87* and Sgr A*

Young BHs discovered with JWST

Coevolution (Or Not) of Supermassive Black Holes and Host Galaxies

John Kormendy[1] and Luis C. Ho[2]

[1]Department of Astronomy, University of Texas at Austin,
2515 Speedway C1400, Austin, TX 78712-1205; email: kormendy@astro.as.utexas.edu

[2]The Observatories of the Carnegie Institution for Science,
813 Santa Barbara Street, Pasadena, CA 91101; email: lho@obs.carnegiescience.edu

Abstract

Supermassive black holes (BHs) have been found in 87 galaxies by dynamical modeling of spatially resolved kinematics. The *Hubble Space Telescope* revolutionized BH research by advancing the subject from its proof-of-concept phase into quantitative studies of BH demographics. Most influential was the discovery of a tight correlation between BH mass $M_\bullet$ and the velocity dispersion σ of the bulge component of the host galaxy. Together with similar correlations with bulge luminosity and mass, this led to the widespread belief that BHs and bulges coevolve by regulating each other's growth. Conclusions based on one set of correlations from $M_\bullet \sim 10^{9.5}\ M_\odot$ in brightest cluster ellipticals to $M_\bullet \sim 10^6\ M_\odot$ in the smallest galaxies dominated BH work for more than a decade.

New results are now replacing this simple story with a richer and more plausible picture in which BHs correlate differently with different galaxy components. A reasonable aim is to use this progress to refine our understanding of BH – galaxy coevolution. BHs with masses of $10^5 - 10^6\ M_\odot$ are found in many bulgeless galaxies. Therefore, classical (elliptical-galaxy-like) bulges are not necessary for BH formation. On the other hand, while they live in galaxy disks, BHs do not correlate with galaxy disks. Also, any $M_\bullet$ correlations with the properties of disk-grown pseudobulges and dark matter halos are weak enough to imply no close coevolution.

The above and other correlations of host galaxy parameters with each other and with $M_\bullet$ suggest that there are four regimes of BH feedback. (1) Local, secular, episodic, and stochastic feeding of small BHs in largely bulgeless galaxies involves too little energy to result in coevolution. (2) Global feeding in major, wet galaxy mergers rapidly grows giant BHs in short-duration, quasar-like events whose energy feedback does affect galaxy evolution. The resulting hosts are classical bulges and coreless-rotating-disky ellipticals. (3) After these AGN phases and at the highest galaxy masses, maintenance-mode BH feedback into X-ray-emitting gas has the primarily negative effect of helping to keep baryons locked up in hot gas and thereby keeping galaxy formation from going to completion. This happens in giant, core-nonrotating-boxy ellipticals. Their properties, including their tight correlations between $M_\bullet$ and core parameters, support the conclusion that core ellipticals form by dissipationless major mergers. They inherit coevolution effects from smaller progenitor galaxies. Also, (4) independent of any feedback physics, in BH growth modes (2) and (3), the averaging that results from successive mergers plays a major role in decreasing the scatter in $M_\bullet$ correlations from the large values observed in bulgeless and pseudobulge galaxies to the small values observed in giant elliptical galaxies.

Table 1 Mass measurements of supermassive black holes in our Galaxy, M 31, and M 32

Galaxy	D (Mpc)	σ_e (km s^{-1})	$M_\bullet$ ($M_{\rm low}, M_{\rm high}$) ($M_\odot$)	$r_{\rm infl}$ (arcsec)	σ_* (arcsec)	$r_{\rm infl}/\sigma_*$	Reference
(1)	(2)	(3)	(4)	(5)	(6)	(7)	(8)
Galaxy			4.41(3.98 – 4.84) e6		0.0146	2868.	Meyer et al. 2012
Galaxy			4.2 (3.9 – 4.6) e6		0.0139	3013.	Yelda et al. 2011
Galaxy	0.00828	105	4.30(3.94 – 4.66) e6	41.9	0.0146	2868.	Genzel, Eisenhauer & Gillessen 2010
Galaxy	0.00828	105	4.30(3.94 – 4.66) e6	41.9	0.0146	2868.	Gillessen et al. 2009a
Galaxy			4.09(3.74 – 4.43) e6		0.0148	2829.	Gillessen et al. 2009b
Galaxy			4.25(3.44 – 4.79) e6		0.0139	3013.	Ghez et al. 2008
Galaxy			3.80(3.60 – 4.00) e6		0.0056	7478.	Ghez et al. 2005
Galaxy			3.7 (3.3 – 4.1) e6		0.0075	5583.	Ghez et al. 2003
Galaxy			3.8 (2.3 – 5.4) e6		0.0155	2702.	Schödel et al. 2002
Galaxy			2.1 (1.3 – 2.8) e6		0.113	371.	Chakrabarty & Saha 2001
Galaxy			3.1 (2.6 – 3.6) e6		0.26	161.	Genzel et al. 2000
Galaxy			2.7 (2.5 – 2.9) e6		0.39	107.	Ghez et al. 1998
Galaxy			2.70(2.31 – 3.09) e6		0.39	107.	Genzel et al. 1997
Galaxy			2.55(2.12 – 2.95) e6		0.39	107.	Eckart & Genzel 1997
Galaxy			2.8 (2.5 – 3.1) e6		2.4	17.4	Genzel et al. 1996
Galaxy			2.0 (0.9 – 2.9) e6		4.9	8.5	Haller et al. 1996
Galaxy			2.9 (2.0 – 3.9) e6		3.4	12.3	Krabbe et al. 1995
Galaxy			2. e6		5	8.4	Evans & de Zeeuw 1994
Galaxy			3. e6		5	8.4	Kent 1992
Galaxy			5.4 (3.9 – 6.8) e6		15	2.8	Sellgren et al. 1990
M 31	0.774	169	1.4 (1.1 – 2.3) e8	5.75	0.053	109.	Bender et al. 2005
M 31			1.0 e8		0.297	19.4	Peiris & Tremaine 2003
M 31			6.1 (3.6 – 8.7) e7		0.052	111.	Bacon et al. 2001
M 31			3.3 (1.5 – 4.5) e7		0.297	19.4	Kormendy & Bender 1999
M 31			6.0 (5.8 – 6.2) e7		0.297	19.4	Magorrian et al. 1998
M 31			9.5 (7 – 10) e7		0.42	13.7	Emsellem & Combes 1997
M 31			7.5 e7		0.56	10.3	Tremaine 1995
M 31			8.0 e7		0.42	13.7	Bacon et al. 1994
M 31			5 (4.5 – 5.6) e7		0.59	9.7	Richstone, Bower & Dressler 1990
M 31			3.8 (1.1 – 11) e7		0.56	10.3	Kormendy 1988a
M 31			5.6 (3.4 – 7.8) e7		0.59	9.7	Dressler & Richstone 1988
M 32	0.805	77	2.45(1.4 – 3.5) e6	0.46	0.052	8.76	van den Bosch & de Zeeuw 2010
M 32			2.9 (2.7 – 3.1) e6		0.052	8.76	Verolme et al. 2002
M 32			3.5 (2.3 – 4.6) e6		0.052	8.76	Joseph et al. 2001
M 32			2.4 (2.2 – 2.6) e6		0.23	1.98	Magorrian et al. 1998
M 32			3.9 (3.1 – 4.7) e6		0.050	9.11	van der Marel et al. 1998a
M 32			3.9 (3.3 – 4.5) e6		0.050	9.11	van der Marel et al. 1997a, 1997b
M 32			3.2 (2.6 – 3.7) e6		0.23	1.98	Bender, Kormendy & Dehnen 1996
M 32			2.1 (1.8 – 2.3) e6		0.34	1.34	Dehnen 1995
M 32			2.1 e6		0.34	1.34	Qian et al. 1995
M 32			2.1 (1.7 – 2.4) e6		0.34	1.34	van der Marel et al. 1994a
M 32			2.2 (0.8 – 3.5) e6		0.59	0.77	Richstone, Bower & Dressler 1990
M 32			9.3 e6		0.59	0.77	Dressler & Richstone 1988
M 32			7.5 (3.5–11.5) e6		0.76	0.60	Tonry 1987
M 32			5.8 e6		1.49	0.31	Tonry 1984

Lines based on HST spectroscopy are in red. Column 2 is the assumed distance. Column 3 is the stellar velocity dispersion inside the "effective radius" that encompasses half of the light of the bulge. Column 4 is the measured BH mass with the one-sigma range that includes 68 % of the probability in parentheses. Only the top four $M_\bullet$ values for the Galaxy include distance uncertainties in the error bars. Column 5 is the radius of the sphere of influence of the BH; the line that lists $r_{\rm infl}$ contains the adopted $M_\bullet$. Column 6 is the effective resolution of the spectroscopy, estimated as in Kormendy (2004). It is a radius that measures the blurring effects of the telescope point-spread function or "PSF," the slit width or aperture size, and the pixel size. The contribution of the telescope is estimated by the dispersion $\sigma_{*\rm tel}$ of a Gaussian fitted to the core of the average radial brightness profile of the PSF. In particular, the HST PSF has $\sigma_{*\rm tel} \simeq 0''036$ from a single-Gaussian fit to the PSF model in van der Marel, de Zeeuw & Rix (1997a).

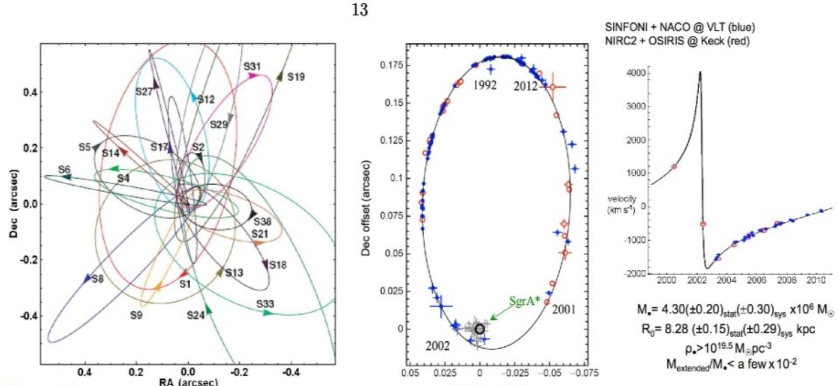

Figure 5

(*left*) Orbits of individual stars near the Galactic center. (*right*) Orbit of star S2 around the BH and associated radio source Sgr A* based on observations of its position from 1992 to 2012. Results from the Ghez group using the Keck telescope and from the Genzel group using the Europen Very Large Telescope (VLT) are combined. This figure is updated from Genzel, Eisenhauer & Gillessen (2010) and is kindly provided by Reinhard Genzel.

These results establish the existence and mass of the central dark object beyond any reasonable doubt. They also eliminate astrophysical plausible alternatives to a BH. These include brown dwarfs and stellar remnants (e. g., Maoz 1995, 1998; Genzel et al. 1997, 2000; Ghez et al. 1998, 2005) and even fermion balls (Ghez et al. 2005; GEG10). Boson balls (Torres et al. 2000; Schunck & Mielke 2003; Liebling & Palenzuela 2012) are harder to exclude; they are highly relativistic, they do not have hard surfaces, and they are consistent with dynamical mass and size constraints. But a boson ball is like the proverbial elephant in a tree: it is OK where it is, but how did it ever get there? GEG10 argue that boson balls are inconsistent with astrophysical constraints based on AGN radiation. Also, the Sołtan (1982) argument implies that at least most of the central dark mass observed in galaxies grew by accretion in AGN phases, and this quickly makes highly relativistic objects collapse into BHs. Finally (Fabian 2013), X-ray AGN observations imply that we see, in some objects, material interior to the innermost stable circular orbit of a non-rotating BH; this implies that these BHs are rotating rapidly and excludes boson balls as alternatives to all central dark objects. Arguments against the most plausible BH alternatives – failed stars and dead stars – are also made for other galaxies in Maoz (1995, 1998) and in Bender et al. (2005). Exotica such as sterile neutrinos or dark matter WIMPs could still have detectable (small) effects, but we conclude that they no longer threaten the conclusion that we are detecting supermassive black holes.

KR95 was titled "Inward Bound – The Search for Supermassive Black Holes in Galactic Nuclei." HST has taken us essentially one order of magnitude inward in radius. A few other telescopes take us closer. But mostly, we are still working at 10^4 to 10^5 Schwarzschild radii. In our Galaxy, we have observed individual stars in to $\sim$ 500 Schwarzschild radii. Only the velocity profiles of relativistically broadened Fe Kα lines (e. g., Tanaka et al. 1995; Fabian 2013) probe radii that are comparable to the Schwarzschild radius. So we are still inward bound. Joining up our measurements made at thousands of r_S with those probed by Fe Kα emission requires that we robustly integrate into our story the rich and complicated details of AGN physics; that is, the narrow– and broad–emission-line regions. That journey still has far to go.

Massive graviton theories

- M. Fierz and W.Pauli-1939
- Zakharov; Veltman, van Dam – 1970
- Vainshtein - 1972
- Boulware, Deser -- 1972
- Logunov, Mestvirishvili, Gershtein et al. (RTG)
- Visser – 1998 (review on such theories)
- Rubakov, Tinyakov – 2008
- de Rham et al.—2011 -- 2016

Journal of Cosmology and Astroparticle Physics
An IOP and SISSA journal

Constraining the range of Yukawa gravity interaction from S2 star orbits II: bounds on graviton mass

A.F. Zakharov,[a,b,c,d,e] P. Jovanović,[f] D. Borka[g] and V. Borka Jovanović[g]

[a]National Astronomical Observatories of Chinese Academy of Sciences, Datun Road 20A, Beijing, 100012 China
[b]Institute of Theoretical and Experimental Physics, 117259 Moscow, Russia
[c]National Research Nuclear University MEPhI (Moscow Engineering Physics Institute), 115409, Moscow, Russia
[d]Bogoliubov Laboratory for Theoretical Physics, JINR, 141980 Dubna, Russia
[e]North Carolina Central University, Durham, NC 27707, U.S.A.
[f]Astronomical Observatory, Volgina 7, 11060 Belgrade, Serbia
[g]Atomic Physics Laboratory (040), Vinča Institute of Nuclear Sciences, University of Belgrade, P.O. Box 522, 11001 Belgrade, Serbia

E-mail: zakharov@itep.ru, pjovanovic@aob.rs, dusborka@vin.bg.ac.rs, vborka@vin.bg.ac.rs

Received May 4, 2016
Accepted May 7, 2016
Published May 20, 2016

Abstract. Recently LIGO collaboration discovered gravitational waves [1] predicted 100 years ago by A. Einstein. Moreover, in the key paper reporting about the discovery, the joint LIGO & VIRGO team presented an upper limit on graviton mass such as $m_g < 1.2 \times 10^{-22} eV$ [1] (see also more details in another LIGO paper [2] dedicated to a data analysis to obtain such a small constraint on a graviton mass). Since the graviton mass limit is so small the authors concluded that their observational data do not show violations of classical general relativity. We consider another opportunity to evaluate a graviton mass from phenomenological consequences of massive gravity and show that an analysis of bright star trajectories could bound graviton mass with a comparable accuracy with accuracies reached with gravitational wave interferometers and expected with forthcoming pulsar timing observations for gravitational wave detection. It gives an opportunity to treat observations of

JCAP05(2016)045

 doi:10.1088/1475-7516/2016/05/045

Constraints on graviton mass from S2 trajectory

- AFZ, D. Borka, P. Jovanovic, V. Borka Jovanovic gr-qc: 1605.00913v; JCAP (2016) :
- $\lambda_g > 2900$ AU = 4.3×10^{11} km with P=0.9 or
- $m_g < 2.9 \times 10^{-21}$ eV $= 5.17 \times 10^{-54}$ g
- Hees et al. PRL (2017) slightly improved our estimates with their new data $m_g < 1.6 \times 10^{-21}$ eV (see discussion below)

NEWS: Help PDG determine which products to keep in the future. Please anwer our survey.

pdgLive Home > graviton > graviton MASS

graviton MASS

INSPIRE search

It is likely that the graviton is massless. More than fifty years ago Van Dam and Veltman (VANDAM 1970), Iwasaki (IWASAKI 1970), and Zakharov (ZAKHAROV 1970) almost simultaneously showed that in the linear approximation a theory with a finite graviton mass does not approach GR as the mass approaches zero. Attempts have been made to evade this "vDVZ discontinuity" by invoking modified gravity or nonlinear theory by De Rahm (DE-RHAM 2017) and others. More recently, the analysis of gravitational wave dispersion has led to bounds that are largely independent of the underlying model, even if not the strongest. We quote the best of these as our best limit.

Experimental limits have been set based on a Yukawa potential (YUKA), dispersion relation (DISP), or other modified gravity theories (MGRV).

The following conversions are useful: 1 eV = 1.783×10^{-33} g = $1.957 \times 10^{-6} m_e$; λ_C = (1.973×10^{-7} m)×(1 eV/m_g).

VALUE (eV)	*DOCUMENT ID*		*TECN*	*COMMENT*
$< 5 \times 10^{-23}$	[1] ABBOTT	2019	DISP	LIGO Virgo catalog GWTC-1
• • We do not use the following data for averages, fits, limits, etc. • •				
$< 3.2 \times 10^{-23}$	[2] BERNUS	2020	YUKA	Planetary ephemeris INPOP19a
$< 2 \times 10^{-28}$	[3] SHAO	2020	DISP	Binary pulsar Galileon radiation
$< 7 \times 10^{-23}$	[4] BERNUS	2019	YUKA	Planetary ephemeris INPOP17b
$< 3.1 \times 10^{-20}$	[5] MIAO	2019	DISP	Binary pulsar orbital decay rate
$< 1.4 \times 10^{-29}$	[6] DESAI	2018	YUKA	Gal cluster Abell 1689
$< 5 \times 10^{-30}$	[7] GUPTA	2018	YUKA	Using SPT-SZ
$< 3 \times 10^{-30}$	[7] GUPTA	2018	YUKA	Using Planck all-sky SZ
$< 1.3 \times 10^{-29}$	[7] GUPTA	2018	YUKA	Using redMaPPer SDSS-DR8
$< 6 \times 10^{-30}$	[8] RANA	2018	YUKA	Weak lensing in massive clusters
$< 8 \times 10^{-30}$	[9] RANA	2018	YUKA	SZ effect in massive clusters
$< 1.0 \times 10^{-23}$	[10] WILL	2018	YUKA	Perihelion advances of planets
$< 7 \times 10^{-23}$	[1] ABBOTT	2017	DISP	Combined dispersion limit from three BH mergers
$< 1.2 \times 10^{-22}$	[1] ABBOTT	2016	DISP	Combined dispersion limit from two BH mergers
$< 2.9 \times 10^{-21}$	[11] ZAKHAROV	2016	YUKA	S2 star orbit
$< 5 \times 10^{-23}$	[12] BRITO	2013	MGRV	Spinning black holes bounds
$< 6 \times 10^{-32}$	[13] GRUZINOV	2005	MGRV	Solar System observations
$< 6 \times 10^{-32}$	[14] CHOUDHURY	2004	YUKA	Weak gravitational lensing
$< 9.0 \times 10^{-34}$	[15] GERSHTEIN	2004	MGRV	From Ω_{tot} value assuming RTG
$< 8 \times 10^{-20}$	[16, 17] FINN	2002	DISP	Binary pulsar orbital period decrease
$< 7 \times 10^{-23}$	TALMADGE	1988	YUKA	Solar system planetary astrometric data
$< 1.3 \times 10^{-29}$	[18] GOLDHABER	1974	YUKA	Rich clusters
$< 7 \times 10^{-28}$	HARE	1973	YUKA	Galaxy
$< 8 \times 10^{4}$	HARE	1973	YUKA	2γ decay

[1] ABBOTT 2019 , ABBOTT 2017 , and ABBOTT 2016 limits assume a dispersion relation for gravitational waves modified relative to GR.

[2] BERNUS 2020 use the latest solution of the ephemeris INPOP (19a) in order to improve the constraint in BERNUS 2019 on the existence of a Yukawa suppression to the Newtonian potential, generically associated to a gravitons mass.

[3] SHAO 2020 sets limit, 95% CL, based on non-observation of excess gravitational radiation in 14 well-timed binary pulsars in the context of the cubic Galileon model.

[4] BERNUS 2019 use the planetary ephemeris INPOP 17b to constraint the existence of a Yukawa suppression to the Newtonian potential, generically associated to a gravitons mass.

[5] MIAO 2019 90% CL limit is based on orbital period decay rates of 9 binary pulsars using a Bayesian prior uniform in graviton mass. Limit becomes $< 5.2 \times 10^{-21}$ eV for a prior uniform in ln(m_g).

[6] DESAI 2018 limit based on dynamical mass models of galaxy cluster Abell 1689.

VALUE (eV) DOCUMENT ID TECN COMMENT

[7] GUPTA 2018 obtains graviton mass limits using stacked clusters from 3 disparate surveys.

[8] RANA 2018 limit, 68% CL, obtained using weak lensing mass profiles out to the radius at which the cluster density falls to 200 times the critical density of the Universe. Limit is based on the fractional change between Newtonian and Yukawa accelerations for the 50 most massive galaxy clusters in the Local Cluster Substructure Survey. Limits for other CL's and other density cuts are also given.

[9] RANA 2018 limit, 68% CL, obtained using mass measurements via the SZ effect out to the radius at which the cluster density falls to 500 times the critical density of the Universe for 182 optically confirmed galaxy clusters in an Altacama Cosmology Telescope survey. Limits for other CL's and other density cuts are also given.

[10] WILL 2018 limit from perihelion advances of the planets, notably Earth, Mars, and Saturn. Alternate analysis yields $< 6 \times 10^{-24}$.

[11] ZAKHAROV 2016 constrains range of Yukawa gravity interaction from S2 star orbit about black hole at Galactic center. The limit is $< 2.9 \times 10^{-21}$ eV for $\delta = 100$.

[12] BRITO 2013 explore massive graviton (spin-2) fluctuations around rotating black holes.

[13] GRUZINOV 2005 uses the DGP model (DVALI 2000) showing that non-perturbative effects restore continuity with Einstein's equations as the gravition mass approaches zero, then bases his limit on Solar System observations.

[14] CHOUDHURY 2004 concludes from a study of weak-lensing data that masses heavier than about the inverse of 100 Mpc seem to be ruled out if the gravitation field has the Yukawa form.

[15] GERSHTEIN 2004 use non-Einstein field relativistic theory of gravity (RTG), with a massive graviton, to obtain the 95% CL mass limit implied by the value of Ω_{tot} = 1.02 ± 0.02 current at the time of publication.

[16] FINN 2002 analyze the orbital decay rates of PSR B1913+16 and PSR B1534+12 with a possible graviton mass as a parameter. The combined frequentist mass limit is at 90%CL.

[17] As of 2020, limits on dP/dt are now about 0.1% (see T. Damour, "Experimental tests of gravitational theory," in this *Review*).

[18] GOLDHABER 1974 establish this limit considering the binding of galactic clusters, corrected to Planck h_0 = 0.67.

References:

BERNUS	2020	PR D102 021501	Constraint on the Yukawa suppression of the Newtonian potential from the planetary ephemeris INPOP19a
SHAO	2020	PR D102 024069	New Graviton Mass Bound from Binary Pulsars
ABBOTT	2019	PR D100 104036	Tests of General Relativity with the Binary Black Hole Signals from the LIGO-Virgo Catalog GWTC-1
BERNUS	2019	PRL 123 161103	Constraining the mass of the graviton with the planetary ephemeris INPOP
MIAO	2019	PR D99 123015	Bounding the mass of graviton in a dynamic regime with binary pulsars
DESAI	2018	PL B778 325	Limit on graviton mass from galaxy cluster Abell 1689
GUPTA	2018	ANP 399 85	Limit on graviton mass using stacked galaxy cluster catalogs from SPT-SZ, Planck-SZ and SDSS-redMaPPer
RANA	2018	PL B781 220	Bounds on graviton mass using weak lensing and SZ effect in galaxy clusters
WILL	2018	CQG 35 17LT01	Solar system versus gravitational-wave bounds on the graviton mass
ABBOTT	2017	PRL 118 221101	GW170104: Observation of a 50-Solar-Mass Binary Black Hole Coalescence at Redshift 0.2
ABBOTT	2016	PRL 116 061102	Observation of Gravitational Waves from a Binary Black Hole Merger
ZAKHAROV	2016	JCAP 1605 045	Constraining the range of Yukawa gravity interaction from S2 star orbits II: Bounds on graviton mass
BRITO	2013	PR D88 023514	Massive Spin-2 Fields on Black Hole Spacetimes: Instability of the Schwarzschild and Kerr Solutions and Bounds on the Graviton Mass
GRUZINOV	2005	NAST 10 311	On the Graviton Mass
CHOUDHURY	2004	ASP 21 559	Probing Large Distance Higher Dimensional Gravity from Lensing Data
GERSHTEIN	2004	PAN 67 1596	Graviton Mass, Quintessence and Oscillatory Character of the Universe Evolution
FINN	2002	PR D65 044022	Bounding the Mass of the Graviton using Binary Pulsar Observations
TALMADGE	1988	PRL 61 1159	Model Independent Constraints on Possible Modifications of Newtonian Gravity
GOLDHABER	1974	PR D9 1119	Mass of the Graviton
HARE	1973	CJP 51 431	Mass of the Graviton

The publication of the *Review of Particle Physics* is supported by US DOE, CERN, MEXT (Japan), and INFN (Italy). Individual collaborators receive support for their PDG activities from their respective funding agencies.

In a recent paper GRAVITY collaboration quoted 8 our papers

A&A, 698, L15 (2025)
https://doi.org/10.1051/0004-6361/202554676

Astronomy & Astrophysics

LETTER TO THE EDITOR

Exploring the presence of a fifth force at the Galactic Center

GRAVITY Collaboration*: K. Abd El Dayem[1], R. Abuter[4], N. Aimar[10,7], P. Amaro Seoane[14,2,18], A. Amorim[8,7], J. P. Berger[3,4], H. Bonnet[4], G. Bourdarot[2], W. Brandner[5], V. Cardoso[7,15], Y. Clénet[1], R. Davies[2], P. T. de Zeeuw[19], A. Drescher[2], A. Eckart[6,13], F. Eisenhauer[2,17], H. Feuchtgruber[2], G. Finger[2], N. M. Förster Schreiber[2], A. Foschi[1,2,**], P. Garcia[10,7], E. Gendron[1], R. Genzel[2,11], S. Gillessen[2], M. Hartl[2], X. Haubois[9], F. Haussmann[2], T. Henning[5], S. Hippler[5], M. Horrobin[6], L. Jochum[9], L. Jocou[3], A. Kaufer[9], P. Kervella[1], S. Lacour[1,4], V. Lapeyrère[1], J.-B. Le Bouquin[3], P. Léna[1], D. Lutz[2], F. Mang[2], N. More[2], J. Osorno[1], T. Ott[2], T. Paumard[1], K. Perraut[3], G. Perrin[1], S. Rabien[2], D. C. Ribeiro[2], M. Sadun Bordoni[2], S. Scheithauer[5], J. Shangguan[20], T. Shimizu[2], J. Stadler[12,2], O. Straub[2,16], C. Straubmeier[6], E. Sturm[2], L. J. Tacconi[2], I. Urso[1], F. Vincent[1], S. D. von Fellenberg[13,2], E. Wieprecht[2], and J. Woillez[4]

(Affiliations can be found after the references)

Received 21 March 2025 / Accepted 1 May 2025

ABSTRACT

Aims. We investigate the presence of a Yukawa-like correction to Newtonian gravity at the Galactic Center, leading to a new upper limit on the intensity of such a correction.
Methods. We performed a Markov chain Monte Carlo (MCMC) analysis using the astrometric and spectroscopic data of star S2 collected at the Very Large Telescope by GRAVITY, NACO, and SINFONI instruments, covering the period from 1992 to 2022.
Results. The precision of the GRAVITY instrument allows us to derive the most stringent upper limit at the Galactic Center for the intensity of the Yukawa contribution ($\propto \alpha e^{-\lambda r}$) of $|\alpha| < 0.003$ for a scale length of $\lambda = 3 \cdot 10^{13}$ m (~ 200 AU). This is an improvement on all estimates obtained in previous works by roughly one order of magnitude.

Key words. gravitation – celestial mechanics – Galaxy: center

1. Introduction

General relativity (GR) is the most widely recognized theory of gravity today. Its predictions have been extensively tested on Solar System scales and using gravitational waves emission by black holes (BHs) and binary pulsars (Will 2014, 2018a; Nitz et al. 2021). Until now, no significant deviation from GR

One way to address these inconsistencies between theory and experiments is to directly modify GR, giving rise to a plethora of possible extended theories of gravity (ETG). In particular, a Yukawa-like interaction emerges quite naturally in the weak field limit of several ETGs; for instance, scalar-tensor-vector theories (Moffat 2006), massive gravity theories (Visser 1998; Hinterbichler 2012), theo-

Ciência e a Tecnologia), to ESO and the Paranal staff, and to the many scientific and technical staff members in our institutions, who helped to make NACO, SINFONI, and GRAVITY a reality. This project has received funding from the European Union's Horizon 2020 research and innovation programme under the Marie Sklodowska-Curie grant agreement No 101007855. We acknowledge the financial support provided by FCT/Portugal through grants 2022.01324.PTDC, PTDC/FIS-AST/7002/2020, UIDB/00099/2020 and UIDB/04459/2020. J.S. acknowledge the National Science Foundation of China (12233001) and the National Key R&D Program of China (2022YFF0503401).

References

Adkins, G. S., & McDonnell, J. 2007, Phys. Rev. D, 75, 082001
Alsing, J., Berti, E., Will, C. M., & Zaglauer, H. 2012, Phys. Rev. D, 85, 064041
Alves, M. F. S., Toniato, J. D., & Rodrigues, D. C. 2024, Phys. Rev. D, 109, 044045
Bars, I., & Visser, M. 1986, Phys. Rev. Lett., 57, 25
Bergé, J. 2017, in 52nd Rencontres de Moriond on Gravitation 191
Borka, D., Jovanović, P., Jovanović, V. B., & Zakharov, A. F. 2013, JCAP, 11, 050
Borka, D., Jovanović, V. B., Capozziello, S., Zakharov, A. F., & Jovanović, P. 2021, Universe, 7, 407
Capozziello, S., Borka, D., Jovanović, P., & Jovanović, V. B. 2014, Phys. Rev. D, 90, 044052
Capozziello, S., Harko, T., Koivisto, T. S., Lobo, F. S. N., & Olmo, G. J. 2015, Universe, 1, 199
Carroll, S. M., Mantry, S., Ramsey-Musolf, M. J., & Stubbs, C. W. 2009, Phys. Rev. Lett., 103, 011301
Catanzarite, J. H. 2010, arXiv e-prints [arXiv:1008.3416]
de Laurentis, M., De Martino, I., & Della Monica, R. 2023, Rept. Prog. Phys., 86, 104901
de Martino, I., & della Monica, R., & de Laurentis, M., 2021, Phys. Rev. D, 104, L101502
Della Monica, R., de Martino, I., & de Laurentis, M. 2022, MNRAS, 510, 4757
Eckart, A., & Genzel, R. 1996, Nature, 383, 415
Esposito, G. 2011, arXiv e-prints [arXiv:1108.3269]
Fienga, A., & Minazzoli, O. 2024, Living Rev. Rel., 27, 1
Foreman-Mackey, D., Hogg, D. W., Lang, D., & Goodman, J. 2013, PASP, 125, 306
Frieman, J. A., & Gradwohl, B.-A. 1991, Phys. Rev. Lett., 67, 2926
Ghez, A. M., Duchêne, G., Matthews, K., et al. 2003, ApJ, 586, L127
Gillessen, S., Eisenhauer, F., Trippe, S., et al. 2009a, ApJ, 692, 1075
Gillessen, S., Eisenhauer, F., Fritz, T. K., et al. 2009b, ApJ, 707, L114
Gradwohl, B.-A., & Frieman, J. A. 1992, ApJ, 398, 407
GRAVITY Collaboration (Abuter, R., et al.) 2018, A&A, 615, L15
GRAVITY Collaboration (Abuter, R., et al.) 2020, A&A, 636, L5
GRAVITY Collaboration (Abuter, R., et al.) 2022, A&A, 657, L12
GRAVITY Collaboration (Abd El Dayem, K., et al.) 2024, A&A, 692, A242
Grould, M., Vincent, F. H., Paumard, T., & Perrin, G. 2017, A&A, 608, A60
Hees, A., Do, T., Ghez, A. M., et al. 2017, Phys. Rev. Lett., 118, 211101
Hees, A., Folkner, W. M., Jacobson, R. A., & Park, R. S. 2014, Phys. Rev. D, 89, 102002
Hinterbichler, K. 2012, Rev. Mod. Phys., 84, 671
Hofmann, F., & Müller, J. 2018, Class. Quant. Grav., 35, 035015
Hoyle, C. D., Schmidt, U., Heckel, B. R., et al. 2001, Phys. Rev. Lett., 86, 1418
Iorio, L. 2024, General Post-Newtonian Orbital Effects: From Earth's Satellites to the Galactic Centre (Cambridge University Press)
Jovanović, P., Borka, D., Borka Jovanović, V., & Zakharov, A. F. 2021, Eur. Phys. J. D, 75, 145
Jovanović, P., Jovanović, V. B., Borka, D., & Zakharov, A. F. 2023, JCAP, 03, 056
Jovanović, P., Jovanović, V. B., Borka, D., & Zakharov, A. F. 2024a, Phys. Rev. D, 109, 064046
Jovanović, P., Borka Jovanović, V., Borka, D., & Zakharov, A. F. 2024b, Symmetry, 16, 397
Kiefer, C. 2023, arXiv e-prints [arXiv:2302.13047]
Konopliv, A. S., Asmar, S. W., Folkner, W. M., et al. 2011, Icarus, 211, 401
Losada, V. d. M., Della Monica, R., de Martino, I., & De Laurentis, M. 2025, A&A, 694, A280
Mariani, V., Fienga, A., Minazzoli, O., Gastineau, M., & Laskar, J. 2023, Phys. Rev. D, 108, 024047
Massey, R., Kitching, T., & Richard, J. 2010, Rept. Prog. Phys., 73, 086901
Moffat, J. W. 2006, JCAP, 03, 004
Nitz, A. H., Capano, C. D., Kumar, S., et al. 2021, ApJ, 922, 76
Peebles, P. J. E., & Ratra, B. 2003, Rev. Mod. Phys., 75, 559
Perivolaropoulos, L. 2010, Phys. Rev. D, 81, 047501
Plewa, P. M., Gillessen, S., Eisenhauer, F., et al. 2015, MNRAS, 453, 3234
Poisson, E., & Will, C. 2012, Gravity: Newtonian, Post-Newtonian, Relativistic (Cambridge: Cambridge University Press), 1
Reid, M. J., & Brunthaler, A. 2020, ApJ, 892, 39
Sabha, N., et al. 2012, A&A, 545, A70
Salucci, P. 2019, Astron. Astrophys. Rev., 27, 2
Schödel, R., Ott, T., Genzel, R., et al. 2002, Nature, 419, 694
Shankaranarayanan, S., & Johnson, J. P. 2022, Gen. Relativ. Gravitation, 54, 44
Tan, Y., & Lu, Y. 2024, Phys. Rev. D, 109, 044047
Touboul, P., et al. 2022, Phys. Rev. Lett., 129, 121102
Tsai, Y.-D., Wu, Y., Vagnozzi, S., & Visinelli, L. 2023, JCAP, 04, 031
Tsai, Y.-D., Farnocchia, D., Micheli, M., Vagnozzi, S., & Visinelli, L. 2024, Commun. Phys., 7, 311
Vagnozzi, S., et al. 2023, Class. Quant. Grav., 40, 165007
van Albada, T. S., Bahcall, J. N., Begeman, K., & Sancisi, R. 1985, ApJ, 295, 305
Visser, M. 1998, Gen. Rel. Grav., 30, 1717
Weinberg, S. 1989, Rev. Mod. Phys., 61, 1
Will, C. M. 2014, Living Rev. Rel., 17, 4
Will, C. M. 2018a, Theory and Experiment in Gravitational Physics (Cambridge University Press)
Will, C. M. 2018b, Class. Quant. Grav., 35, 17LT01
Zakharov, A. F., Jovanovic, P., Borka, D., & Jovanovic, V. B. 2016, JCAP, 05, 045
Zakharov, A. F., Jovanović, P., Borka, D., & Borka Jovanović, V. 2018, JCAP, 04, 050

---

[1] LIRA, Observatoire de Paris, Université PSL, CNRS, Sorbonne Université, Université de Paris, 5 place Jules Janssen, 92195 Meudon, France
[2] Max Planck Institute for Extraterrestrial Physics, Giessenbachstraße 1, 85748 Garching, Germany
[3] Univ. Grenoble Alpes, CNRS, IPAG, 38000 Grenoble, France
[4] European Southern Observatory, Karl-Schwarzschild-Straße 2, 85748 Garching, Germany
[5] Max Planck Institute for Astronomy, Königstuhl 17, 69117 Heidelberg, Germany
[6] 1st Institute of Physics, University of Cologne, Zülpicher Straße 77, 50937 Cologne, Germany
[7] CENTRA – Centro de Astrofísica e Gravitação, IST, Universidade de Lisboa, 1049-001 Lisboa, Portugal
[8] Universidade de Lisboa – Faculdade de Ciências, Campo Grande 1749-016, Lisboa, Portugal
[9] European Southern Observatory, Casilla 19001, Santiago 19, Chile
[10] Faculdade de Engenharia, Universidade do Porto, rua Dr. Roberto Frias, 4200-465 Porto, Portugal
[11] Departments of Physics & Astronomy, Le Conte Hall, University of California, Berkeley, CA 94720, USA
[12] Max Planck Institute for Astrophysics, Karl-Schwarzschild-Straße 1, 85748 Garching, Germany
[13] Max Planck Institute for Radio Astronomy, auf dem Hügel 69, 53121 Bonn, Germany
[14] Institute of Multidisciplinary Mathematics, Universitat Politècnica de València, València, Spain
[15] Center of Gravity, Niels Bohr Institute, Blegdamsvej 17, 2100 Copenhagen, Denmark
[16] ORIGINS Excellence Cluster, Boltzmannstraße 2, 85748 Garching, Germany
[17] Department of Physics, Technical University of Munich, 85748 Garching, Germany
[18] Higgs Centre for Theoretical Physics, Edinburgh, UK
[19] Leiden University, 2311 EZ Leiden, The Netherlands
[20] The Kavli Institute for Astronomy and Astrophysics, Peking University, Beijing 100871, China

World Scientific Series in Astrophysics

The Encyclopedia of Cosmology

Set 2: Frontiers in Cosmology

Volume 1
Modified Gravity

Editor-in-chief

Giovanni G Fazio
Center for Astrophysics | Harvard & Smithsonian, USA

Claudia de Rham & Andrew J Tolley
Imperial College London, UK

World Scientific

NEW JERSEY • LONDON • SINGAPORE • BEIJING • SHANGHAI • HONG KONG • TAIPEI • CHENNAI

modification $\mu(a)$ of Kepler's third law:

$$\frac{a^3}{T^2} = \frac{M_\odot(1+\mu(a))}{4(2\pi)^3 M_{\rm Pl}^2}, \tag{3.10}$$

where a and T are the semi-major axis and the period of the planet's orbit. In GR, $\mu = 0$, while in models of modified gravity, μ can depart from unity in some regime and acquire a non-trivial radius dependence, $\mu = \mu(a)$. Comparing the ratio a^3/T^2 of various planets provides a powerful way to test GR with the best bounds given by comparison of the ratio for the Earth and the Moon (Talmadge *et al.*, 1988).

Besides modifying Kepler's third law and including fifth force effects, modifications of the standard Newtonian potential can lead to an additional precession beyond that expected from GR and the fifth forces. This implies that even theories that do not involve any additional degrees of freedom or carry no fifth force effects can still lead to an additional advance of the perihelion on top of GR's expected precession. These effects are typically less constrained than the corrections to Kepler's third law but should still be under control.

3.4.5 *Black holes and stellar solutions*

All of the constraints on planetary orbits within the solar system are also applicable to the orbits of stars in the vicinity of black holes, including Sagittarius A*, with S2-like stars orbiting the black hole within distances comparable to that in the solar system as observed by the **W.M. KECK observatory** (Eckart and Genzel, 1996; Ghez *et al.*, 2005a,b; Gillessen *et al.*, 2009; Meyer *et al.*, 2012) leading to competitive tests of modified gravity (Borka *et al.*, 2012, 2013; Zakharov *et al.*, 2016).

In parallel, the modification of the black hole solution itself in theories of modified gravity can be matched against its shadow as observed by the **Event Horizon Telescope** (Akiyama *et al.*, 2022a) and has already been used to constrain models of modified gravity (Akiyama *et al.*, 2022b; Psaltis *et al.*, 2020; Shaikh, 2023; Vagnozzi *et al.*, 2022; Zakharov, 2022). The potential presence of hair, superradiance and other effects modifying the black hole structure near the horizon could provide competitive tests of modified gravity in the future.

In addition, modifications of gravity can affect the **sequence of stars** and structure of other astrophysical systems. The presence of additional degrees of freedom that often go along with modified gravity, when equilibrated in a stellar core, can drive new stellar instabilities which would manifest in **mass gaps in black hole populations** (see Straight *et al.*, 2020 for an example). Modified gravity effects can also change the equilibrium structure of main sequence stars, modifying the relation between their mass and luminosity (stars are typically brighter in theories of gravity involving a Chameleon-like screened scalar field like in $f(R)$), an effect which is then reflected in their radii and ages (Davis *et al.*, 2012). Reviews on other astrophysical tests of modified gravity can be found in Alves Batista *et al.* (2021); Baker *et al.* (2021); Sakstein (2020).

Shadow reconstructions for M87* and Sgr A* are based on three pillars: Synchrotron radiation, VLBI concept, GR in a strong gravitational field

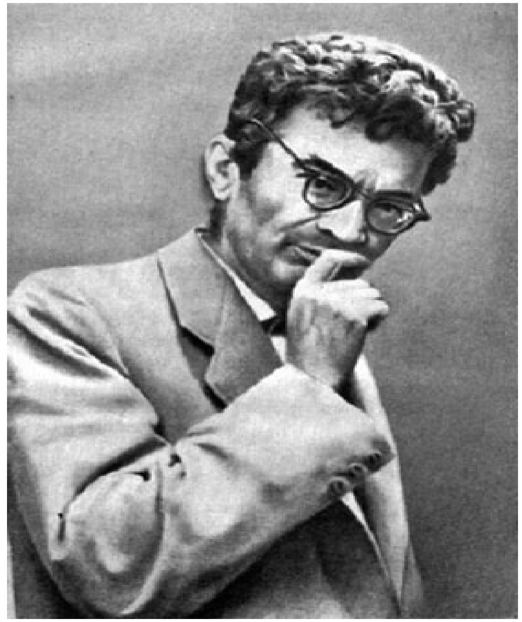

I. Pomeranchuk, The maximum energy that primary cosmic ray electrons can have on the Earth's surface due to radiation in the Earth's magnetic field, J. Phys. USSR, 2, 356 (1940)

D. Ivanenko and I. Pomeranchuk, On the Maximal Energy Attainable in a Betatron, Phys. Rev. 65, 343 (1944)

L.A. Artsimovich and I. Pomeranchuk, The maximum energy that primary cosmic ray electrons can have on the Earth's surface due to radiation in the Earth's magnetic field, J. Phys. USSR, 2, 267 (1945)

Elder, F. R., Gurewitsch, A. M., Langmuir, R. V., & Pollock, H. C. Radiation from Electrons in a Synchrotron. Physical Review, 71(11), 829 (1947)

In 1950 D. Ivanenko, A. A. Sokolov and I. Pomeranchuk were awarded the State prize of the second grade for works on synchrotron radiation, presented in book “Classical Field Theory”

Synchrotron radiation plays a key role in many astrophysical objects (including BH's and pulsars (Crab Nebula)) . In 1946 they predicted emission in radio band from solar corona. In May 1947 they participated in Brazil expedition

The Soviet expedition in Brazil for solar eclipse observations in 20 May 1947 where S. E. Khaikin and B. M. Chikhachev discovered radio emission from solar corona during the solar eclipse aboard the “Griboedov” ship

The idea of VLBI observation was introduced by L. I. Matveenko (1929—2019) in 1960s and it was realized in Soviet – US joint radio observations in 1970s. Matveenko proposed also a project of a ground – space interferometer. This idea was realized later by Japanese (HALCA, VSOP, 1997) and Russian Astronomers (Radioastron, 2011) .

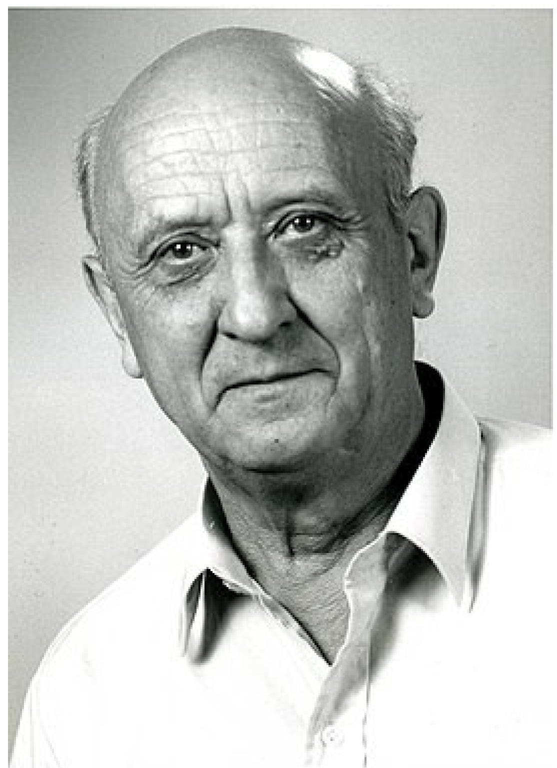

EHT shadow reconstruction for M87* and Sgr A* observed in April 2017

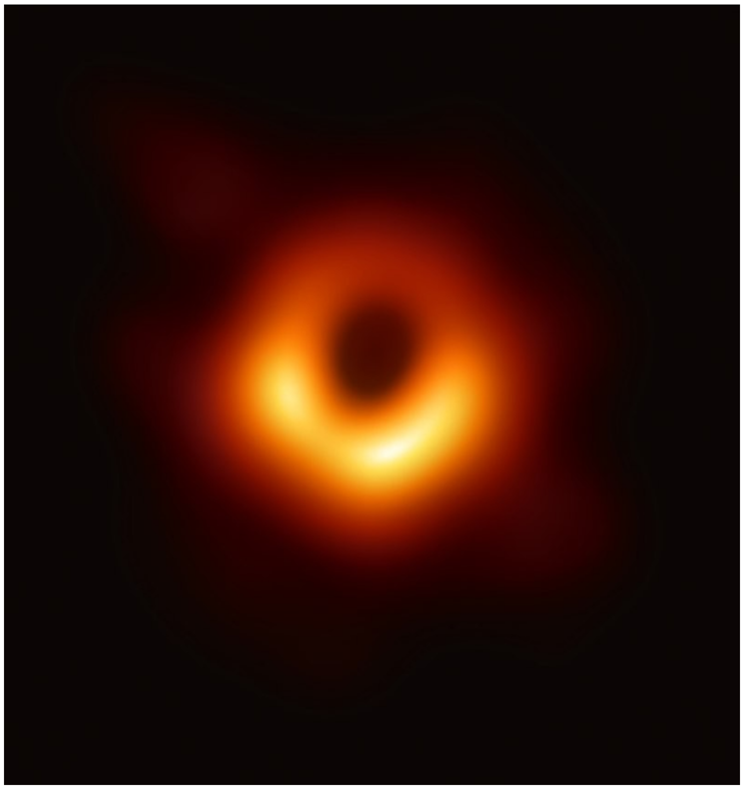

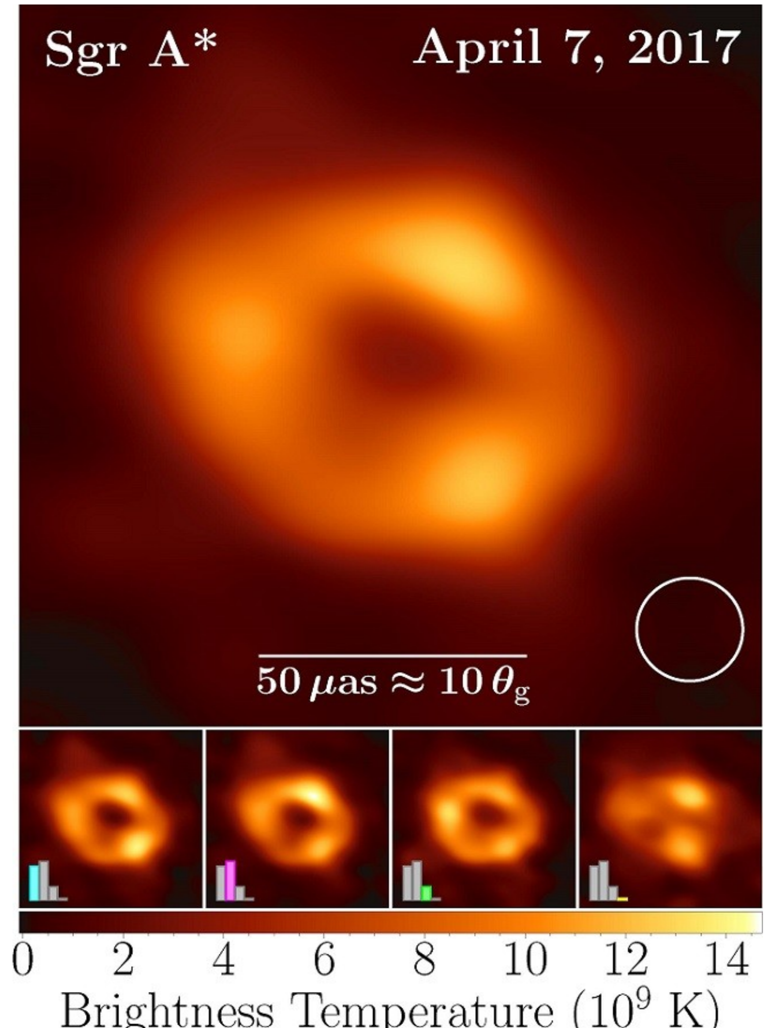

For about 20 years we declared black holes (for theorists) are dark spots (shadows) for observers and reported these ideas in many institutes located in different countries (Russia, Serbia, China, Bulgaria, Switzerland, Italy, Greece, Germany, USA, UK, India, Pakistan, Australia, Spain, France). These ideas were also reported at EHT meetings.

When our predictions concerning GC shadow were confirmed a majority of colleagues forgot them and did not mention them. Similarly, when I noted in a comment that an opportunity for GC shadow using Millimetron space – ground observations was firstly discussed in our paper (2005), three (!!!) anonymous referees did not disprove a correctness of my statement but they reacted in a negative way and they simultaneously wrote that it was not modest and ethic to request an additional citation.

International Journal of Modern Physics D | Online Ready

Shadows near supermassive black holes: From a theoretical concept to GR test

Alexander F. Zakharov

https://doi.org/10.1142/S0218271823400047 |

Abstract

General relativity (GR) passed many astronomical tests but in majority of them GR predictions have been tested in a weak gravitational field approximation. Around 50 years ago a shadow was introduced by Bardeen as a purely theoretical concept but due to an enormous progress in observational and computational facilities this theoretical prediction has been confirmed and the most solid argument for an existence of supermassive black holes in Sgr A* and M87* has been obtained.

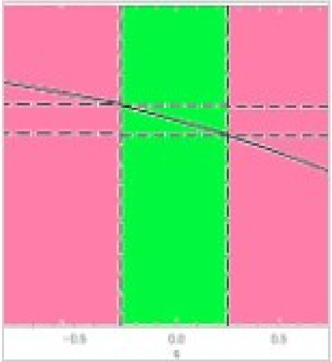

Shadows near supermassive black holes: From a theoretical concept to GR test

International Journal of Modern Physics D

Alexander F. Zakharov

At the initial stage of development of GR and quantum mechanics gedanken(thought) experiments were very popular in a discussion of specific features of new theories. To discuss observations signatured of black holes J. M. Bardeen considered features of an existence of bright screen which is located behind a Kerr black hole in the case of an observer is located in the equatorial plane. In these considerations it was assumed that photons emitted by a luminous screen do not interact with a matter around a black hole.

Clearly, this gedanken experiment looked rather artificial since first, there are no luminous screens behind astrophysical black holes, second, masses of black holes were estimated not precisely and a majority of astrophysical black holes were black holes with stellar masses but even now shadows around these black holes are too small to be detected, third, it was not clear how to detect a darkness or to distinguish it from a faintness.

Available online at www.sciencedirect.com
SCIENCE DIRECT®
ELSEVIER
New Astronomy 10 (2005) 479–489
New Astronomy
www.elsevier.com/locate/newast

Measuring the black hole parameters in the galactic center with RADIOASTRON

A.F. Zakharov [a,b,c,*], A.A. Nucita [d], F. DePaolis [d], G. Ingrosso [d]

[a] *Institute of Theoretical and Experimental Physics, 25, B. Cheremushkinskaya st., Moscow 117259, Russia*
[b] *Space Research Centre of Lebedev Physics Institute, Moscow, Russia*
[c] *Joint Institute for Nuclear Research, Dubna, Russia*
[d] *Dipartimento di Fisica, Universita di Lecce and INFN, Sezione di Lecce, Italy*

Received 19 January 2005; accepted 21 February 2005
Available online 23 March 2005
Communicated by F. Melchiorri

Abstract

Recently, Holz and Wheeler (2002) [ApJ 578, 330] considered a very attracting possibility to detect retro-MACHOs, i.e., retro-images of the Sun by a Schwarzschild black hole. In this paper, we discuss glories (mirages) formed near rapidly rotating Kerr black hole horizons and propose a procedure to measure masses and rotation parameters analyzing these forms of mirages. In some sense that is a manifestation of gravitational lens effect in the strong gravitational field near black hole horizon and a generalization of the retro-gravitational lens phenomenon. We analyze the case of a Kerr black hole rotating at arbitrary speed for some selected positions of a distant observer with respect to the equatorial plane of a Kerr black hole. Some time ago Falcke, Melia, Agol (2000) [ApJ 528, L13S] suggested to search shadows at the Galactic Center. In this paper, we present the boundaries for shadows. We also propose to use future radio interferometer RADIOASTRON facilities to measure shapes of mirages (glories) and to evaluate the black hole spin as a function of the position angle of a distant observer.

PACS: 97.60.L; 04.70; 95.30.S; 04.20; 98.62.S

Keywords: Black hole physics; Gravitational lenses; Microlensing

1. Introduction

Recently Holz and Wheeler (2002) have suggested that a Schwarzschild black hole may form retro-images (called retro-MACHOs) if it is illuminated by the Sun. We analyze a rapidly rotating

* Corresponding author. Tel.:+7 095 1299759; fax: +7 095 8839601.
E-mail address: zakharov@itep.ru (A.F. Zakharov).

1384-1076/$ - see front matter
doi:10.1016/j.newast.2005.02.007

ELSEVIER

New Astronomy
Top Cited Article 2005-2010

Awarded to:

Zakharov, A.F., Nucita, A.A., Depaolis, F., Ingrosso, G.

For the paper entitled:

"Measuring the black hole parameters in the galactic center with RADIOASTRON"

This paper was published in:

New Astronomy, Volume 10, Issue 6, 2005

David Clark
Senior Vice President, Physical Sciences I
Amsterdam, The Netherlands

Our proposal

In 2004-2005 we proposed a way to test GR predictions with Radioastron:

Since angular resolution of Radioastron at 1.3 cm is around 8 uas and the size of darkness (shadow) could help us to evaluate a charge, while shape could help us to evaluate a spin (good!)

The shortest wavelength is 1.3 cm (it is too long to detect shadow) (not good for Radioastron!)

So, we propose to test GR predictions about shape and size of BH images with observations. Astronomy is dealing with images. Therefore, establishing the correspondence of theoretical image and reconstructed image using observational data is an aim for further observations.

AFZ et al., NA (2005): “In our old paper https://ui.adsabs.harvard.edu/.../2005NewA...10.../abstract

we wrote at the end "In spite of the difficulties of measuring the shapes of images near black holes is so attractive challenge to look at the ‘‘faces’’ of black holes because namely the mirages outline the ‘‘faces’’ and

correspond to fully general relativistic description of a region near black hole horizon without any assumption about a specific model for astrophysical processes around black holes (of course we assume that there are sources illuminating black hole surroundings). No doubt that the rapid growth of observational facilities will give a chance to measure the mirage shapes using not only RADIOASTRON facilities but using also other instruments and spectral bands (for example, X-ray interferometer MAXIM (White, 2000; Cash et al., 2000) or sub-mm VLBI array (Miyoshi, 2004)). Astro Space Centre of Lebedev Physics Institute proposed except the RADIOASTRON mission and developed also space based interferometers (Millimetron and Sub-millimetron) for future observations in mm and sub-mm bands. These instruments could be used for the determination of shadow shapes.“

Therefore, the shadows may be reconstructed from ground or space -- ground VLBI observations in mm or sub-mm bands. EHT results confirmed these predictions.

Measuring the black hole parameters in the Galactic Center with Radioastron

- Let us consider an illumination of black holes. Then retro-photons form caustics around black holes or mirages around black holes or boundaries around shadows.
- (Zakharov, Nucita, DePaolis, Ingrosso,
- New Astronomy 10 (2005) 479; astro-ph/0411511)

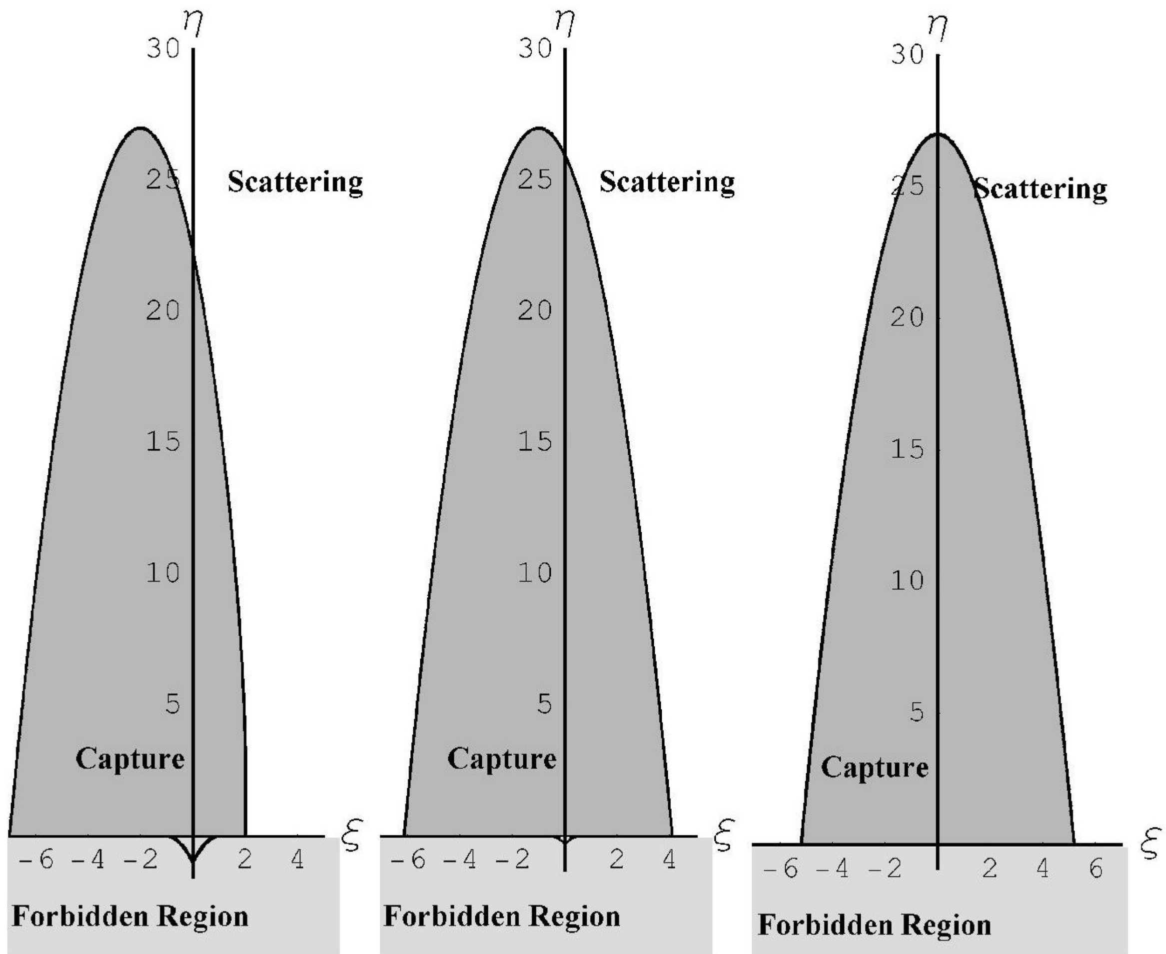

Fig. 1. Different types for photon trajectories and spin parameters ($a = 1., a = 0.5, a = 0.$). Critical curves separate capture and scatter regions. Here we show also the forbidden region corresponding to constants of motion $\eta < 0$ and $(\xi, \eta) \bar{\in} M$ as it was discussed in the text.

OXFORD SCIENCE PUBLICATIONS

INTERNATIONAL SERIES OF
MONOGRAPHS ON PHYSICS 69

The Mathematical Theory of Black Holes

S. Chandrasekhar

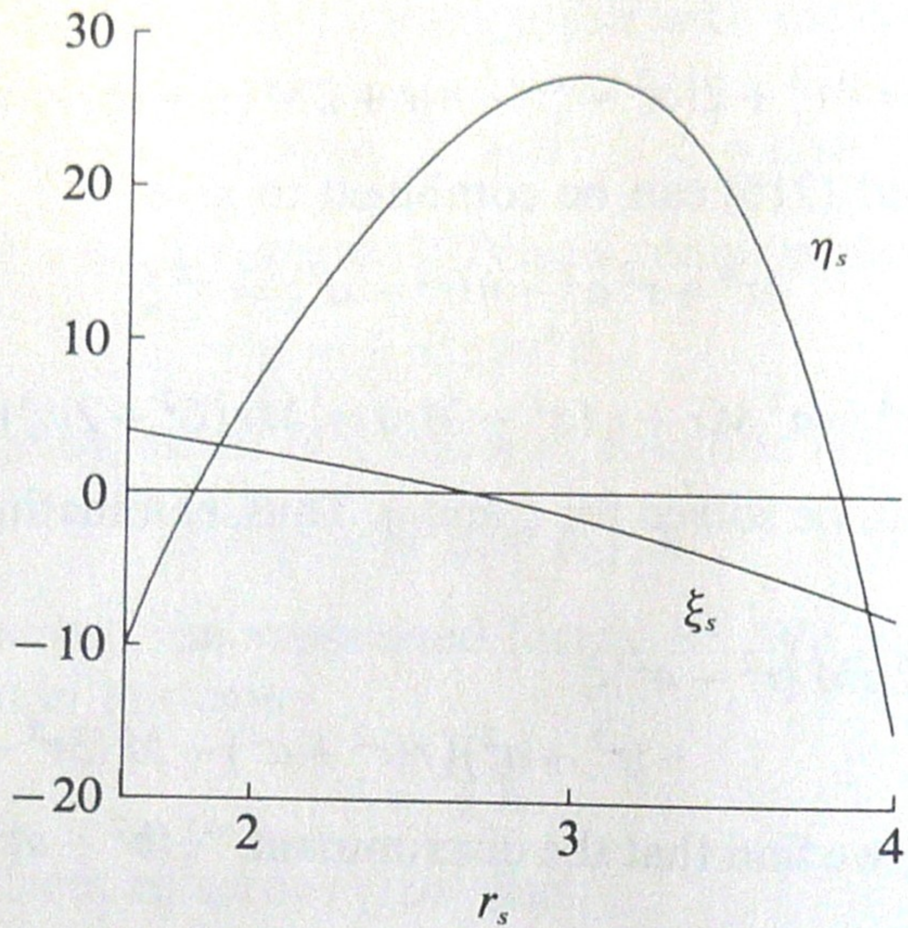

FIG. 34. The locus (ξ_s, η_s) determining the constants of the motion for three-dimensional orbits of constant radius described around a Kerr black-hole with $a = 0.8$. The unit of length along the abscissa is M.

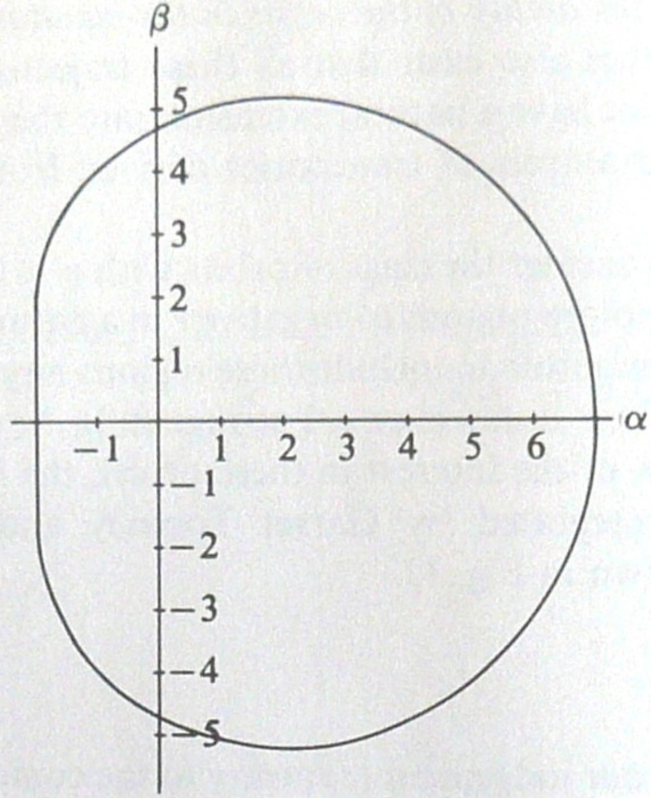

FIG. 38. The apparent shape of an extreme ($a = M$) Kerr black-hole as seen by a distant observer in the equatorial plane, if the black hole is in front of a source of illumination with an angular size larger than that of the black hole. The unit of length along the coordinate axes α and β (defined in equation (241) is M.

black hole from infinity, the apparent shape will be determined by

$$(\alpha, \beta) = [\xi, \sqrt{\eta(\xi)}]. \tag{242}$$

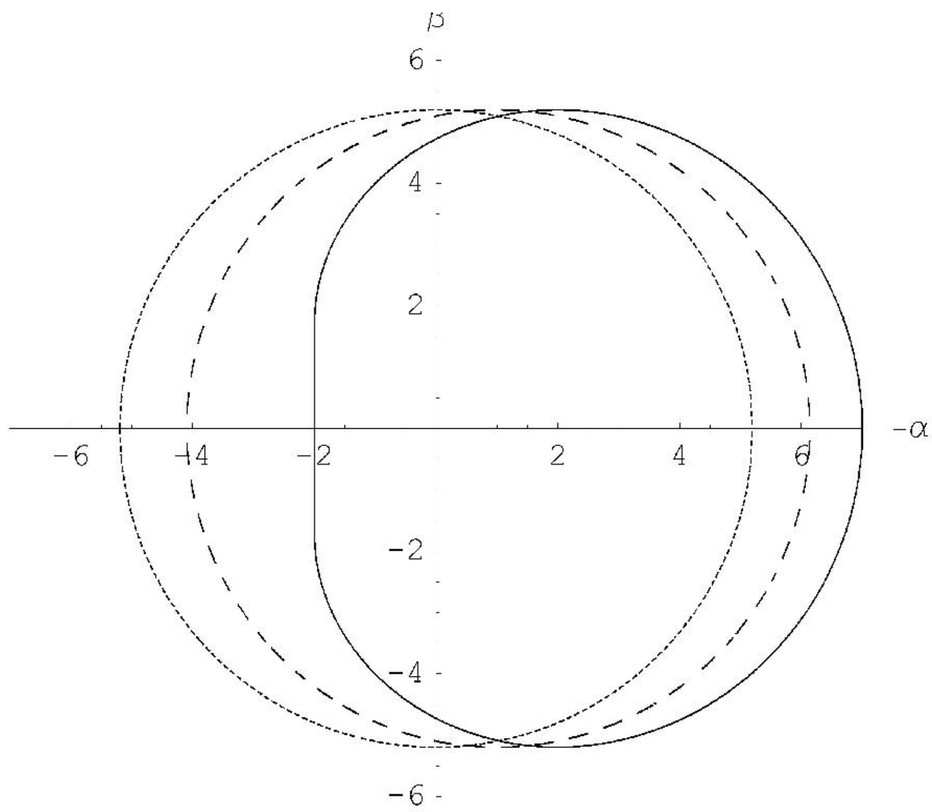

Fig. 2. Mirages around black hole for equatorial position of distant observer and different spin parameters. The solid line, the dashed line and the dotted line correspond to $a = 1, a = 0.5, a = 0$ correspondingly

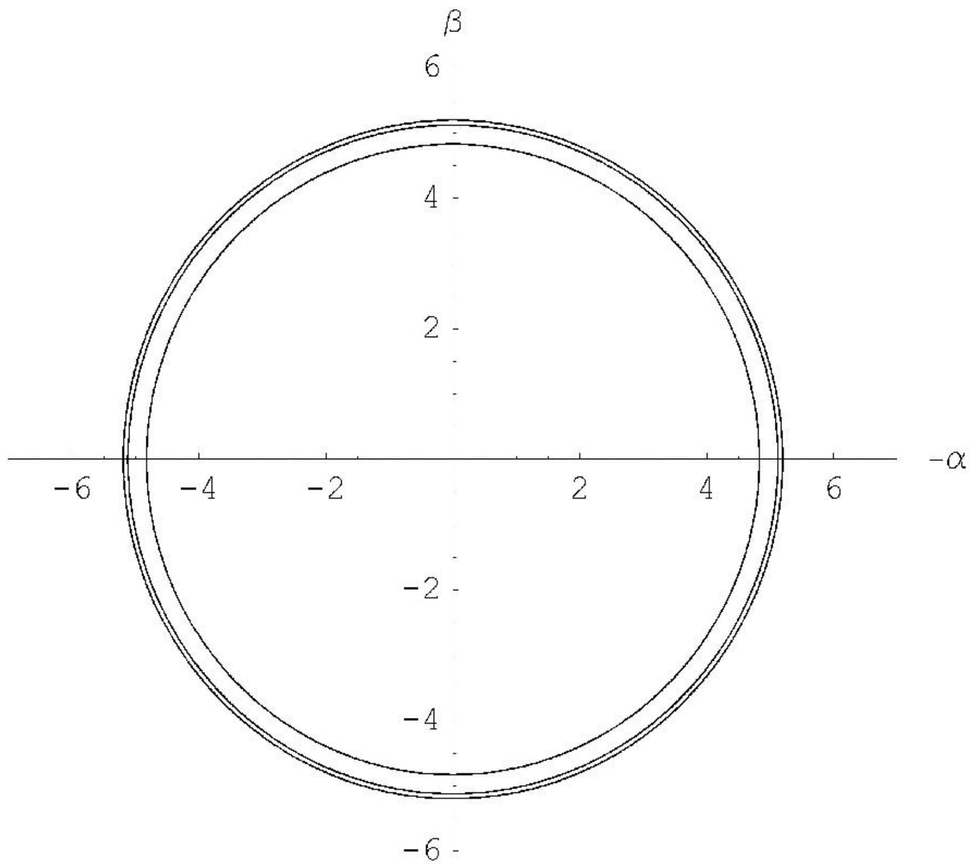

Fig. 3. Mirages around a black hole for the polar axis position of distant observer and different spin parameters ($a = 0, a = 0.5, a = 1$). Smaller radii correspond to greater spin parameters.

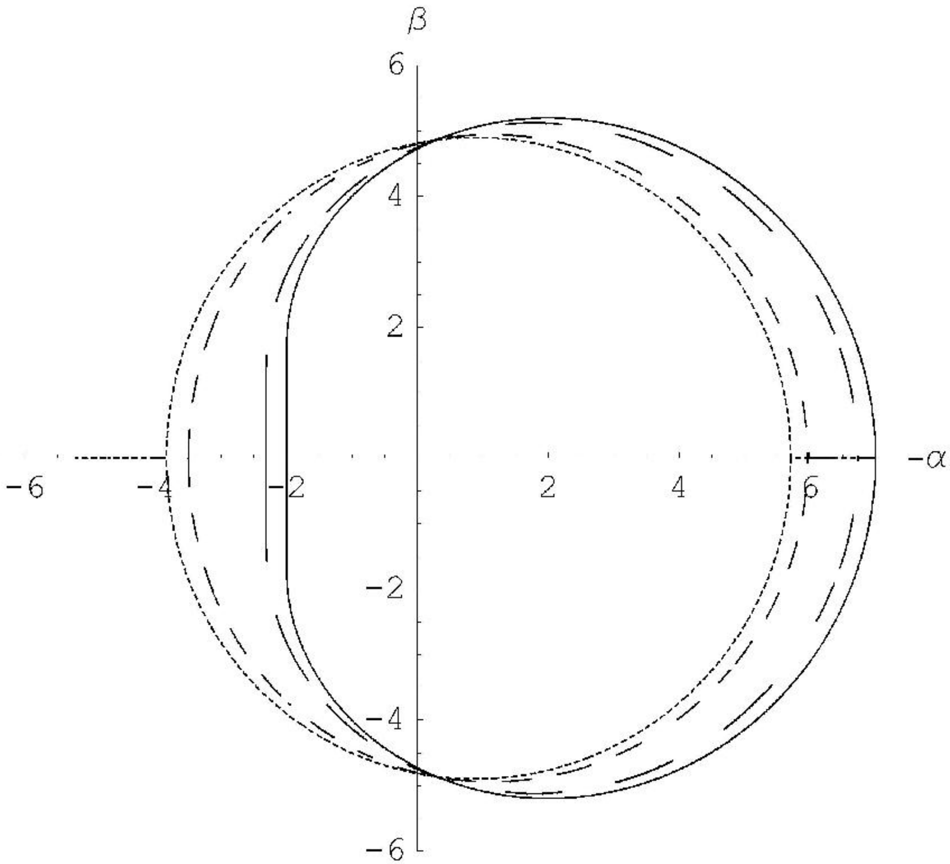

Fig. 5. Mirages around black hole for different angular positions of a distant observer and the spin $a = 1$. Solid, long dashed, short dashed and dotted lines correspond to $\theta_0 = \pi/2, \pi/3, \pi/6$ and $\pi/8$, respectively.

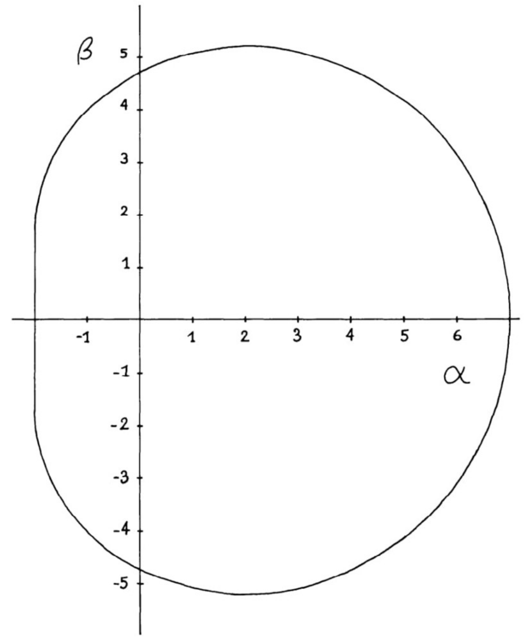

Figure 6. The apparent shape of an extreme ($a = m$) Kerr black hole as seen by a distant observer in the equatorial plane, if the black hole is in front of a source of illumination with an angular size larger than that of the black hole.

is largest there and because of the gravitational focusing effects associated with the bending of the rays toward the equatorial plane. Note that the radiation comes out along the flat portion of the apparent boundary of the extreme black hole as plotted in Figure 6.

D. Geometrical Optics

A detailed calculation of the brightness distribution coming from a source near a Kerr black hole requires more of geometrical optics than the calculation of photon trajectories. I will now review some techniques which are useful in making astrophysical calculations in connection with black holes.

The fundamental principle can be expressed as the conservation of photon density in phase space along each photon trajectory. A phase space element $d^3x\, d^3p$, the product of a proper spatial volume element and a physical momentum-space volume element in a local observer's frame of reference, is a Lorentz invariant, so the particular choice of local observer is arbitrary. The density $N(x^a, p^{(\beta)})$ is defined

James Maxwell Bardeen passed away on June 20, 2022
(Shadows +Kerr BHs as engines for quasars)

John Bardeen (1908 -1991), the father of J. M. Bardeen. E. Wigner was J. Bardeen' supervisor

Direct Measurements of Black Hole Charge with Future Astrometrical Missions

A.F. Zakharov[1,2,3], F. De Paolis[4], G. Ingrosso[4], A.A. Nucita[4]

[1] Institute of Theoretical and Experimental Physics, 25, B.Cheremushkinskaya st., Moscow, 117259, Russia,

[2] Astro Space Centre of Lebedev Physics Institute, 84/32, Profsoyuznaya st., Moscow, 117810, Russia,

[3] Joint Institute for Nuclear Research, Dubna, Russia

[4] Department of Physics, University of Lecce and INFN, Section of Lecce, Via Arnesano, I-73100 Lecce, Italy

Received / accepted

Abstract. Recently, Zakharov et al. (2005a) considered the possibility of evaluating the spin parameter and the inclination angle for Kerr black holes in nearby galactic centers by using future advanced astrometrical instruments. A similar approach which uses the characteristic properties of gravitational retro-lensing images can be followed to measure the charge of Reissner-Nordström black hole. Indeed, in spite of the fact that their formation might be problematic, charged black holes are objects of intensive investigations. From the theoretical point of view it is well-known that a black hole is described by only three parameters, namely, its mass M, angular momentum J and charge Q. Therefore, it would be important to have a method for measuring all these parameters, preferably by model independent way. In this paper, we propose a procedure to measure the black hole charge by using the size of the retro-lensing images that can be revealed by future astrometrical missions. A discussion of the Kerr-Newmann black hole case is also offered.

Table 1. The fringe sizes (in micro arcseconds) for the standard and advanced apogees B_{max} (350 000 and 3 200 000 km, respectively).

B_{max}(km)\λ(cm)	92	18	6.2	1.35
3.5×10^5	540	106	37	8
3.2×10^6	59	12	4	0.9

4. The space RADIOASTRON interferometer

The space-based radio telescope RADIOASTRON[1] is planned to be launched within few next years[2]. This space-based 10-m radio telescope will be used for space – ground VLBI observations. The measurements will have extremely high angular resolutions, namely about 1–10 μas (in particular about 8 μas at the shortest wavelength of 1.35 cm and a standard orbit[3], and could be about 0.9 μas for the high orbit configuration at the same wavelength. Four wave bands will be used corresponding to λ = 1.35 cm, λ = 6.2 cm, λ = 18 cm, λ = 92 cm (see Table 1). A detailed calculation of the high-apogee evolving orbits (B_{max}) can be done, once the exact launch time is known.

After several years of observations, it should be possible to move the spacecraft to a much higher orbit (with apogee radius about 3.2 million km), by additional spacecraft maneuvering using the gravitational force of the Moon. The fringe sizes (in μas) for the apogee of the above-mentioned orbit and for all RADIOASTRON wavelengths are given in Table 1.

By comparing Figs. 1, 2 and Table 1, one can see that there are non-negligible chances to observe such mirages around the black hole at the Galactic Center and in nearby AGNs and microquasars in the radio-band using RADIOASTRON facilities.

We also mention that this high resolution in radio band will be achieved also by Japanese VLBI project VERA (VLBI Exploration of Radio Astrometry), since the angular resolution aimed at will be at the 10 μas level (Sawad-Satoh 2000; Honma 2001). Therefore, the only problem left is to have a powerful enough radio source to illuminate a black hole in order to have retro-lensing images detectable by such radio VLBI telescopes as RADIOASTRON or VERA.

[1] See web-site `http://www.asc.rssi.ru/radioastron/` for more information.

[2] This project was proposed by the Astro Space Center (ASC) of Lebedev Physical Institute of the Russian Academy of Sciences (RAS) in collaboration with other institutions of RAS and RosAviaKosmos. Scientists from 20 countries are developing the scientific payload for the satellite by providing by ground-based support to the mission.

[3] The satellite orbit will have high apogee, and its rotation period around Earth will be 9.5 days, which evolves as a result of the weak gravitational perturbations from the Moon and the Sun. The perigee has been planned to be between 10^4 and 7×10^4 km and the apogee between 310 and 390 thousand kilometers. The basic orbit parameters will be the following: the orbital period is P = 9.5 days, the semi-major axis is a = 189 000 km, the eccentricity is e = 0.853, the perigee is H = 29 000 km.

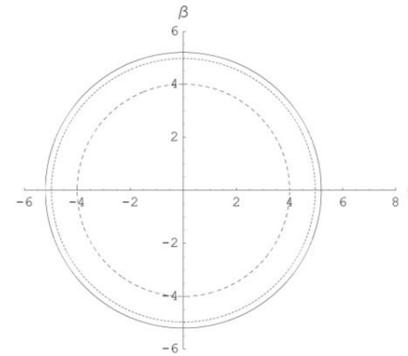

Fig. 1. Shadow (mirage) sizes are shown for selected charges of black holes Q = 0 (solid line), Q = 0.5 (short dashed line), and Q = 1 (long dashed line).

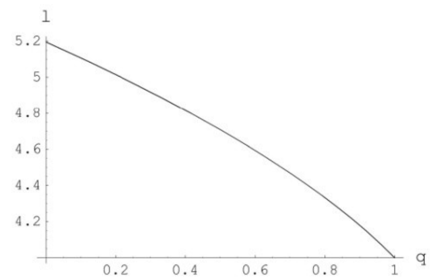

Fig. 2. The mirage radius l is shown as a function of the black hole charge q (l and q are given in units of M).

5. Searches for mirages near Sgr A^* with RADIOASTRON

Radio, near-infrared, and X-ray spectral band observations are developing very rapidly (Lo et al. 1998, 1999; Genzel et al. 2003; Ghez et al. 2004; Baganoff et al. 2001, 2003; Bower et al. 2002, 2003; Narayan 2003; Bower et al. 2004)[4], and it is known that Sgr A^* harbors the closest massive black hole with mass estimated to be 4.07×10^6 $M_\odot$ (Bower et al. 2004; Melia & Falcke 2001; Ghez et al. 2003; Schodel et al. 2003).

Following the idea of Falcke et al. (2000) and of Zakharov et al. (2005a,b,c,d) we propose to use the VLBI technique to observe mirages around massive black holes and, in particular, towards the black hole at Galactic Center. To evaluate the shadow shape Falcke et al. (2000) used the ray-tracing technique. The boundaries of the shadows are black hole mirages.

[4] An interesting idea to use radio pulsars to investigate the region nearby black hole horizon was proposed recently by Pfahl & Loeb (2003).

PHYSICAL REVIEW D **90**, 062007 (2014)

Constraints on a charge in the Reissner-Nordström metric for the black hole at the Galactic Center

Alexander F. Zakharov*

North Carolina Central University, Durham, North Carolina 27707, USA; Institute of Theoretical and Experimental Physics, Moscow 117218, Russia; Joint Institute for Nuclear Research, Dubna 141980, Russia; Institute for Computer Aided Design of RAS, 123056 Moscow, Russia; and National Research Nuclear University (NRNU MEPHI), 115409 Moscow, Russia

(Received 5 March 2013; published 9 September 2014)

Using an algebraic condition of vanishing discriminant for multiple roots of fourth-degree polynomials, we derive an analytical expression of a shadow size as a function of a charge in the Reissner-Nordström (RN) metric [1,2]. We consider shadows for negative tidal charges and charges corresponding to naked singularities $q = \mathcal{Q}^2/M^2 > 1$, where $\mathcal{Q}$ and M are black hole charge and mass, respectively, with the derived expression. An introduction of a negative tidal charge q can describe black hole solutions in theories with extra dimensions, so following the approach we consider an opportunity to extend the RN metric to negative $\mathcal{Q}^2$, while for the standard RN metric $\mathcal{Q}^2$ is always non-negative. We found that for $q > 9/8$, black hole shadows disappear. Significant tidal charges $q = -6.4$ (suggested by Bin-Nun [3–5]) are not consistent with observations of a minimal spot size at the Galactic Center observed in mm-band; moreover, these observations demonstrate that a Reissner-Nordström black hole with a significant charge $q \approx 1$ provides a better fit of recent observational data for the black hole at the Galactic Center in comparison with the Schwarzschild black hole.

DOI: 10.1103/PhysRevD.90.062007 PACS numbers: 04.80.Cc, 04.20.-q, 04.50.Gh, 04.70.Bw

I. INTRODUCTION

Soon after the discovery of general relativity (GR), the first solutions corresponding to spherical symmetric black holes were found [1,2,6]; however, initially people were rather sceptical about possible astronomical applications of the solutions corresponding to black holes [7] (see also, for instance, one of the first textbooks on GR [8]). Even after an introduction to the black hole concept by Wheeler [9] (he used the term in his public lecture in 1967 [10]), we did not know too many examples where we really need GR models with strong gravitational fields that arise near black hole horizons to explain observational data. The cases where we need strong field approximation are very important since they give an opportunity to check GR predictions in a strong field limit; therefore, one could significantly constrain alternative theories of gravity.

One of the most important options to test gravity in the strong field approximation is analysis of relativistic line shape as it was shown in [11], with assumptions that a line emission is originated at a circular ring area of a flat accretion disk. Later on, such signatures of the Fe $K\alpha$ line have been found in the active galaxy MCG-6-30-15 [12]. Analyzing the spectral line shape, the authors concluded the emission region is so close to the black hole horizon that one has to use Kerr metric approximation [13] to fit observational data [12]. Results of simulations of iron $K\alpha$ line formation are given in [14,15] (where we used our approach [16]); see also [17] for a more recent review of the subject.

Now there are two basic observational techniques to investigate a gravitational potential at the Galactic Center, namely, (a) monitoring the orbits of bright stars near the Galactic Center to reconstruct a gravitational potential [18] (see also a discussion about an opportunity to evaluate black hole dark matter parameters in [19] and an opportunity to constrain some class of an alternative theory of gravity [20]) and (b) measuring in mm band, with VLBI technique, the size and shape of shadows around the black hole, giving an alternative possibility to evaluate black hole parameters. The formation of retro-lensing images (also known as mirages, shadows, or "faces" in the literature) due to the strong gravitational field effects nearby black holes has been investigated by several authors [21–24].

Theories with extra dimensions admit astrophysical objects (supermassive black holes in particular) which are rather different from standard ones. Tests have been proposed when it would be possible to discover signatures of extra dimensions in supermassive black holes since the gravitational field may be different from the standard one in the GR approach. So, gravitational lensing features are different for alternative gravity theories with extra dimensions and general relativity.

Recently, Bin-Nun [3–5] discussed the possibility that the black hole at the Galactic Center is described by the tidal Reissner-Nordström metric which may be admitted by the Randall-Sundrum II braneworld scenario [25]. Bin-Nun suggested an opportunity of evaluating the black hole

*zakharov@itep.ru

$$\mathrm{Dis}(s_1,s_2,s_3,s_4)=\begin{vmatrix}1&1&1&1\\X_1&X_2&X_3&X_4\\X_1^2&X_2^2&X_3^2&X_4^2\\X_1^3&X_2^3&X_3^3&X_4^3\end{vmatrix}^2=\begin{vmatrix}4&p_1&p_2&p_3\\p_1&p_2&p_3&p_4\\p_2&p_3&p_4&p_5\\p_3&p_4&p_5&p_6\end{vmatrix}. \quad (20)$$

Expressing the polynomials $p_k (1 \le k \le 6)$ in terms of the polynomials $s_k (1 \le k \le 4)$ and using Newton's equations we calculate the polynomials and discriminant of the family X_1, X_2, X_3, X_4 in roots of the polynomial $R(r)$; we obtain

$$p_1 = s_1 = 0, \quad p_2 = -2s_2, \quad p_3 = 3s_3,$$
$$p_4 = 2s_2^2 - 4s_4, \quad p_5 = -5s_3s_2,$$
$$p_6 = -2s_2^3 + 3s_3^2 + 6s_4s_2, \quad (21)$$

where $s_1 = 0, s_2 = -l, s_3 = -2l, s_4 = -ql$, corresponding to the polynomial $R(r)$ in Eq. (8). The discriminant Dis of the polynomial $R(r)$ has the form

$$\mathrm{Dis}(s_1,s_2,s_3,s_4)=\begin{vmatrix}4&0&2l&-6l\\0&2l&-6l&2l(l+2q)\\2l&-6l&2l(l+2q)&-10l^2\\-6l&2l(l+2q)&-10l^2&2l^2(l+6+3q)\end{vmatrix}$$
$$= 16l^3[l^2(1-q) + l(-8q^2 + 36q - 27) - 16q^3]. \quad (22)$$

The polynomial $R(r)$ thus has a multiple root if and only if

$$l^3[l^2(1-q) + l(-8q^2 + 36q - 27) - 16q^3] = 0. \quad (23)$$

Excluding the case $l = 0$, which corresponds to a multiple root at $r = 0$, we find that the polynomial $R(r)$ has a multiple root for $r \ge r_+$ if and only if

$$l^2(1-q) + l(-8q^2 + 36q - 27) - 16q^3 = 0. \quad (24)$$

If $q = 0$, we obtain the well-known result for a Schwarzschild black hole [38,39,49], $l_{cr} = 27$, or $\xi_{cr} = 3\sqrt{3}$ [where l_{cr} is the positive root of Eq. (24)]. If $q = 1$, then $l = 16$, or $\xi_{cr} = 4$, which also corresponds to numerical results given in paper [50]. The photon capture cross section for an extreme charged black hole turns out to be considerably smaller than the capture cross section of a Schwarzschild black hole. The critical value of the impact parameter, characterizing the capture cross section for a RN black hole, is determined by the equation

$$l_{cr} = \frac{(8q^2 - 36q + 27) + \sqrt{D_1}}{2(1-q)}, \quad (25)$$

where $D_1 = (8q^2 - 36q + 27)^2 + 64q^3(1-q) = -512(q - \frac{9}{8})^3$. It is clear from the last relation that there are circular unstable photon orbits only for $q \le \frac{9}{8}$ (see also results in [37] about the same critical value). Substituting Eq. (25) into the expression for the coefficients of the polynomial $R(r)$ it is easy to calculate the radius of the unstable circular photon orbit (which is the same as the minimum periastron distance). The orbit of a photon moving from infinity with the critical impact parameter, determined in accordance with Eq. (25) spirals into circular orbit. To find a radius of photon unstable orbit we will solve Eq. (7) substituting l_{cr} in the relation. From trigonometric formula for roots of cubic equation we have

$$r_{crit} = 2\sqrt{\frac{l_{cr}}{6}}\cos\frac{\alpha}{3}, \quad (26)$$

where

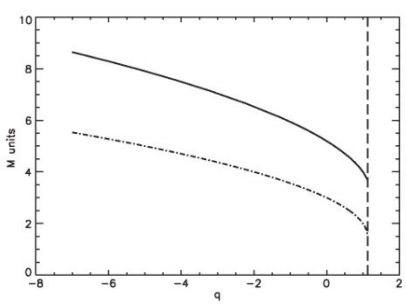

FIG. 1. Shadow (mirage) radius (solid line) and radius of the last circular unstable photon orbit (dot-dashed line) in M units as a function of q. The critical value $q = 9/8$ is shown with dashed vertical line.

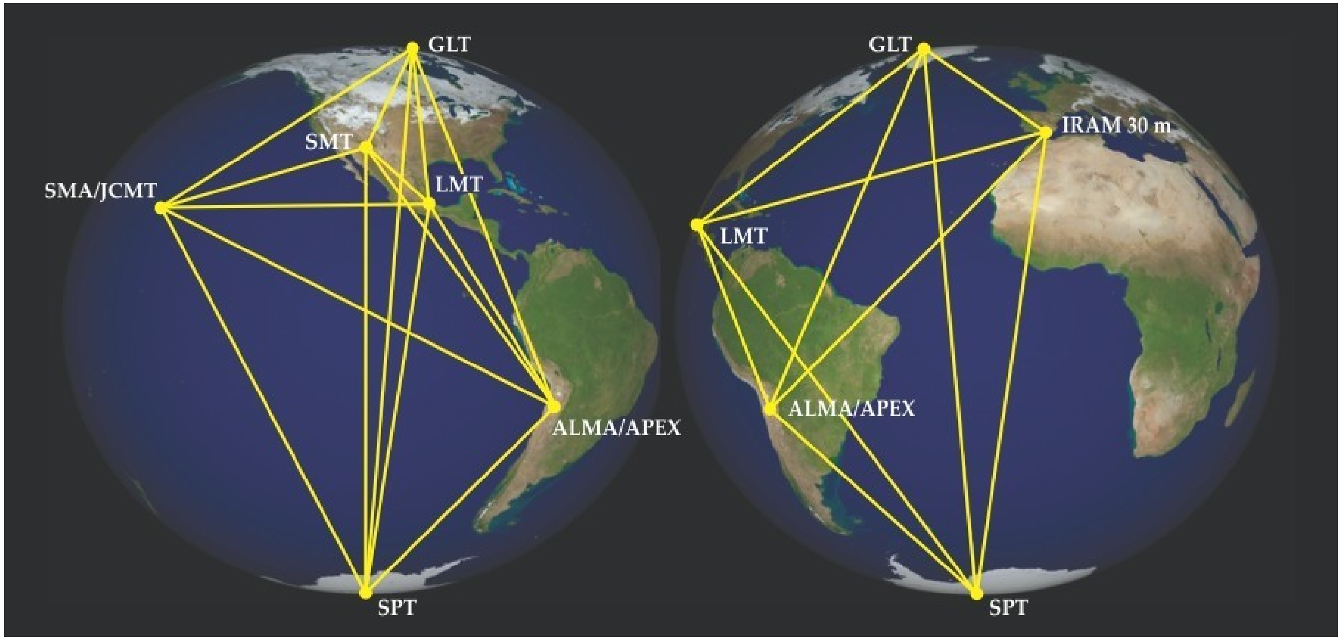

Figure 2. ***The Event Horizon Telescope*** *is a global array of millimeter telescopes (see http://eventhorizontelescope.org/array) that aims to take the first pictures of black holes. (Courtesy of Dan Marrone/University of Arizona.)*

Published in: Dimitrios Psaltis; Feryal Özel; *Physics Today* **2018,** 71, 70-71.

DOI: 10.1063/PT.3.3906

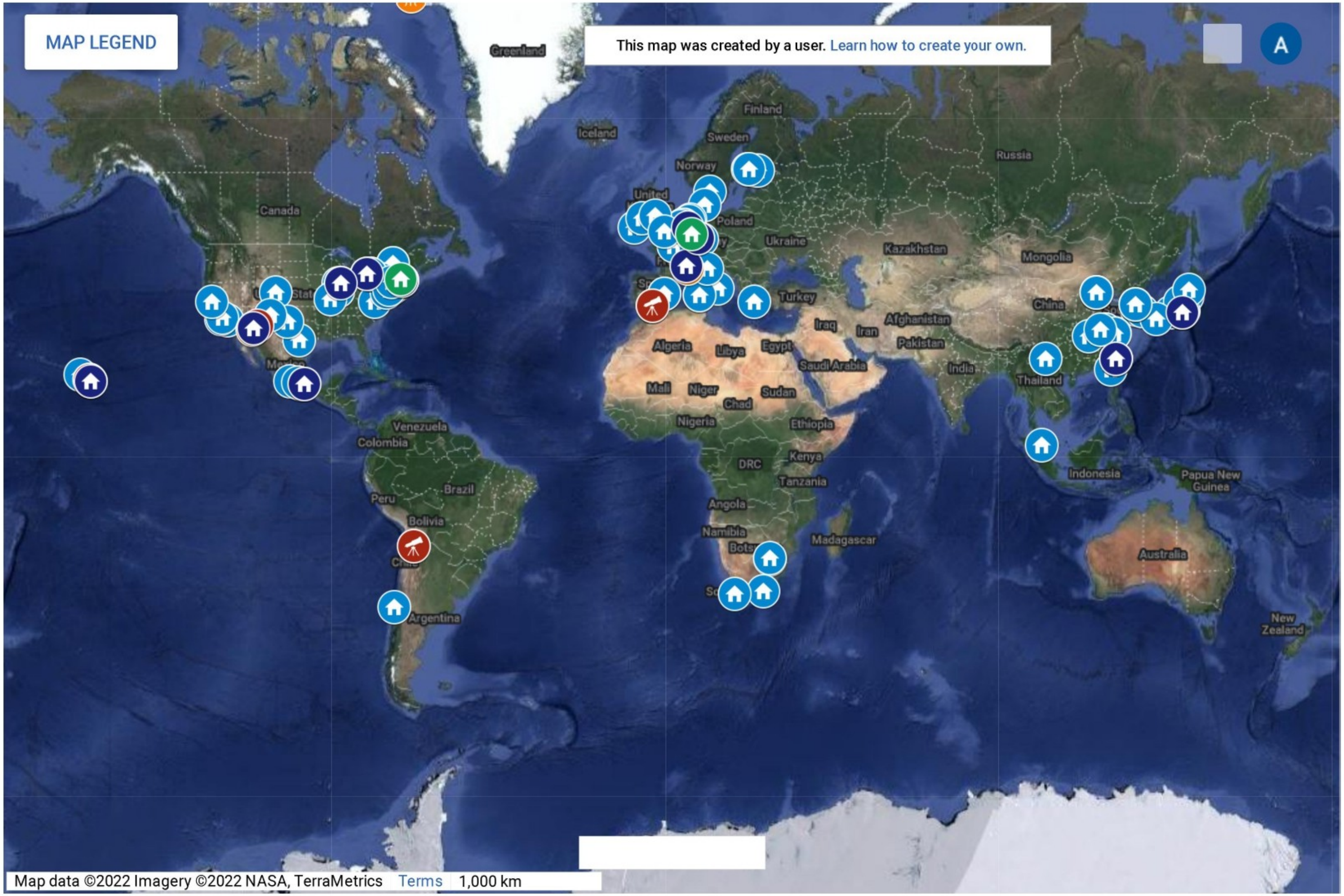
MAP LEGEND
This map was created by a user. Learn how to create your own.
A
Greenland
Iceland
Finland
Sweden
Norway
Russia
Canada
Poland
Ukraine
Kazakhstan
Mongolia
Turkey
China
Iraq
Iran
Afghanistan
Pakistan
Algeria
Libya
Egypt
Saudi Arabia
India
Thailand
Mali
Niger
Sudan
Chad
Nigeria
Ethiopia
Venezuela
Colombia
DRC
Kenya
Tanzania
Indonesia
Papua New Guinea
Brazil
Peru
Bolivia
Angola
Namibia
Madagascar
Australia
Argentina
New Zealand
Map data ©2022 Imagery ©2022 NASA, TerraMetrics Terms 1,000 km

EHT team: “Similarly, for the EHT, the data we take only tells us only a piece of the story, as there are an infinite number of possible images that are perfectly consistent with the data we measure. But not all images are created equal— some look more like what we think of as images than others. To chose the best image, we essentially take all of the infinite images that explain our telescope measurements, and rank them by how reasonable they look. We then choose the image (or set of images) that looks most reasonable. “

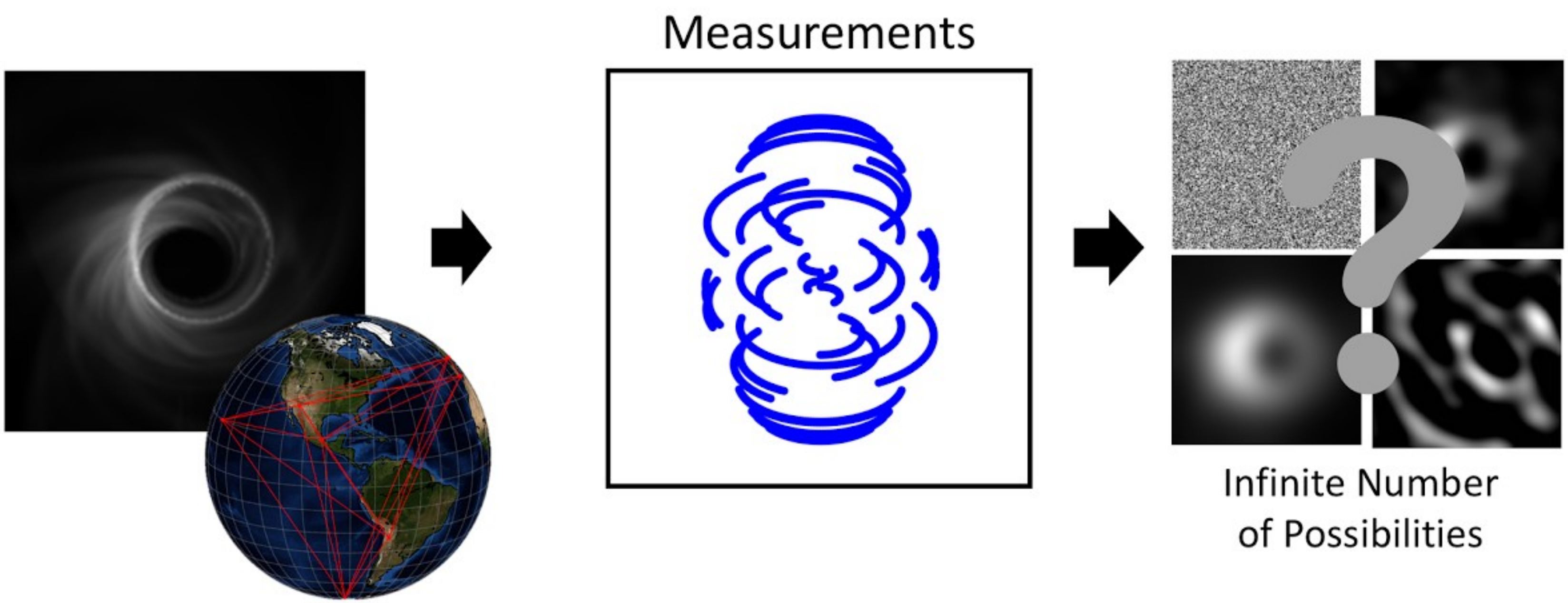

Constraints on black-hole charges with the 2017 EHT observations of M87*

Prashant Kocherlakota,[1] Luciano Rezzolla,[1–3] Heino Falcke,[4] Christian M. Fromm,[5,6,1] Michael Kramer,[7] Yosuke Mizuno,[8,9] Antonios Nathanail,[9,10] Héctor Olivares,[4] Ziri Younsi,[11,9] Kazunori Akiyama,[12,13,5] Antxon Alberdi,[14] Walter Alef,[7] Juan Carlos Algaba,[15] Richard Anantua,[5,6,16] Keiichi Asada,[17] Rebecca Azulay,[18,19,7] Anne-Kathrin Baczko,[7] David Ball,[20] Mislav Baloković,[5,6] John Barrett,[12] Bradford A. Benson,[21,22] Dan Bintley,[23] Lindy Blackburn,[5,6] Raymond Blundell,[6] Wilfred Boland,[24] Katherine L. Bouman,[5,6,25] Geoffrey C. Bower,[26] Hope Boyce,[27,28] Michael Bremer,[29] Christiaan D. Brinkerink,[4] Roger Brissenden,[5,6] Silke Britzen,[7] Avery E. Broderick,[30–32] Dominique Broguiere,[29] Thomas Bronzwaer,[4] Do-Young Byun,[33,34] John E. Carlstrom,[35,22,36,37] Andrew Chael,[38,39] Chi-kwan Chan,[20,40] Shami Chatterjee,[41] Koushik Chatterjee,[42] Ming-Tang Chen,[26] Yongjun Chen (陈永军),[43,44] Paul M. Chesler,[5] Ilje Cho,[33,34] Pierre Christian,[45] John E. Conway,[46] James M. Cordes,[41] Thomas M. Crawford,[22,35] Geoffrey B. Crew,[12] Alejandro Cruz-Osorio,[9] Yuzhu Cui,[47,48] Jordy Davelaar,[49,16,4] Mariafelicia De Laurentis,[50,9,51] Roger Deane,[52–54] Jessica Dempsey,[23] Gregory Desvignes,[55] Sheperd S. Doeleman,[5,6] Ralph P. Eatough,[56,7] Joseph Farah,[6,5,57] Vincent L. Fish,[12] Ed Fomalont,[58] Raquel Fraga-Encinas,[4] Per Friberg,[23] H. Alyson Ford,[59] Antonio Fuentes,[14] Peter Galison,[5,60,61] Charles F. Gammie,[62,63] Roberto García,[29] Olivier Gentaz,[29] Boris Georgiev,[31,32] Ciriaco Goddi,[4,64] Roman Gold,[65,30] José L. Gómez,[14] Arturo I. Gómez-Ruiz,[66,67] Minfeng Gu (顾敏峰),[43,68] Mark Gurwell,[6] Kazuhiro Hada,[47,48] Daryl Haggard,[27,28] Michael H. Hecht,[12] Ronald Hesper,[69] Luis C. Ho (何子山),[70,71] Paul Ho,[17] Mareki Honma,[47,48,72] Chih-Wei L. Huang,[17] Lei Huang (黄磊),[43,68] David H. Hughes,[66] Shiro Ikeda,[13,73–75] Makoto Inoue,[17] Sara Issaoun,[4] David J. James,[5,6] Buell T. Jannuzi,[20] Michael Janssen,[7] Britton Jeter,[31,32] Wu Jiang (江悟),[43] Alejandra Jimenez-Rosales,[4] Michael D. Johnson,[5,6] Svetlana Jorstad,[76,77] Taehyun Jung,[33,34] Mansour Karami,[30,31] Ramesh Karuppusamy,[7] Tomohisa Kawashima,[78] Garrett K. Keating,[6] Mark Kettenis,[79] Dong-Jin Kim,[7] Jae-Young Kim,[33,7] Jongsoo Kim,[33] Junhan Kim,[20,25] Motoki Kino,[13,80] Jun Yi Koay,[17] Yutaro Kofuji,[47,72] Patrick M. Koch,[17] Shoko Koyama,[17] Carsten Kramer,[29] Thomas P. Krichbaum,[7] Cheng-Yu Kuo,[81,17] Tod R. Lauer,[82] Sang-Sung Lee,[33] Aviad Levis,[25] Yan-Rong Li (李彦荣),[83] Zhiyuan Li (李志远),[84,85] Michael Lindqvist,[46] Rocco Lico,[14,7] Greg Lindahl,[6] Jun Liu (刘俊),[7] Kuo Liu,[7] Elisabetta Liuzzo,[86] Wen-Ping Lo,[17,87] Andrei P. Lobanov,[7] Laurent Loinard,[88,89] Colin Lonsdale,[12] Ru-Sen Lu (路如森),[43,44,7] Nicholas R. MacDonald,[7] Jirong Mao (毛基荣),[90–92] Nicola Marchili,[86,7] Sera Markoff,[42,93] Daniel P. Marrone,[20] Alan P. Marscher,[76] Iván Martí-Vidal,[18,19] Satoki Matsushita,[17] Lynn D. Matthews,[12] Lia Medeiros,[94,20] Karl M. Menten,[7] Izumi Mizuno,[23] James M. Moran,[5,6] Kotaro Moriyama,[12,47] Monika Moscibrodzka,[4] Cornelia Müller,[7,4] Gibwa Musoke,[42,4] Alejandro Mus Mejías,[18,19] Hiroshi Nagai,[13,48] Neil M. Nagar,[95] Masanori Nakamura,[96,17] Ramesh Narayan,[5,6] Gopal Narayanan,[97] Iniyan Natarajan,[54,52,98] Joseph Neilsen,[99] Roberto Neri,[29] Chunchong Ni,[31,32] Aristeidis Noutsos,[7] Michael A. Nowak,[100] Hiroki Okino,[47,72] Gisela N. Ortiz-León,[7] Tomoaki Oyama,[47] Feryal Özel,[20] Daniel C. M. Palumbo,[5,6] Jongho Park,[17] Nimesh Patel,[6] Ue-Li Pen,[30,101–103] Dominic W. Pesce,[5,6] Vincent Piétu,[29] Richard Plambeck,[104] Aleksandar PopStefanija,[97] Oliver Porth,[42,9] Felix M. Pötzl,[7] Ben Prather,[62] Jorge A. Preciado-López,[30] Dimitrios Psaltis,[20] Hung-Yi Pu,[105,17,30] Venkatessh Ramakrishnan,[95] Ramprasad Rao,[26] Mark G. Rawlings,[23] Alexander W. Raymond,[5,6] Angelo Ricarte,[5,6] Bart Ripperda,[106,16] Freek Roelofs,[4] Alan Rogers,[12] Eduardo Ros,[7] Mel Rose,[20] Arash Roshanineshat,[20] Helge Rottmann,[7] Alan L. Roy,[7] Chet Ruszczyk,[12] Kazi L. J. Rygl,[86] Salvador Sánchez,[107] David Sánchez-Arguelles,[66,67] Mahito Sasada,[47,108] Tuomas Savolainen,[109,110,7] F. Peter Schloerb,[97] Karl-Friedrich Schuster,[29] Lijing Shao,[7,71] Zhiqiang Shen (沈志强),[43,44] Des Small,[79] Bong Won Sohn,[33,34,111] Jason SooHoo,[12] He Sun (孙赫),[25] Fumie Tazaki,[47] Alexandra J. Tetarenko,[112] Paul Tiede,[31,32] Remo P. J. Tilanus,[4,64,113,20] Michael Titus,[12] Kenji Toma,[114,115] Pablo Torne,[7,107] Tyler Trent,[20] Efthalia Traianou,[7] Sascha Trippe,[116] Ilse van Bemmel,[79] Huib Jan van Langevelde,[79,117] Daniel R. van Rossum,[4] Jan Wagner,[7] Derek Ward-Thompson,[118] John Wardle,[119] Jonathan Weintroub,[5,6] Norbert Wex,[7] Robert Wharton,[7] Maciek Wielgus,[5,6] George N. Wong,[62] Qingwen Wu (吴庆文),[120] Doosoo Yoon,[42] André Young,[4] Ken Young,[6] Feng Yuan (袁峰),[43,68,121] Ye-Fei Yuan (袁业飞),[122] J. Anton Zensus,[7] Guang-Yao Zhao,[14] and Shan-Shan Zhao[43]

(EHT Collaboration)

[1]*Institut für Theoretische Physik, Goethe-Universität, Max-von-Laue-Strasse 1, 60438 Frankfurt, Germany*
[2]*Frankfurt Institute for Advanced Studies, Ruth-Moufang-Strasse 1, 60438 Frankfurt, Germany*
[3]*School of Mathematics, Trinity College, Dublin 2, Ireland*
[4]*Department of Astrophysics, Institute for Mathematics, Astrophysics and Particle Physics (IMAPP), Radboud University, P.O. Box 9010, 6500 GL Nijmegen, Netherlands*
[5]*Black Hole Initiative at Harvard University, 20 Garden Street, Cambridge, Massachusetts 02138, USA*

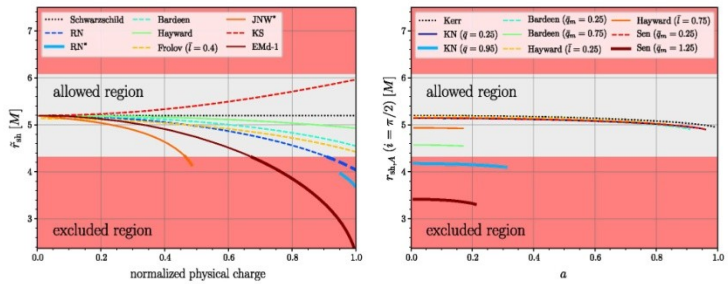

FIG. 2. Left: shadow radii $\tilde{r}_{sh}$ for various spherically symmetric black-hole solutions, as well as for the JNW and RN naked singularities (marked with an asterisk), as a function of the physical charge normalized to its maximum value. The gray/red shaded regions refer to the areas that are 1-σ consistent/inconsistent with the 2017 EHT observations and highlight that the latter set constraints on the physical charges (see also Fig. 3 for the EMd-2 black hole). Right: shadow areal radii $r_{sh,A}$ as a function of the dimensionless spin a for four families of black-hole solutions when viewed on the equatorial plane ($i = \pi/2$). Also in this case, the observations restrict the ranges of the physical charges of the Kerr-Newman and the Sen black holes (see also Fig. 3).

independent charges—can also produce shadow radii that are incompatible with the EHT observations; we will discuss this further below. The two EMd black-hole solutions (1 and 2) correspond to fundamentally different field contents, as discussed in [70].

We report in the right panel of Fig. 2 the shadow areal radius $r_{sh,A}$ for a number of stationary black holes, such as Kerr [72], Kerr-Newman (KN) [73], Sen [74], and the rotating versions of the Bardeen and Hayward black holes [75]. The data refers to an observer inclination angle of $i = \pi/2$, and we find that the variation in the shadow size with spin at higher inclinations (of up to $i = \pi/100$) is at most about 7.1% (for $i = \pi/2$, this is 5%); of course, at zero-spin the shadow size does not change with inclination. The shadow areal radii are shown as a function of the dimensionless spin of the black hole $a \coloneqq J/M^2$, where J is its angular momentum, and for representative values of the additional parameters that characterize the solutions. Note that—similar to the angular momentum for a Kerr black hole—the role of an electric charge or the presence of a de Sitter core (as in the case of the Hayward black holes) is to reduce the apparent size of the shadow. Furthermore, on increasing the spin parameter, we recover the typical trend that the shadow becomes increasingly noncircular, as encoded, e.g., in the distortion parameter δ_{sh} defined in [57,83] (see Appendix). Also in this case, while the regular rotating Bardeen and Hayward solutions are compatible with the present constraints set by the 2017 EHT observations, the Kerr-Newman and Sen families of black holes can produce shadow areal radii that lie outside of the 1-σ region allowed by the observations.

To further explore the constraints on the excluded regions for the Einstein-Maxwell-dilaton 2 and the Sen black holes, we report in Fig. 3 the relevant ranges for these two solutions. The Einstein-Maxwell-dilaton 2 black holes are nonrotating but have two physical charges expressed by the coefficients $0 < \bar{q}_e < \sqrt{2}$ and $0 < \bar{q}_m < \sqrt{2}$, while the Sen black holes spin (a) and have an additional electromagnetic charge $\bar{q}_m$. Also in this case, the gray/red shaded regions refer to the areas that are consistent/inconsistent with the 2017 EHT observations. The figure shows rather easily that for these two black-hole families there are large

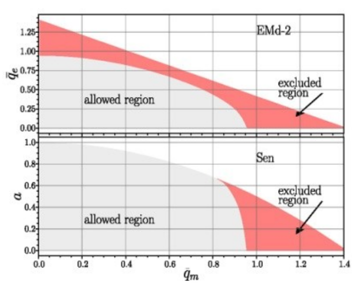

FIG. 3. Constraints set by the 2017 EHT observations on the nonrotating Einstein-Maxwell-dilaton 2 and on the rotating Sen black holes. Also in this case, the gray/red shaded regions refer to the areas that are 1-σ consistent/inconsistent with the 2017 EHT observations).

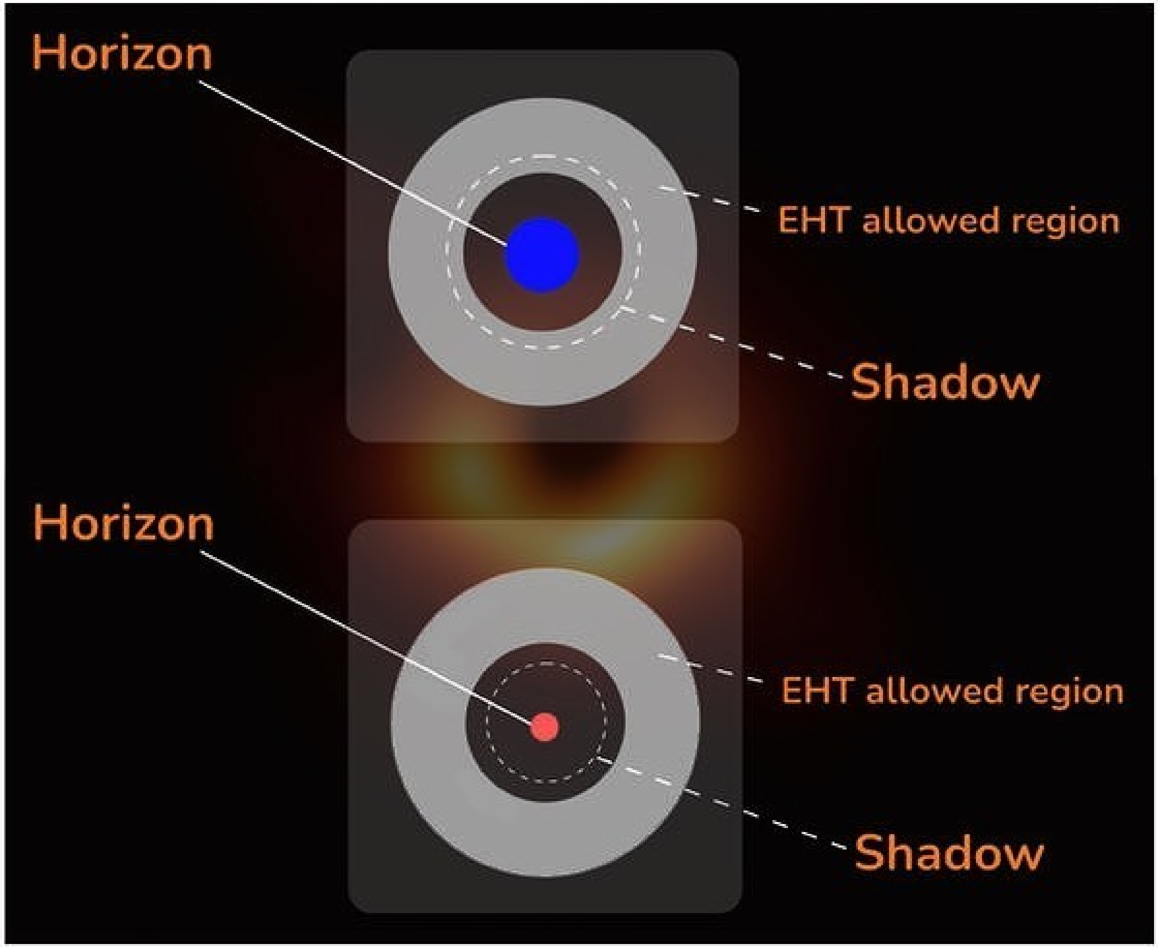
Horizon
EHT allowed region
Shadow
Horizon
EHT allowed region
Shadow

Zakharov, Universe, 2022; arxiv:2108.01533; charge constraint on M87* (for Sgr A* D=51.8±2.3 uas, 12.05.2022). For M87 D=D_Sch (1±0.17)

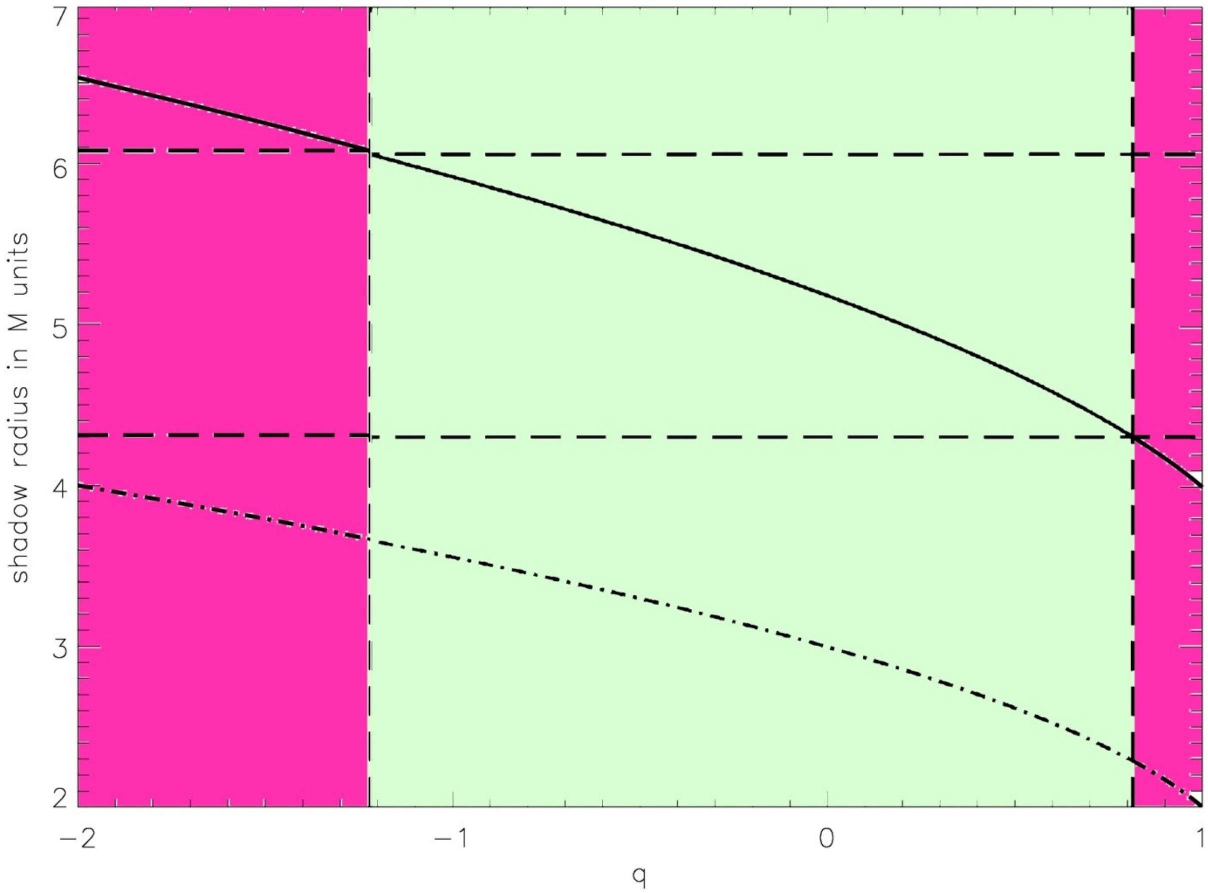

Sgr A* shadow discovery by EHT (reported on May 12, 2022)
Press Conferences around the world (Video Recordings):

Garching, Germany - European Southern Observatory
Madrid, Spain - Consejo Superior de Investigaciones Científicas
México D.F., Mexico - Consejo Nacional de Ciencia y Tecnología
Rome, Italy - Istituto Nazionale di Astrofisica
Santiago de Chile - ALMA Observatory
Washington D.C., USA - National Science Foundation
Tokyo, Japan - National Astronomical Observatory of Japan

For Sgr A* D=51.8±2.3 uas, (EHT collaboration, 12.05.2022)

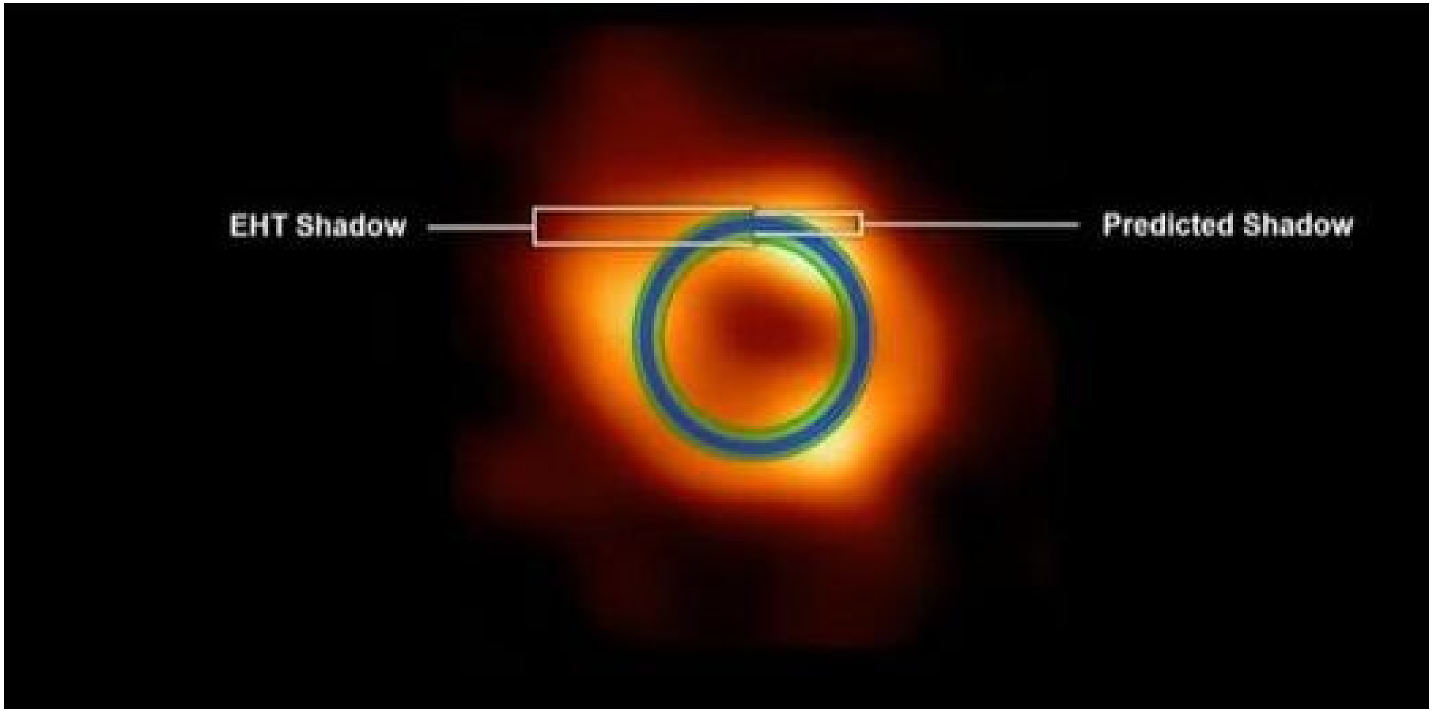

A. F. Zakharov, Physics of Particle and Nuclei Lett. (2023)

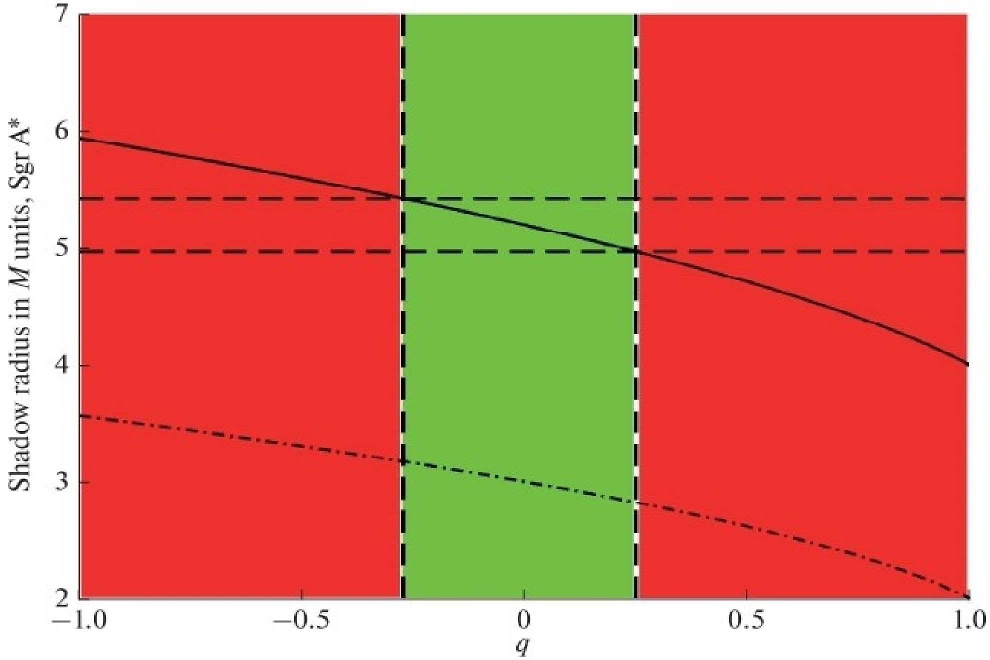

Fig. 1. Shadow radius (solid curve) and radius of the last circular unstable photon orbit (dashed-and-dotted curve) in units M as a function q. Following work [30], we believe that $\theta_{\rm sh\ SgrA^*} \approx (51.8 \pm 2.3)$ μas at a confidence level of 68%. The horizontal dashed lines correspond to the restrictions on the size of the radius in units M. Accordingly, red vertical stripes for q are inconsistent with these estimates of the size of the shadow in the HC.

Circular photon orbits = Shadow existence

ISSN 1547-4771, Physics of Particles and Nuclei Letters, 2025, Vol. 22, No. 3, pp. 568–575. © Pleiades Publishing, Ltd., 2025.
Russian Text © The Author(s), 2025, published in Pis'ma v Zhurnal Fizika Elementarnykh Chastits i Atomnogo Yadra, 2025.

PHYSICS OF ELEMENTARY PARTICLES AND ATOMIC NUCLEI. THEORY

Shadows and Circular Photon Orbits: Consideration of Some Cases of Generalizations of Kerr–Newman Black Holes

A. F. Zakharov[a, b, *]

[a] *National Research Center "Kurchatov Institute," Moscow, 123182 Russia*
[b] *Bogoliubov Laboratory of Theoretical Physics, Joint Institute for Nuclear Research, Moscow oblast, Dubna, 141980 Russia*
**e-mail: alex.fed.zakharov@gmail.com*

Received October 16, 2024; revised November 25, 2024; accepted December 2, 2024

Abstract—In our paper published in 2005, it was predicted that the shadow near the Galactic Center (GC) black hole could be reconstructed from results of observations of the global VLBI system operating in the millimeter or submillimeter range. This prediction became reality in 2022, when shadows near black holes in the GC and the center of the galaxy M87 (in 2019) were reconstructed from data of observations of the Event Horizon Telescope collaboration, and these results led to the appearance of a large number of theoretical papers that considered constraints on both alternative models of galactic centers and alternative theories of gravity. For Schwarzschild, Kerr, and Reissner–Nordström black holes, the impact parameters corresponding to circular photon orbits determine the shadow shape and size; however, as was shown in the abovementioned paper, in the cases of some metrics, the existence of circular photon orbits is possible, though shadows for these metrics are not formed. A number of recent papers (including one published in the journal *PEPAN Letters*) have put forth, without evidence, alternative models of galactic centers in which parameters corresponding to circular photon orbits determine the shadow shape and size.

DOI: 10.1134/S1547477125700177

1. INTRODUCTION

General Relativity (GR), proposed in 1915 by Einstein, is still the best theory of gravity, notwithstanding the many alternative theories that have been considered (many of which were proposed recently). Initially, the GR predictions were tested in a weak gravitational field limit, but recently it has become possible to test GR in strong gravitational fields. A detailed discussion of the experimental testing of GR effects in the vicinity of astrophysical black holes is given in [1].

In 1973, James Bardeen discussed a thought experiment in which it is assumed that there is a luminous screen behind the black hole [2]. In this case, the observer would see a small dark spot (shadow) against the background of the screen. For a long time, this model had no application to astrophysical black holes, since there is no bright screen behind the black hole in astronomy, and also for a long time, the stellar-mass black holes in our Galaxy were predominantly considered, for which the shadow size is about a million times smaller than the size of the shadow in the Galac-

20 years ago and found to be quite accurate, the authors of [3] predicted the possibility of reconstructing the shadow in the GC using a ground-based or Earth–space interferometer operating in the millimeter or submillimeter range (in this work, the capabilities of the Millimetron interferometer were also mentioned for the first time for solving such problems). This prediction, made in [3], came true in May 2022, when the Event Horizon Telescope (EHT) collaboration presented the results of the reconstruction of a shadow of our GC (the shadow of supermassive black hole in M87 was reconstructed in 2019). The prediction of the possibility of detecting a shadow in the GC is well known in the world, so, in a recent work by famous Indian and Japanese experts for the theory of gravity [4], it is noted that the idea of reconstructing a shadow of a black hole in the center of Galaxy using global interferometers operating in the millimeter wavelength range was originally put forward in [3].These reconstructions were based on EHT observations conducted in 2017; thus, the analysis of obser-

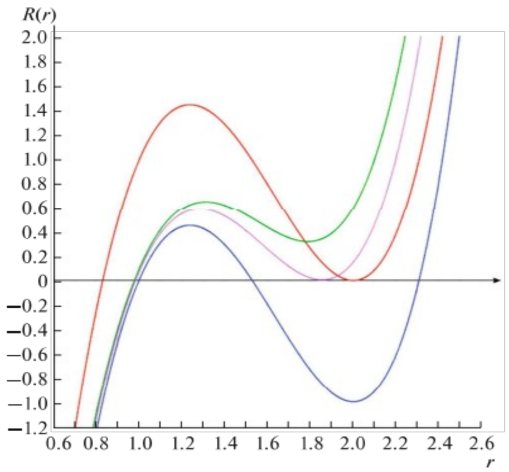

Fig. 3. The red curve corresponds to the case of the extremal Reissner–Nordström metric ($q = 1$) and the limiting value of the impact parameter $\xi = 16$ ($L = 4$). The light purple curve corresponds to the superextreme Reissner–Nordström metric ($q = 1.0625$) and the critical value of the impact parameter corresponding to the unstable circular photon orbit $\xi = 14.922$. The blue curve corresponds to the superextreme Reissner–Nordström metric ($q = 1.0625$) and to the value of the impact parameter greater than the critical value of the impact parameter $\xi = 16$. The green curve corresponds to the superextreme Reissner–Nordström metric ($q = 1.0625$) and to the value of the impact parameter smaller than the critical value of the impact parameter $\xi = 14.5$.

6. EXAMPLE OF CIRCULAR PHOTON ORBITS IN THE ABSENCE OF SHADOWS FOR NAKED REISSNER–NORDSTRÖM SINGULARITIES

Thus, it can be noted that, at spin values $q \leq 1$, black holes have shadows, while for $1 < q \leq 9/8$ there are no shadows, but there are circular photon orbits, and at $q > 9/8$ there are neither circular photon orbits nor shadows. Thus, there is a structural instability in the sense discussed in the works of Poincaré–Pontryagin–Andronov–Anosov and other authors. The need to study structural stability has been noted, e.g., by R. Thom and V.I. Arnold in many of their works (see [29–32] and references therein). In the case of discussing the presence of shadows of the Reissner–Nordström black hole, there is a structural instability in the vicinity of the value $q = 1$, since with any small change in the parameters, the properties of the system change qualitatively (in our case, this is the availability of shadows near black holes), because at values of the limiting charge $q = 1 - \epsilon$ there are shadows, while at $q = 1 + \epsilon$ shadows disappear; i.e., the shadows disappear at supercritical charge values, as does the Reissner–Nordstrom black hole horizon.

The right-hand side of Eq. (22) is shown for some values of parameters in Fig. 3. Namely, the red curve describes the case of the extremal Reissner–Nordström metric ($q = 1$) and the limiting value of a square of the impact parameter $\xi = 16$) ($L = 4$) (in this case, a photon, moving from infinity to the naked singularity, asymptotically approaches the limiting circular photon orbit); the magenta curve corresponds to the superextremal Reissner–Nordström metric ($q = 1.0625$) and the critical value of a square of the impact parameter corresponding to an unstable circular photon orbit $\xi = 14.922$ (in this case, a photon, moving from infinity to the naked singularity, asymptotically approaches the limiting circular photon orbit); the blue curve corresponds to the superextremal Reissner–Nordström metric ($q = 1.0625$) and the value of a square of the impact parameter greater than the critical value of the impact parameter $\xi = 16$ (in this case, after approaching the naked singularity, a photon moves away from it, and, as can be seen from the figure, the turning point is approximately at $r \approx 2.3$); the green curve corresponds to the superextreme Reissner–Nordström metric ($q = 1.0625$) and to a value of the impact parameter smaller than the critical value of a square of the impact parameter (in this case, after approaching the naked singularity, the photon moves away from it, and, as can be seen from the figure, the turning point is approximately at $r \approx 1$); thus, no shadow is formed for the superextreme Reissner–Nordström metric ($q = 1.0625$) (as well as for other values of the parameter $1 < q < 9/8$). For $q > 1$ in the vicinity of the naked singularity, there are neither circular photon orbits nor shadows.

However, the above example does not allow us to assert that black holes have shadows, while naked singularities do not have them, since the authors of [33] showed that there may be shadows in the vicinity of naked singularities.

CONCLUSIONS

Following J. Wheeler and S. Chandrasekhar, it seems natural to consider that the most general solution of the black-hole type for astrophysical applications is determined by the Kerr–Newman metric, while their various generalizations or alternatives, at least for now, are mainly of importance for theoretical research and will take unlikely a dominant position for interpretation of observational data in the near future. As noted earlier for the Schwarzschild, Kerr, and Reissner–Nordström black holes, the impact parameters corresponding to circular photon orbits indeed separate the regions of photon capture and their scat-

ISSN 1063-7788, Physics of Atomic Nuclei, 2025, Vol. 88, No. 1, pp. 154–170.

Galactic Center Shadows: Beyond the Standard Model

A. F. Zakharov[1),2)*]

Received December 5, 2024; revised December 5, 2024; accepted December 24, 2024

Abstract—In 2005 Zakharov et al. predicted an opportunity to reconstruct a shadow in Sgr A* with ground based or space—ground interferometer acting in mm or sub-mm band (the Millimetron was mentioned for such needs). The prediction was confirmed in May 2022 since the Event Horizon Telescope (EHT) Collaboration presented results of a shadow reconstruction for our Galactic Center (the shadow around the supermassive black hole in M87 was reconstructed in 2019). These reconstructions were based on EHT observations done in 2017. In 2005 Zakharov et al. also derived analytical expressions for shadow size as a function of charge for Reissner–Nordström metric and later these results were generalized for a tidal charge case. We discuss opportunities to evaluate parameters of alternative theories of gravity with shadow size estimates done by the EHT Collaboration, in particular, a tidal charge could be estimated from these observations. We also discuss opportunities to use Millimetron facilities for shadow reconstructions in M87* and Sgr A*. In our recent studies we discuss shadow formations for cases where naked singularities, wormholes or more exotic models substitute conventional black holes in galactic centers.

DOI: 10.1134/S106377882570019X

1. INTRODUCTION. ON SHOULDERS OF GIANTS

One of the most famous theorists Steven Weinberg wrote several years ago [1]: "I am a physicist, not a historian, but over the years I have become increasingly fascinated by the history of science. It is an extraordinary story, one of the most interesting in human history. It is also a story in which scientists like myself have a personal stake. Today's research can be aided and illuminated by a knowledge of its past, and for some scientists knowledge of the history of science helps to motivate present work. We hope that our research may turn out to be a part, however small, of the grand historical tradition of natural science." I believe that these sentences reflect feelings of many other researchers even in the cases if they are not so famous and they are not authors of the Standard Model.

Very often it is very hard to recognize the author name when we mention a theorem, definition or principle. As a well-known example is the following one. People mention Columbus who discovered America but it is not named Columbia. Famous Russian mathematician V.I. Arnold formulated a principle which was generalized by M. Berry and as a result Arnold noted [2] that "Prof. M. Berry once formulated the following two principles: The Arnold Principle: If a notion bears a personal name, then this name is not the name of the discoverer. The Berry Principle: The Arnold Principle is applicable to itself."

Currently the phrase "on the shoulders of giants" is associated with the book which is a compilation of works edited and with commentary by Stephen Hawking [3]; however, more often people reminded the following letter of I. Newton to R. Hooke [4]: "If I have seen further it is by standing on the shoulders of Giants". The letter was signed such as "Your humble Servant Is. Newton" while the correspondence was sent to "For his honoured Friend Mr Robert Hooke". Commenting this famous phrase V. Arnold noted that R. Hooke was rather small, while I. Newton was tall. Very similar ideas were expressed much earlier, really John of Salisbury wrote in 1159 in *Metalogicon* [5]: "Bernard of Chartres used to say that we are like dwarfs sitting on the shoulders of giants so that we are able to see more and further than they, not indeed by reason of the sharpness of our own vision or the height of our bodies, but because we are lifted up on high and raised aloft by the greatness of giants." I. Newton knew claims of a famous British monk and he slightly re-phrased similar ideas. Perhaps, it would be reasonable to remind relations between these two great scientists (Robert Hooke and Isaac Newton). Initially, they have rather friendly conversations concerning different problems [6]. On January 6, 1680 R. Hooke wrote a letter to I. Newton where he assumed that attraction is inversely propor-

[1)]National Research Center—"Kurchatov Institute", Moscow, Russia.

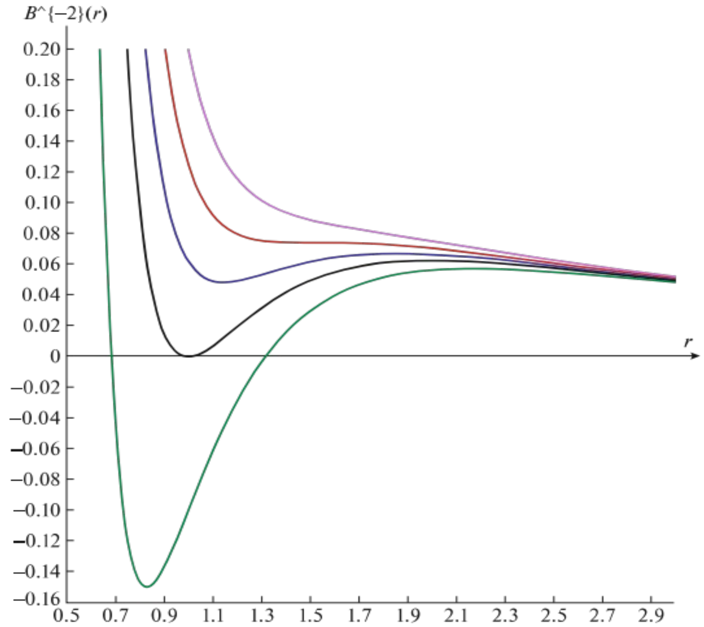

Fig. 3. Graph of the function $B^{-2}(\hat{r})$ for different q, namely for the green curve $q = 0.9$, for the black curve $q = 1$, for the blue curve $q = 1.0625$, for the red curve $q = 1.125$ and for the violet curve $q = 1.2$. From inspection of the curves we conclude that there are shadows for Reissner—Nordström metrics with $q \leq 1$, there are photon circular orbits (but shadows do not exist) for $1 < q \leq 9/8$ while for $q > 9/8$ there are no shadows or circular photon orbits in the vicinity of such a naked singularity.

Thus, it can be noted that for charge values $q \leq 1$ black holes have shadows, while for $1 < q \leq 9/8$ (there are no shadows, but there are circular photon orbits), and for $q > 9/8$ there are neither circular photon orbits nor shadows. Thus, there is structural instability in the sense discussed in the works of Poincaré—Pontryagin—Andronov—Anosov and other authors. The need to study structural stability was written about in many of their works by, for example, R. Thom and V.I. Arnold (see [72—75] and references in these works). In the case of discussing the presence of shadows of the Reissner—Nordström black hole, there is a structural instability in the vicinity of the value $q = 1$, since with any small change in the parameters, the properties of the system qualitatively change (in our case, this is the presence of shadows in the vicinity of black holes), since at the values of the limiting charge $q = 1 - \epsilon$ there are shadows, while at $q = 1 + \epsilon$ the shadows disappear, i.e. the shadows disappear at supercritical values of charge, as does the horizon of the Reissner—Nordström black hole.

However, the above example does not allow us to assert that black holes have shadows, while naked singularities do not, since the authors of [76] showed that there may be shadows in the vicinity of naked singularities.

8. SHADOWS FOR PERTURBED KERR BLACK HOLES

In this section we describe a sketch for a proof that in some cases conditions for circular photon orbits determine shadows as it was done for Kerr metric in [55]. We consider small perturbations of the Kerr metric $\tilde{g}_{\mu\nu}$ that could arise as a result of considering alternative theories of gravity. Moreover, we assume that when considering geodesics in such metrics it is possible to apply Carter's approach, in which the Hamilton—Jacobi equation allows separation of variables. In this case, it is necessary to introduce Chandrasekhar constants of motion for photons (ξ, η) and therefore, for radial motion we have the following equation

$$\left(\frac{d\hat{r}}{d\sigma}\right)^2 = \hat{\mathcal{R}}(\hat{r}, \xi, \eta), \quad (50)$$

NATURAL SCIENCE REVIEW
NATURAL SCIENCE REVIEW **00** 00 (2025)
nsr.jinr.int

Shadow in the Galactic Center: Theoretical Concept – Prediction – Realization

A. F. Zakharov*[1,2]

[1] *National Research Center – Kurchatov Institute, Moscow, Russia*
[2] *Bogoliubov Laboratory of Theoretical Physics, Joint Institute for Nuclear Research, Dubna, Russia*

Abstract

General Relativity (GR) was created in November 1915 and since its creation and up to now this theory has undergone many tests. The first realistic cosmological models were proposed in the works of Friedman, written in the 1920s. For a long time Friedman's cosmological works were actually banned in Soviet Union due to philosophical reasons, since the models where the birth and evolution of the Universe occurs were considered ideologically unacceptable. Due to great achievements in relativity and cosmology and due to increasing interest to these branches of of science in last decades we recall a development of relativistic astrophysics and contribution of Russian researchers in these studies. Since one of the world leaders in physical cosmology A. A. Friedman passed away in September 1925, it is reasonable to outline the main achievements of physical cosmology over the past 100 years. We discuss also observational and theoretical achievements in confirmations of relativistic observational predictions for black holes, including the closest supermassive black hole in our Galactic Center. We outline an evolution of black hole shadow from the purely theoretical concept to observable quantities for supermassive black holes in Sgr A* and M87*.

Keywords: Foundations of GR, Cosmology, Supermassive black holes, Galactic Center, M87*, Synchrotron radiation, VLBI observations

1. 110 years of success of GR development

General relativity (GR) was developed by A. Einstein after intensive conversations with D. Hilbert in November 1915 [1–5]. In spite of difficulties to create a consistent quantum gravity in numerous attempts done by different authors [6–11] classical GR passed all possible tests at different scales.

In 1917 a truly revolutionary event in cosmological studies has taken place since the Universe started to be a subject for studies not only by philosophers but also by physicists as well [12]. In this year A. Einstein obtained the first cosmological model of static Universe based on his theory of relativity [13]. In this paper Einstein assumed that the spatial distribution of matter in the Universe is uniformly isotropic and homogeneous (now it is called the cosmological principle). Many consequent researchers used the principle in their studies after him. Later,

*Corresponding author e-mail address: alex.fed.zakharov@gmail.com

https://doi.org/doi/number
Received: 30 April 2025; Revised: 19 June 2025; Accepted: 19 June 2025; Published: XX Month 2025

metric. Then, we obtain from Eq. (1)

$$A(r)\left(\frac{dt}{d\lambda}\right)^2 - A^{-1}(r)\left(\frac{dr}{d\lambda}\right)^2 + r^2\left(\frac{d\phi}{d\lambda}\right)^2 = 0, \tag{2}$$

since

$$\left(\frac{dt}{d\lambda}\right)^2 = \frac{E^2}{A^2(r)}, \tag{3}$$

we obtain

$$\left(\frac{dr}{d\lambda}\right)^2 = \left(\frac{E^2}{A(r)} - \frac{L^2}{r^2}\right)A(r), \tag{4}$$

or

$$\left(\frac{dr}{d\lambda}\right)^2 = \left(\frac{1}{A(r)} - \frac{b^2}{r^2}\right)\frac{A(r)}{E^2}, \tag{5}$$

where $b = L/E$. Therefore, the photon motion can only in regions where

$$\frac{1}{A(r)} \geq \frac{b^2}{r^2}, \tag{6}$$

or

$$B(r) \leq \frac{1}{b^2}, \tag{7}$$

where $B(r) = A(r)/r^2$. If we define function $A(r) = 1 - 2/r$ for $r \geq 3$, while $A(r) = r^2/27$ for $r < 3$ (therefore, $B(r) = (1 - 2/r)/r^2$ for $r \geq 3$ and $B(r) = 1/27$ for $r < 3$. As we noted above we could compare Eq. (6) from Friedman paper [22] and Eqs. (4) or (5) and our Fig. 1 with Figure in [22]. It is not strange since in both papers the authors were searching regions where some functions are positive.

If we conduct a thought experiment like Rutherford's experiment on the scattering of photons by a Schwarzschild black hole, we will not be able, even in principle, to distinguish the metric of a black hole from a metric where the function $A(r)$ is replaced by a modified one in the interval $2 < r < 3$. Similarly, if we use bound orbits to test the black hole metric, the Schwarzschild metric will be indistinguishable from the modified metric considered above and done in Eq. () , since the probe body tests gravity only in the range of radial coordinate periapsis to apoapsis but in this region the metric in Eq. () coincides with Schwarzschild one. We have considered only two ways to test the metric of a compact object, but even when considering other approaches there are limitations to the inference that the processing of observations leads to the conclusion that there is a Schwarzschild and/or Kerr black hole. It is probably more correct in this case to say that this black hole model describes the observational data best among the alternatives considered.

9. Conclusions

In this article we recalled some fragments of the development of physics and astronomy in Russia, not all of them are well known even to specialists. The remarkable words of S. Weinberg about the history of physics come to mind. At the end of his life this famous scientist worked in GR and astronomy and wrote several outstanding books on these subjects [244–247]. In one of his last popular book Weinberg emphasized an importance of history of science and wrote:"I am a physicist, not a historian, but over the years I have become increasingly fascinated by the

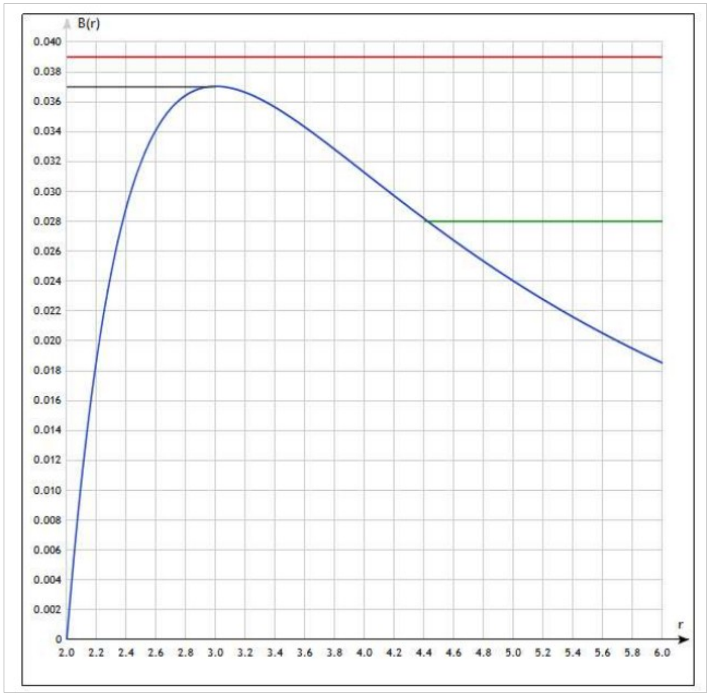

Figure 1. Blue curve represents $(1-2/r)/r^2$ for all r. Function $B(r)$ corresponds to the blue curve for $r \geq 3$ and corresponds to the black horizontal straight line $B(r) = 1/27$ for $r < 3$. Red horizontal straight line $b = 5.063$ $(B(r) = 0.039)$ corresponds to capture of photon, the green horizontal straight line $b = 6$ $(B(r) = 0.028$ for $r > 4.4)$ corresponds to the case when photon moves from infinity toward the until $r \approx 4.4$, at this point photon turns and moves to infinity again. Critical impact parameter $b = 3\sqrt{3}$ separates scatter and capture regions for the impact parameters. It is the same as for the Schwarzschild metric.

history of science. It is an extraordinary story, one of the most interesting in human history. It is also a story in which scientists like myself have a personal stake. Today's research can be aided and illuminated by a knowledge of its past, and for some scientists knowledge of the history of science helps to motivate present work" [248].

Unfortunately, in Russia the achievements of domestic scientists were sometimes hushed up, thereby giving additional bonuses to foreign scientists. In this context, one can recall the underestimation of the importance of Friedman's work on cosmology, since Soviet philosophers and ideologists insisted that the Universe is infinite in time and space. On May 2, 1946, P. L. Kapitsa wrote a letter to Stalin, asking for support for the publication of Gumilevsky's book "Russian Engineers", in particular, Kapitsa wrote [249] "it is clear from Gumilevsky's book that a large number of the largest engineering initiatives were born in our country, we ourselves were almost unable to develop them, often often the failure to use innovation is that

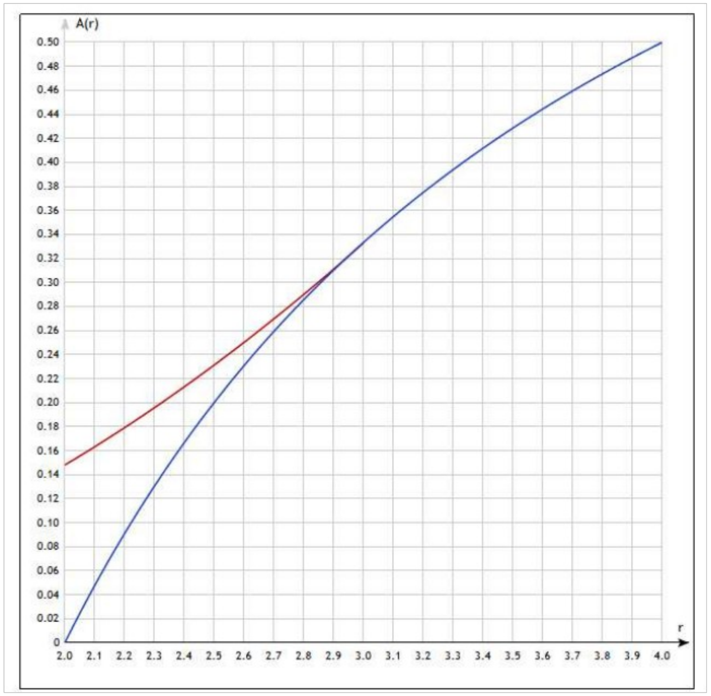

Figure 2. Blue curve presents function $A(r)$ for the Schwarzschild, while red curve corresponds to our modified $A(r)$. These red and blue curves are different only for $r < 3$.

we usually underestimated our own and overestimated foreign...Many of the organizational shortcomings still exist today, and one of the main ones is the underestimation of one's own and overestimation of foreign forces....After all, excessive modesty is an even greater disadvantage than excessive self-confidence...We will do this successfully [to develop national technology] only when we believe in the talent of our scientist and engineer..." A number of measures were taken that led to the acceleration of the country's technological development, the social status of scientists was raised, but such ugly campaigns as the fight against sycophancy and cosmopolitanism also arose. Perhaps Kapitsa's letter to Stalin influenced his determination to begin the fight against servility to the West. Soviet writer and poet K. M. Simonov recalled that one at the meeting with writers Stalin said: "There is an issue which is very important which writers need to be interested in. This is the theme of Soviet patriotism. If we take our average intelligentsia, scientific intelligentsia, professors, doctors, they have not developed a sufficient sense of conscientious patriotism. They have an unjustified admiration for foreign culture. They all feel like minors, not one hundred percent, they are used to considering themselves in the position of eternal students... First the Germans, then the French, there was admiration for foreigner" [250].

As an example of the disgusting campaign to combat cosmopolitanism and servility in 1940s

Are we sure that there is SMBH in GC?

If we select the best model from the finite number of opportunities SMBH may be chosen as the best option, however, it is very hard to prove that alternative models are excluded. Usually, in physics, there is no theorem on the uniqueness of the model for the observed phenomena.

Physics and Astronomy

In contrast to experimental physics we cannot control all parameters in astronomical system. In astronomy we have an opportunity only to observe, therefore we have to point out what, where and when to observe in the sky.

Example. All astrophysical BHs are surrounded with bulk distribution of matter (dust, gas, DM and stellar clusters near SMBH). If uncertainties in shadow reconstruction due bulk matter distribution are around 10^{-6} there is no reason to consider shadow deviation at a level 10^{-7}.

ЖЭТФ, 2024, том 165, вып. 4, стр. 508–515

НЕЛОКАЛЬНЫЕ ГРАВИТАЦИОННЫЕ ТЕОРИИ И ИЗОБРАЖЕНИЯ ТЕНЕЙ ЧЕРНЫХ ДЫР

С. О. Алексеев [a,b*], *А. А. Байдерин* [b], *А. В. Немтинова* [c], *О. И. Зенин* [b]

[a] *Государственный астрономический институт им. П. К. Штернберга,*
Московский государственный университет им. М. В. Ломоносова
119234, Москва, Россия

[b] *Кафедра квантовой теории и физики высоких энергий, физический факультет,*
Московский государственный университет им. М. В. Ломоносова
119234, Москва, Россия

[c] *Уральский федеральный университет им. первого Президента России Б. Н. Ельцина*
620002, Екатеринбург, Россия

Поступила в редакцию 28 ноября 2023 г.,
после переработки 4 декабря 2023 г.
Принята к публикации 4 декабря 2023 г.

С помощью метода Ньюмена – Яниса получено новое вращающееся решение «черная дыра» (ЧД) в гравитации с нелокальными поправками. Предложен способ учета поправок от квантовой гравитации при моделировании теней ЧД с использованием вращающихся метрик ЧД. Метод применим и для других нелокальных моделей с аналогичной структурой ЧД-решений. Показано, что в будущем при увеличении точности наблюдений и, следовательно, необходимости более точного их теоретического моделирования в некоторых случаях удобнее учитывать полевые и/или нелокальные поправки вместо введения новых полей.

DOI: 10.31857/S0044451024040059

1. ВВЕДЕНИЕ

Идея использования нелокальных членов в действии расширенных моделей гравитации обсуждается довольно продолжительное время [1]. Использование такого подхода дает еще одну возможность построить модель темной энергии. Нелокальные конструкции использовались, например, в моделях Рэндалл – Сандрума [2]. Отметим, что рассмотрение нелокальных членов позволило установить новые ограничения на гравитационные модели, используя

$$L = R + c_1 R^2 + c_2 R_{\mu\nu} R^{\mu\nu} + c_3 R_{\mu\nu\alpha\beta} R^{\mu\nu\alpha\beta} + \\ + \alpha R \log \frac{\Box}{\mu^2} R + \beta R_{\mu\nu} \log \frac{\Box}{\mu^2} R^{\mu\nu} + \\ + \gamma R_{\mu\nu\alpha\beta} \log \frac{\Box}{\mu^2} R^{\mu\nu\alpha\beta}, \quad (1)$$

где R — скаляр Риччи, $R_{\mu\nu}$ и $R_{\mu\nu\alpha\beta}$ — тензоры Риччи и Римана соответственно, c_i, α, β и γ — числовые коэффициенты, определенные в [4]. Решения вида «черная дыра» для действия (1) получено и имеет вид (в сигнатуре $(-,+,+,+)$)

$$ds^2 = -f_t dt^2 + f_r dr^2 + r^2 d\Omega^2, \quad (2)$$

где f_t, f_r — метрические функции,

$$f_t \simeq \left(1 - \frac{2G_n M}{r}\right) - \frac{\hat{\alpha}\hbar G_n^2 M}{r^3} + O(G_n^3),$$

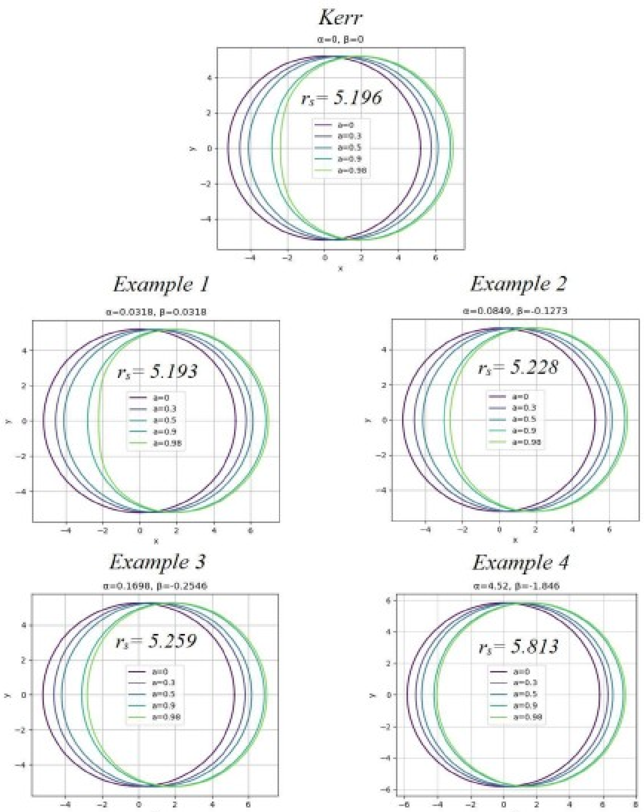

Рис. 2. Профили тени черной дыры при различных a для случая метрики Керра и различных фиксированных полей при угле наклона плоскости вращения $\theta_0 = \pi/2$

4. МОДЕЛИРОВАНИЕ ТЕНИ ЧЕРНОЙ ДЫРЫ ДЛЯ МЕТРИКИ (19)

После нескольких предварительных замечаний можно приступить к расчету зависимости размера тени от α и β. Применяя гравитационные поправки к метрике стабильной звезды, удовлетворяющей уравнению Толмена – Оппенгеймера – Волкова [18], мы вводим новые переменные $\alpha = \hat{\alpha}$ и $\beta = \hat{\beta}$, которые являются модельно-независимыми.

Необходимо отметить, что в качестве примеров мы используем значения коэффициентов из [4]. Таким образом, получены изображения теней ЧД для $M = 1$[1)] и различных значений a для метрики Керра и ее расширения, определенные в [18] (в скалярном поле $\xi = 1/3$), см. рис. 2. Угол плоскости вращения равен $\theta_0 = \pi/2$. Заметим две основные особенности: во-первых, тень смещается от оси симметрии с увеличением a и, во-вторых, тень становится асимметричной вдоль направления x для больших значений a. Обе особенности исчезают при $a \to 0$, когда круглая тень для метрики Шварцшильда восстанавливается. Также заметим, что при угле $\theta_0 = \pi/2$ размер

[1)] Поскольку в реальном случае $M = 10^{44}$, эффект исчезает, как было указано во Введении.

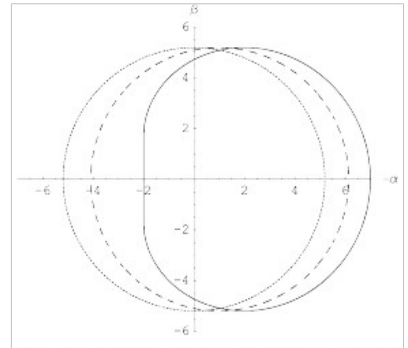

Fig. 2. Mirages around black hole for equatorial position of distant observer and different spin parameters. Solid line, dashed line and dotted lines correspond to $a = 1$, $a = 0.5$, $a = 0$, respectively.

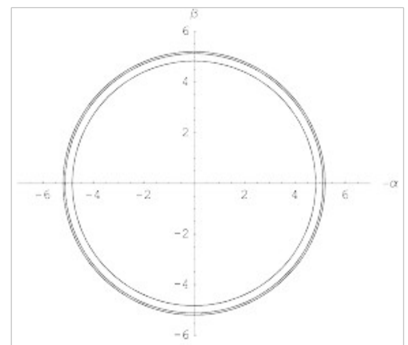

Fig. 3. Mirages around a black hole for the polar position of distant observer and different spin parameters ($a = 0$, $a = 0.5$, $a = 1$). Smaller radii correspond to greater spin parameters.

4. Polar axis observer case

If the observer is located along the polar axis we have $\theta_0 = 0$ and from Eq. (6), we obtain

$$\beta(\alpha) = (\eta_{\text{crit}}(0) + a^2 - \alpha^2(\xi))^{1/2}. \quad (9)$$

or

$$\beta^2(\alpha) + \alpha^2 = \eta_{\text{crit}}(0) + a^2.$$

Thus, mirages around Kerr black hole cles and even for this case in princi evaluate the black hole spin (if the bla is known) taking into account that rad cles weakly depend on the black hole ter. However, one should mention th small difference between radii for di even in the future it is unlikely to be ab black hole spins in this way (see Tabl

5. General case for the angular positio observer

Let us consider different values fo positions of a distant observer θ = π/8 for the spin parameter $a = 0.5$ $\theta = \pi/2$, π/3, π/4 and π/6 for $a = 1$. (F these figures one can see that angu of a distant observer could be evalua mirage shapes only for rapidly rotatin ($a \sim 1$), but there are no chances to angles for slowly rotating black ho even for $a = 0.5$ the mirage shape d too small to be distinguishable by Indeed, mirage shapes weakly depen server angle position for moderate bl parameters.

6. Projected parameters of the space RADIOASTRON interferometer

During this decade the space ra RADIOASTRON will be launched. was initiated by Astro Space Cent Lebedev Physical Institute of Russi of Sciences (RAS) in collaboration institutions of RAS and RosAviaKo tists from 20 countries develop the s load for the satellite and will provi base support of the mission. The pro proved by RAS and RosAviaKos smoothly developing. This space ba radio telescope will be used for s

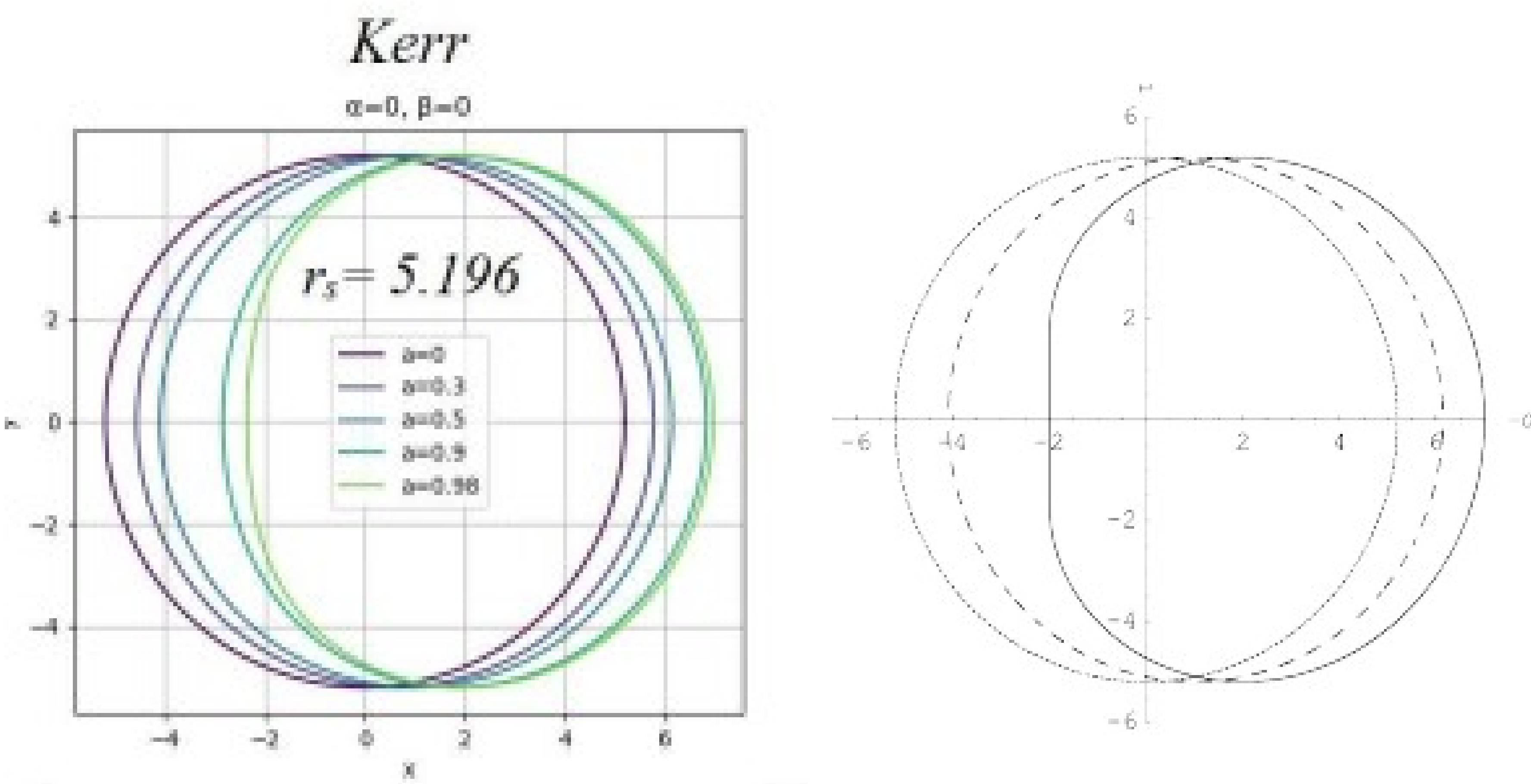

Comparison of these figures Alexeyev et. al (2024) [*a=0, a=0.3, a=0.5, 0.9, 0.98*] and Zakharov et al. (2005) [*a=0, a=0.5, a=1*.]

Concerns on Alexeyev et al. paper (2024)

1. The conventional model for SMBH is describing by Kerr metric (even electric charge is usually considered as negligible). No hair theorem for BHs. There are no observational arguments to violate no hair theorem conditions.

2. “Quantum” black holes approach is applicable for microscopic objects while shadows could observable only for SMBHs. Therefore, such objects look like centaurs which do not exist in nature. The authors increased “quantum” parameters in 10^{44} times but they ignored natural astronomical factors such as bulk distribution of matter. Therefore, the authors from observable phenomena came back to thought experiments. «One step forward, two steps back».

3. The authors discussed an invariance of shadow size in the rotation axis direction for Kerr metric and an equatorial observer (this property was proven in Zakharov et al. (NA, 2005)). The property was discussed for “quantum” rotational black holes without a proof.

4. For K-N BHs circular photon orbits determine shadows but for generalizations of K-N these metrics these two categories are not equivalent. There are examples of circular photon orbits without shadows and shadows without black holes. The authors did not prove that they really deal with shadows (not with circular photon orbits).

5. The authors did not mention that GC shadow was reconstructed by EHT as it was predicted by Zakharov et al. (NA, 2005) in spite of the fact that predictions are realized extremely rarely (usually after observing a phenomenon, its interpretations appear).

COMMENT ON THE ARTICLE "NON-LOCAL GRAVITATIONAL CORRECTIONS IN BLACK HOLE SHADOW IMAGES" BY S. O. ALEXEYEV ET AL.

Alexander F. Zakharov [a,b]

[a] *National Research Center – "Kurchatov Institute", Moscow*

[b] *Bogoliubov Laboratory of Theoretical Physics, JINR, 141980 Dubna, Russia*

Recently Alexeyev et al. published paper (J. Theor. Exper. Phys. v. 165, N 4, p. 508 in Russian; arXiv:2404.16079 [gr-qc], the reference is given also in [1]). In the paper the authors discussed an opportunity of estimating spins from the analysis of the shadow reconstruction of black holes, theoretically considered using the nonlocal gravity model proposed earlier for the description of "quantum" black holes. However, in essence, this paper considered circular photon orbits, and the fact that the corresponding motion parameters determine the shape and size of shadows, similarly to Kerr black holes, remained unproven. It is also remained unproven the statement that for an equatorial observer the shadow size in the direction of rotation of "quantum" black holes remains independent of spin. A long time ago the shadow property was established for the Kerr black hole case.

Many years ago it was shown [2] that if we consider the constants of motion for classical Kerr black holes, the capture region and the scattering region for photons are separated by the Chandrasekar constants of motion (ξ, η) corresponding to circular photon orbits. Thus, for the Kerr metric, the shape and size of the shadow is determined by these critical parameter values (as shown in [3]). As is known, the possibility of shadow reconstruction in the neighborhood of the nearest supermassive black holes is currently under discussion, not only for classical Kerr–Newman black holes, but also for some of their "quantum" generalizations, although in some cases quantum corrections are used to recover shadows in the vicinity of the nearest supermassive black holes. in some cases quantum corrections in the corresponding coefficients are too small for their influence on the physical effects to be detected (this is also noted by the authors of the paper [1]).

If we mean a purely theoretical discussion, we can analyze the differences of shadows for the classical Kerr black hole and its "quantum" generalization, considered in the work of [1], but it is necessary to keep in mind that if we speak about astrophysical black holes, it is necessary to take into account the influence of such factors as the spatial mass distribution, the influence of plasma effects, etc., since the influence of these factors significantly exceeds the difference in the shape and size of shadows for the cases of a classical black hole and its quantum generalization. In paper [3] it is shown that for a classical Kerr black hole in the case of the observer's position in the equatorial plane, the size of the shadow in the direction of the black hole's rotation does not depend on the spin of the black hole. The authors of the paper [1] note that in the examples considered by them the size of shadows for the "quantum" generalization of the Kerr black hole for an observer in the equatorial plane is also independent of spin, however it remains unproven that for additional parameters (due to the use of the model of nonlocal gravitation), the sizes of shadows in the rotation direction for the considered "quantum" generalization of the Kerr black hole for an observer in the equatorial plane, do not depend on spin.

After the discovery of any physical (or astronomical) phenomenon, there is also its theoretical explanation, but very often theoretical predictions are not realized in experiments or astronomical observations. are realized in experiments or astronomical observations, so it is useful to recall that the the idea to use ground-based and ground-based space-based VLBI operating in the millimeter or submillimeter range to reconstruct the shadow in the vicinity of the Galactic center was proposed in [3] (which can naturally be generalized to other supermassive black holes, such as the black hole at the center of the galaxy M87). The possibility of reconstructing the shadow of a black hole at the Galactic Center using global ground-space (and ground-based) interferometers operating in the mm band was *firstly*

nature

NEWS | 04 September 2024

Publishing nightmare: a researcher's quest to keep his own work from being plagiarized

A scientist reviewing a study spotted figures that looked identical to his own, leading to a frustrating campaign to prevent its publication.

By Dan Garisto

When bioinformatician Sam Payne was asked to review a manuscript on a topic relevant to his own work, he agreed – not anticipating just how relevant it would be.

When bioinformatician Sam Payne was asked to review a manuscript on a topic relevant to his own work, he agreed — not anticipating just how relevant it would be.

The manuscript, which was sent to Payne in March, was about a study on the effect of cell sample sizes for protein analysis. "I immediately recognized it," says Payne, who is at Brigham Young University in Provo, Utah. The text, he says, was similar to that of a paper[1] he'd authored three years earlier, but the most striking feature was the plots: several were identical down to the last data point. He fired off an e-mail to the journal, *BioSystems*, which promptly rejected the manuscript.

In July, Payne discovered that the manuscript had been published[2] in the journal *Proteomics*, and he alerted the editors. On 15 August, the journal retracted the paper. An accompanying statement cited "major unattributed overlap between the figures" in it and Payne's work. In response to questions from *Nature*, a spokesperson for Wiley, which publishes *Proteomics*, said, "This paper was simultaneously submitted to multiple journals and included plagiarized images."

RELATED

AI is complicating plagiarism. How should scientists respond?

The retraction statement also stated that four of the authors said they "did not participate in the writing and submission of the article and gave no consent for publication", and that the fifth author did not respond. However, *Nature*'s news team found links between several of the authors and International Publisher, a paper mill based in Moscow. Neither the authors nor International Publisher responded to *Nature*'s requests for comment.

A VERY CLOSE MATCH

The figure on the left appears in a paper published in 2021 by bioinformatician Sam Payne and his co-authors. The figure on the right appears in a paper published in the journal *Proteomics* in May 2024 by other authors. The *Proteomics* paper was retracted in August.

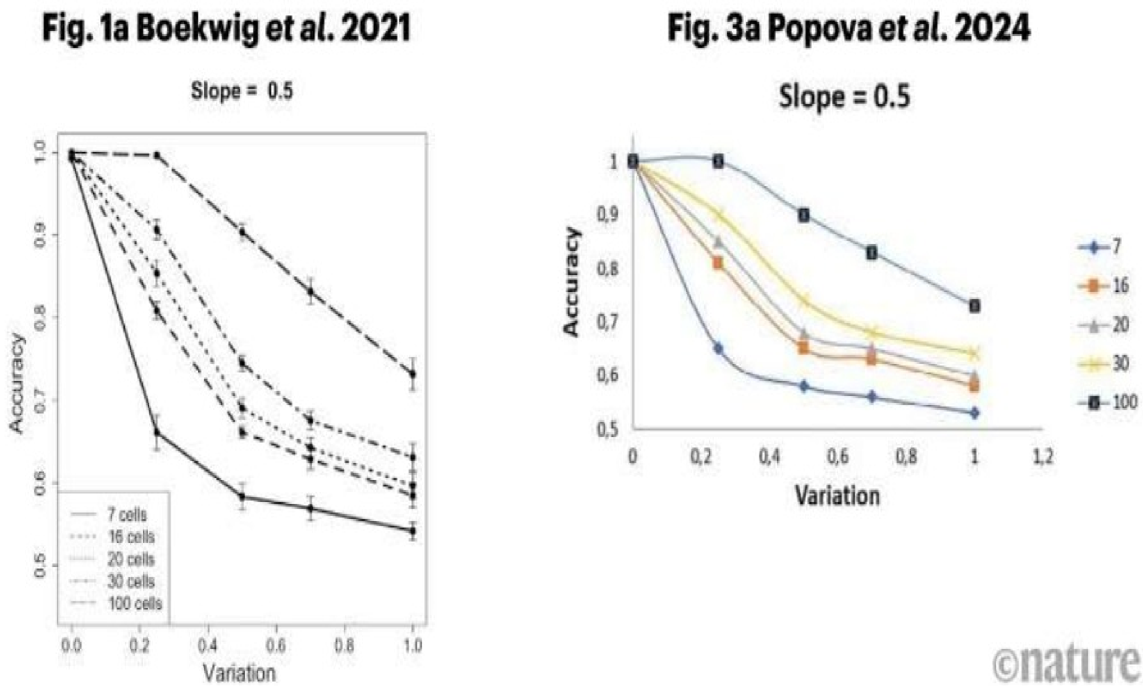

Source: Ref. 1 and Ref. 2

When, months later, he discovered the *Proteomics* paper, he posted a follow-up. “Well. It REALLY happened” – the paper that he had been asked to review had been published. Two weeks later, *Proteomics* retracted the paper, citing


Nature's
10

[Anna Abalkina]... She was shocked to find that a PhD student had plagiarized two of her papers, copying large parts of the works. When she complained, the journal issued only a correction, saying that the author forgot to reference her work. (The student later gave up their degree after Abalkina applied pressure to their university.)

DM or SMBH in our GC?

MGM 16 (July 10, 2021): Saturday round table

https://www.youtube.com/watch?v=pxoq-H4cXqE

Subject: Nature of Galactic Center

Two alternatives: SMBH vs RAR model for DM

Two opponents: R. Genzel vs C. Arguelles

Genzel: «Any theoretical model must
Schwarzschild precession for S2 orbit»

An alternative potential for elliptical trajectories

Monthly Notices of the ROYAL ASTRONOMICAL SOCIETY

MNRAS **505,** L64–L68 (2021) https://doi.org/10.1093/mnrasl/slab051
Advance Access publication 2021 May 20

Hinting a dark matter nature of Sgr A∗ via the S-stars

E. A. Becerra-Vergara,[1,2,3★] C. R. Argüelles,[1,2,4] A. Krut,[1,2] J. A. Rueda[1,2,5,6★] and R. Ruffini[1,2,5,6★]

[1] *ICRANet, Piazza della Repubblica 10, I-65122 Pescara, Italy*
[2] *ICRA, Dip. di Fisica, Sapienza Università di Roma, P.le Aldo Moro 5, I-00185 Rome, Italy*
[3] *GIRG, Escuela de Física, Universidad Industrial de Santander, 680002 Bucaramanga, Colombia*
[4] *Fac. de Ciencias Astron. y Geofísicas, Universidad Nacional de La Plata, Paseo del Bosque, B1900FWA La Plata, Argentina*
[5] *ICRANet-Ferrara, Dip. di Fisica e Scienze della Terra, Università degli Studi di Ferrara, Via Saragat 1, I-44122 Ferrara, Italy*
[6] *INAF, Istituto de Astrofisica e Planetologia Spaziali, Via Fosso del Cavaliere 100, I-00133 Rome, Italy*

Accepted 2021 May 12. Received 2021 May 12; in original form 2021 March 1

ABSTRACT

The motion data of the S-stars around the Galactic Centre gathered in the last 28 yr imply that Sgr A∗ hosts a supermassive compact object of about $4 \times 10^6\,M_\odot$, a result awarded with the Nobel Prize in Physics 2020. A non-rotating black hole (BH) nature of Sgr A∗ has been uncritically adopted since the S-star orbits agree with Schwarzschild geometry geodesics. The orbit of S2 has served as a test of general relativity predictions such as the gravitational redshift and the relativistic precession. The central BH model is, however, challenged by the G2 post-peripassage motion and by the lack of observations on event-horizon-scale distances robustly pointing to its univocal presence. We have recently shown that the S2 and G2 astrometry data are better fitted by geodesics in the spacetime of a self-gravitating dark matter *core–halo* distribution of 56 keV-fermions, '*darkinos*', which also explains the outer halo Galactic rotation curves. This letter confirms and extends this conclusion using the astrometry data of the 17 best-resolved S-stars, thereby strengthening the alternative nature of Sgr A∗ as a dense core of darkinos.

Key words: Elementary particles – Dark matter.

1 INTRODUCTION

The gravitational potential in the Galactic centre (GC) is dominated by a supermassive compact object, Sagittarius A∗ (Sgr A∗), long thought to be a massive black hole (BH) of $\approx 4 \times 10^6\,M_\odot$ (Ghez et al. 2005, 2008; Genzel, Eisenhauer & Gillessen 2010; Gravity Collaboration 2018b). From the observational viewpoint, this inference on the nature of Sgr A∗ mainly comes from the nearly Keplerian orbits of tens of stars belonging to the S-star cluster (Gillessen et al. 2009a, 2017), whose motions are well described by geodesics in the Schwarzschild spacetime geometry. The most important S-cluster member is S2 which, with an orbital period of about 16 yr and a pericentre of about 1500 Schwarzschild radii, has the most compact orbit around Sgr A∗. The S2 orbit data have allowed to test general relativity predictions such as the relativistic redshift (see e.g. Gravity Collaboration 2018a; Do et al. 2019) and precession (see e.g. Parsa et al. 2017; Gravity Collaboration 2020). However, not every news is good for the BH model; it is challenged by the G2 motion which cannot be explained by any geodesics in the BH geometry (Plewa et al. 2017; Gillessen et al. 2019), as well as by very scarce data at event-horizon-scale distances from Sgr A∗, robustly pointing to a univocal central BH presence (see e.g. Yuan & Narayan 2014; Bouffard et al. 2019).

In view of the above, we have dived into the possibility of an alternative nature for Sgr A∗ based on the fermionic dark matter (DM) profile predicted by the Ruffini–Argüelles–Rueda (RAR) model (Ruffini, Argüelles & Rueda 2015; Argüelles et al. 2018). In the RAR model, the DM distribution in galaxies is obtained from the general relativity field equations, assuming it as a self-gravitating system of fermions at finite temperature in equilibrium and distributed in phase space according to the Fermi–Dirac statistics including a particle energy cut-off that gives to the configuration, a finite size (see Argüelles et al. 2018, for more details). We hereafter refer to these neutral, massive DM fermions as '*darkinos*'. The RAR model leads to a *dense core–diluted halo* density profile in which the darkinos are: (1) in a quantum degenerate regime within the nearly uniform core, (2) followed by an intermediate quantum-classical regime in the density fall-off and plateau phase, and (3) finally in a Boltzmann regime in the outer halo that follows a power-law density ending with a nearly exponential cut-off defining the galaxy border. There is a bunch of astrophysical consequences of the *core–halo* profile of darkinos derived from the RAR model. In Argüelles et al. (2018), it has been shown that it explains the rotation curves of the Milky Way outer halo. In Argüelles et al. (2019), this agreement has been shown to apply as well to other galaxy types ranging from dwarfs to big ellipticals and galaxy clusters. These results have further enticed attention on the darkinos microphysics, e.g. their self-interactions (Argüelles et al. 2016; Yunis et al. 2020a) and interaction with neutrinos (Penacchioni, Civitarese & Argüelles 2020) as well as in their macrophysics, e.g. their lensing properties (Gómez et al. 2016), their influence in the dynamics of binaries (Gómez & Rueda 2017), their halo formation and stability on cosmological time-scales (Argüelles et al. 2020), and their role in the large- and small-scale structure formation (Yunis, Argüelles & López Nacir 2020b).

★ E-mail: eduar.becerra@icranet.org (EAB-V); jorge.rueda@icra.it (JAR); ruffini@icra.it (RR)

June 2, 2021

222

Astronomy & Space \ Astronomy

What if the black hole at the center of the Milky Way is actually a mass of dark matter?

REPORT

by Bob Yirka , Phys.org

Would you like to receive trending story notifications on your smartphone?

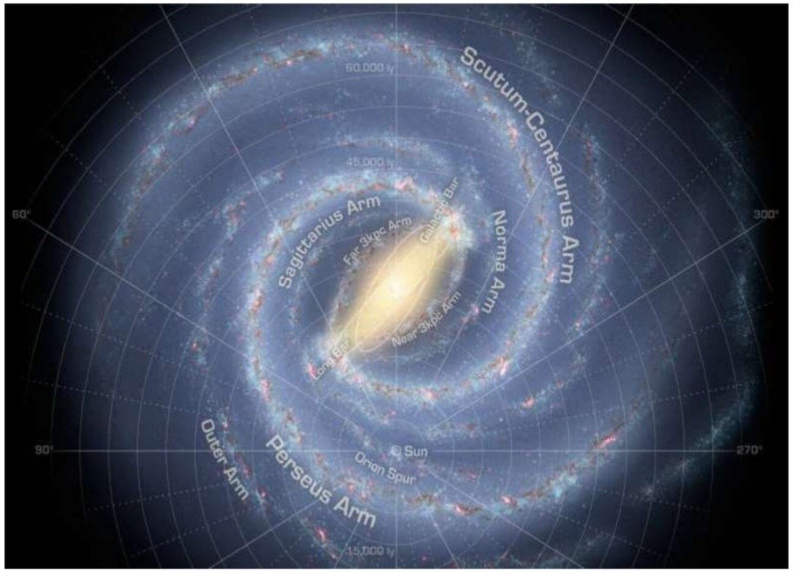

Credit: CC0 Public Domain

A team of researchers at the International Center for Relativistic Astrophysics has found evidence that suggests Sagittarius A* is not a massive black hole but is instead a mass of dark matter. In their paper published in the journal *Monthly Notices of the Royal Astronomical Society: Letters*, the group describes the evidence they found and how it has stood up to testing.

The Center of the Milky Way Might Not Be a Black Hole After All

Well, that would change some things.

// BY CAROLINE DELBERT JUN 16, 2021

PAKIN SONGMOR / GETTY IMAGES

- **The center of the Milky Way could be dark matter instead of a supermassive black hole, according to a new study.**
- **The study is based on observations of the objects that orbit closest to the center.**
- **If it's true, this could help explain how supermassive black holes originate.**

What if the center of our galaxy isn't a supermassive black hole after all, but instead, a massive amount of dark matter? That would flip our long-held understanding of the Milky Way, but in a new study, scientists from Italy, Argentina, and Colombia say the evidence stacks up.

➞ You think space is badass. So do we. Let's explore it together.

The idea of a supermassive black hole at the center of the Milky Way is well-established, based partly on the orbit of specific stars like S0-2. Scientists study

Space

The black hole at the centre of the Milky Way may be something even more mysterious, scientists say

The centre of our galaxy could be a cluster of dark matter, not a supermassive black hole

Adam Smith | Wednesday 02 June 2021 10:22

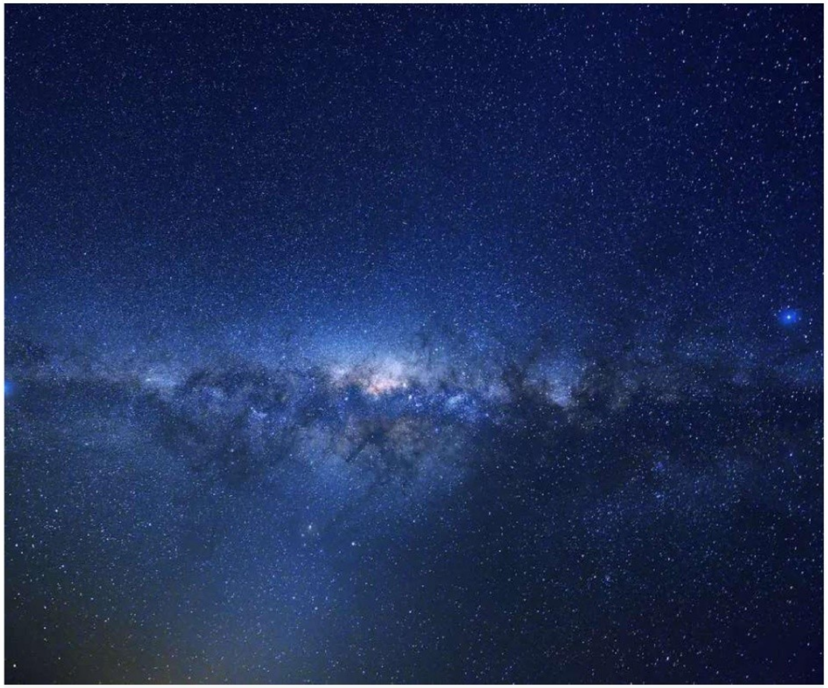

(Getty Images)

Leer en Español

MEDIA INAF
The online newsletter of the National Institute of Astrophysics

NOT A SINGULARITY BUT A THICKNESS OF DARK MATTER

Black hole in the center of the Milky Way? There are those who say no

*A new theory offers an alternative explanation to the nature of Sgr A *, the supermassive compact object at the center of our galaxy: while the commonly accepted hypothesis is that it is a black hole, a study led by IcraNet researchers and published in May on Mnras Letters shows that they could be "darkinos" - particles of dark matter - in high concentration. Media Inaf interviewed one of the authors of the article, astrophysicist Jorge Armando Rueda Hernández*

Marco Malaspina 06/15/2021 Tweet Condividi 895

What if there is no singularity at the center of the Milky Way? What if our galaxy's heart of darkness actually hides not a supermassive black hole - as most astrophysicists believe - but a dense agglomeration of dark matter ? The hypothesis, illustrated in a study published at the end of May in *Mnras Letters* , may seem out of time: perhaps the Nobel Prize was awarded just last year to Reinhard Genzel and Andrea Ghez precisely for the discovery of Sagittarius A * , home of the black hole of four million solar masses that resides right in the center of our galaxy? On closer inspection, however, the reasons for the Nobel Prize to Genzel and Ghez do not speak of *black hole* , but more broadly of the *compact object* supermassive (*supermassive compact object*). What other object - more or less compact - could we ever deal with?

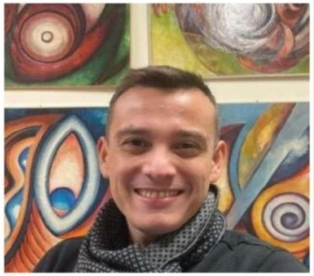

Jorge Armando Rueda Hernández, astrophysicist at IcraNet, co-author of the study published May 20 in Monthly Notices of the Royal Astronomical Society: Letters

According to the authors of the article published in *Mnras Letters* , it could be a condensate of *darkinos* - particles of dark matter, in fact. And it is a scenario that would not only concern the Milky Way, but many other galaxies. Among the authors of the study, led by EA Becerra-Vergara of IcraNet , there is a Colombian astrophysicist - he is originally from Bucaramanga - in Italy for the past fifteen years: he arrived in 2006 for a doctorate in relativistic astrophysics at Sapienza, then also become a professor at iCraNet, first in Rome and now at the University of Ferrara. His name is **Jorge Armando Rueda Hernández** , we interviewed him.

A&A 641, A34 (2020)
https://doi.org/10.1051/0004-6361/201935990

Astronomy & Astrophysics

Geodesic motion of S2 and G2 as a test of the fermionic dark matter nature of our Galactic core

E. A. Becerra-Vergara[1,2,3], C. R. Argüelles[1,2,4], A. Krut[1,2], J. A. Rueda[1,2,5,6,7], and R. Ruffini[1,2,5,6,8]

[1] ICRANet, Piazza della Repubblica 10, 65122 Pescara, Italy
e-mail: eduar.becerra@icranet.org
[2] ICRA, Dipartimento di Fisica, Sapienza Università di Roma, P.le Aldo Moro 5, 00185 Rome, Italy
e-mail: jorge.rueda@icra.it, ruffini@icra.it
[3] Grupo de Investigación en Relatividad y Gravitación, Escuela de Física, Universidad Industrial de Santander, A. A. 678, Bucaramanga 680002, Colombia
[4] Facultad de Ciencias Astronómicas y Geofísicas, Universidad Nacional de La Plata, Paseo del Bosque, B1900FWA La Plata, Argentina
[5] ICRANet-Ferrara, Dipartimento di Fisica e Scienze della Terra, Università degli Studi di Ferrara, Via Saragat 1, 44122 Ferrara, Italy
[6] Dipartimento di Fisica e Scienze della Terra, Università degli Studi di Ferrara, Via Saragat 1, 44122 Ferrara, Italy
[7] INAF, Istituto de Astrofisica e Planetologia Spaziali, Via Fosso del Cavaliere 100, 00133 Rome, Italy
[8] INAF, Viale del Parco Mellini 84, 00136 Rome, Italy

Received 30 May 2019 / Accepted 22 July 2020

ABSTRACT

The motion of S-stars around the Galactic center implies that the central gravitational potential is dominated by a compact source, Sagittarius A* (Sgr A*), which has a mass of about $4 \times 10^6\, M_\odot$ and is traditionally assumed to be a massive black hole (BH). The explanation of the multiyear accurate astrometric data of the S2 star around Sgr A*, including the relativistic redshift that has recently been verified, is particularly important for this hypothesis and for any alternative model. Another relevant object is G2, whose most recent observational data challenge the scenario of a massive BH: its post-pericenter radial velocity is lower than expected from a Keplerian orbit around the putative massive BH. This scenario has traditionally been reconciled by introducing a drag force on G2 by an accretion flow. As an alternative to the central BH scenario, we here demonstrate that the observed motion of both S2 and G2 is explained in terms of the *dense core – diluted halo* fermionic dark matter (DM) profile, obtained from the fully relativistic Ruffini-Argüelles-Rueda (RAR) model. It has previously been shown that for fermion masses 48–345 keV, the RAR-DM profile accurately fits the rotation curves of the Milky Way halo. We here show that the solely gravitational potential of such a DM profile for a fermion mass of 56 keV explains (1) all the available time-dependent data of the position (orbit) and line-of-sight radial velocity (redshift function z) of S2, (2) the combination of the special and general relativistic redshift measured for S2, (3) the currently available data on the orbit and z of G2, and (4) its post-pericenter passage deceleration without introducing a drag force. For both objects, we find that the RAR model fits the data better than the BH scenario: the mean of reduced chi-squares of the time-dependent orbit and z data are $\langle\bar{\chi}^2\rangle_{\rm S2,RAR} \approx 3.1$ and $\langle\bar{\chi}^2\rangle_{\rm S2,BH} \approx 3.3$ for S2 and $\langle\bar{\chi}^2\rangle_{\rm G2,RAR} \approx 20$ and $\langle\bar{\chi}^2\rangle_{\rm G2,BH} \approx 41$ for G2. The fit of the corresponding z data shows that while for S2 we find comparable fits, that is, $\bar{\chi}^2_{z,\rm RAR} \approx 1.28$ and $\bar{\chi}^2_{z,\rm BH} \approx 1.04$, for G2 the RAR model alone can produce an excellent fit of the data, that is, $\bar{\chi}^2_{z,\rm RAR} \approx 1.0$ and $\bar{\chi}^2_{z,\rm BH} \approx 26$. In addition, the critical mass for gravitational collapse of a degenerate 56 keV-fermion DM core into a BH is $\sim 10^8\, M_\odot$. This result may provide the initial seed for the formation of the observed central supermassive BH in active galaxies, such as M 87.

Key words. Galaxy: center – Galaxy: kinematics and dynamics – Galaxy: structure – dark matter – elementary particles

1. Introduction

The monitoring of the motion of the so-called S-stars near the Galactic center over the past decades has revealed that the gravitational potential in which they move is dominated by a massive compact source at the center, Sagittarius A* (Sgr A*; Gillessen et al. 2009, 2017). The S-star dynamics implies a mass for Sgr A* of $\approx 4.1 \times 10^6\, M_\odot$, which is traditionally associated in the literature with a massive black hole (BH; Gravity Collaboration 2018a; Ghez et al. 2008; Genzel et al. 2010).

Of the objects that move near and around Sgr A*, S2 and G2 are the most interesting. The star S2 describes an elliptical orbit that is focused on Sgr A* and has a period of 16.05 yr and the second closest pericenter of the S-stars, $r_{p(S2)} \approx 0.6$ mpc (Gillessen et al. 2009, 2017). The S2 orbit constrains the Sgr A* mass best, but its pericenter at $\sim 1500\, r_{\rm Sch}$ from Sgr A* is too far to univocally infer a putative massive BH of Schwarzschild radius $r_{\rm Sch} = 2GM_{\rm BH}/c^2$, where $M_{\rm BH}$ is its mass.

The most recent measurements of the motion of G2 after the peripassage around Sgr A* represent a further challenge for the hypothesis of a massive BH. The G2 radial velocity is lower than that from a Keplerian motion around the massive BH, which has been reconciled by introducing the action of a drag force exerted by an accretion flow (Plewa et al. 2017; Gillessen et al. 2019).

Our aim here is to show that the *dense core – diluted halo* DM density distribution of a general relativistic system of 56 keV fermions, following the extended Ruffini-Argüelles-Rueda (RAR) model (Argüelles et al. 2018, 2019a) instead explains the orbits of S2 and G2 without invoking the massive BH or a drag force. We use the most complete data of the S2 orbit over the last 26 yr (Gillessen et al. 2017; Gravity Collaboration 2018b), including the recent data released by Do et al. (2019), and the four-year data of the G2 motion after its pericenter passage (Gillessen et al. 2019).

2. Ruffini-Argüelles-Rueda model of dark matter

The Ruffini-Argüelles-Rueda (RAR) model equilibrium equations consist of the Einstein equations in spherical symmetry for a perfect fluid energy-momentum tensor. Pressure and density are given by Fermi-Dirac statistics, and the closure relations are determined by the Klein and Tolman conditions of thermodynamic equilibrium (Ruffini et al. 2015). The solution to this system of equations leads to a continuous and novel *dense core – diluted halo* DM profile from the center all the way to the galactic halo (see Siutsou et al. 2015; Argüelles et al. 2016; Mavromatos et al. 2017, for its applications). Similar *core-halo* profiles with applications to fermionic DM were also obtained in Bilic et al. (2002) and more recently in Chavanis et al. (2015) from a statistical approach within Newtonian gravity.

The above corresponds to the original version of the RAR model, with a unique family of density profile solutions that behaves as $\rho(r) \propto r^{-2}$ at large radial distances from the center. This treatment was extended in Argüelles et al. (2018), by introducing a cutoff in momentum space in the distribution function (DF; i.e., accounting for particle-escape effects) that allows defining the galaxy border (see Appendix A). This extension of the RAR model was successfully applied to explain the Milky Way rotation curve, as shown in Fig. 1, implying a more general *dense core – diluted halo* behavior for the DM distribution as follows:

– A DM core with radius r_c (defined at the first maximum of the twice-peaked rotation curve), whose value is shown to be inversely proportional to the particle mass m, in which the density is nearly uniform. This central core is supported against gravity by the fermion degeneracy pressure, and general relativistic effects are appreciable.

– Then, there is an intermediate region characterized by a sharply decreasing density where quantum corrections are still important, followed by an extended and diluted plateau. This region extends until the halo scale-length r_h is achieved (defined at the second maximum of the rotation curve).

– Finally, the DM density reaches a Boltzmann regime supported by thermal pressure with negligible general relativistic effects, and shows a behavior $\rho \propto r^{-n}$ with $n > 2$ that is due to the phase-space distribution cutof. This leads to a DM halo bounded in radius (i.e., $\rho \approx 0$ occurs when the particle escape energy approaches zero).

As was explicitly shown in Argüelles et al. (2019b,a, 2018), this type of *dense core – diluted halo* density profile suggests that the DM might explain the mass of the dark compact object in Sgr A* as well as the halo mass. It applies not only to the Milky Way, but also to other galactic structures from dwarfs and ellipticals to galaxy clusters (Argüelles et al. 2019a). Specifically, a Milky Way analysis (Argüelles et al. 2018) has shown that this DM profile can indeed explain the dynamics of the closest S-cluster stars (including S2) around Sgr A*, all the way to the halo rotation curve without changing the baryonic bulge-disk components. The analysis of the S-stars was made through a simplified circular velocity analysis in general relativity, constraining the allowed fermion mass to $mc^2 \approx 50-345$ keV. We extend this analysis by fully reconstructing the geodesic of the object in full general relativity, and apply it to S2 and G2. Figure 1 shows the DM density profile and its contribution to the rotation curve for the Milky Way for 56 keV DM fermions.

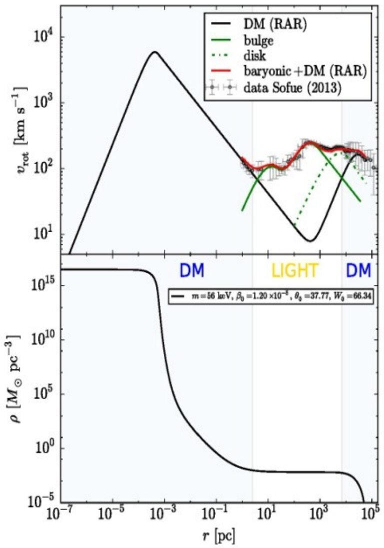

Fig. 1. Milky Way rotation curve and DM density profile from the extended RAR model with a core mass of $M_c = M(r_c) = 3.5 \times 10^6\, M_\odot$. *Top*: DM (black) and baryonic (bulge + disk) contribution to the rotation curve v_{rot} (total in red). *Bottom*: DM density profile. The baryonic model and the data are taken from Sofue (2013). The parameters of the extended RAR model in this case are fermion mass $mc^2 = 56$ keV, temperature parameter $\beta_0 = 1.1977 \times 10^{-5}$, degeneracy parameter $\theta_0 = 37.7656$, and energy cutoff parameter $W_0 = 66.3407$. For the RAR model fitting of the Milky Way, we follow Argüelles et al. (2018); see also Appendix A.

3. Orbit and radial velocity of S2 and G2

To obtain the S2 or G2 positions (orbit) and the corresponding line-of-sight radial velocity (i.e., the redshift function; see Appendix B) at each time, we solved the equations of motion for a test particle (see Appendix C) in the gravitational field produced by two possible scenarii that we describe below.

1. A central Schwarzschild massive BH. Gravity Collaboration (2018b) reported a BH mass of $M_{BH} = 4.1 \times 10^6\, M_\odot$ from the fit of the most recent measurements of the position and velocity of S2. The more recent analysis by Do et al. (2019) reported a BH mass of $3.975 \times 10^6\, M_\odot$. These works used a second-order post-Newtonian (2PN) model to describe the object motion. In order to compare and contrast the BH and the DM-RAR hypotheses on the same ground, that is, using the same analysis method and treatment, we performed our own fit of the data for the BH case using a full general relativistic modeling by solving the equations of motion in the Schwarzschild metric (see Appendix C). From our analysis of S2, we obtain model parameters that are very similar (but not

PERGAMON

Progress in Particle and Nuclear Physics 48 (2002) 291–300

Progress in Particle and Nuclear Physics

http://www.elsevier.com/locate/npe

The Dynamics of Stars Near Sgr A* and Dark Matter at the Center and in the Halo of the Galaxy

N. BILIĆ†, F. MUNYANEZA, G. B. TUPPER and R. D. VIOLLIER‡

Institute of Theoretical Physics and Astrophysics,

Department of Physics, University of Cape Town, Private Bag, Rondebosch 7701, South Africa

November 26, 2001

Abstract

After a discussion of the properties of degenerate fermion balls, we analyze the orbits of the star S0-1, which has the smallest projected distance to Sgr A*, in the supermassive black hole as well as in the fermion ball scenarios of the Galactic center. It is shown that both scenarios are consistent with the data, as measured during the last six years by Genzel et al. and Ghez et al. We then consider a self-gravitating ideal fermion gas at nonzero temperature as a model for the Galactic halo. The Galactic halo of mass $\sim 2 \times 10^{12} M_\odot$ enclosed within a radius of $\sim$ 200 kpc implies the existence of a supermassive compact dark object at the Galactic center that is in hydrostatic and thermal equilibrium with the halo. The central object has a maximal mass of $\sim 2.3 \times 10^6 M_\odot$ within a minimal radius of $\sim$ 18 mpc or $\sim$ 21 light-days for fermion masses $\sim$ 15 keV. We thus conclude that both the supermassive compact dark object and the halo could be made of the same weakly interacting $\sim$ 15 keV particle.

1. Introduction

In the past, self-gravitating neutrino matter has been suggested as a model for quasars, with neutrino masses in the 0.2keV $\lesssim m \lesssim$ 0.5MeV range [1]. More recently, supermassive compact objects consisting of weakly interacting degenerate fermionic matter, with fermion masses in the $10 \lesssim m/\text{keV} \lesssim 20$ range, have been proposed [2, 3, 4, 5, 6] as an alternative to the supermassive black holes that are believed to reside at the centers of many galaxies.

So far the masses of $\sim$ 20 supermassive compact dark objects at the galactic centers have been measured [7]. The most massive compact dark object ever observed is located at the center of M87 in the Virgo cluster, and it has a mass of $\sim 3 \times 10^9 M_\odot$ [8]. If we identify this object of maximal mass with a degenerate fermion ball at the Oppenheimer-Volkoff (OV) limit [9], i.e., $M_{\rm OV} = 0.54 M_{\rm Pl}^3 m^{-2} g^{-1/2} \simeq 3 \times 10^9 M_\odot$ [4], where $M_{\rm Pl} = \sqrt{\hbar c/G}$, this allows us to fix the fermion mass to $m \simeq 15$ keV for a spin and particle-antiparticle degeneracy factor of $g = 2$. Such a relativistic object would have a radius of $R_{\rm OV} = 4.45 R_{\rm S} \simeq 1.5$ light-days, where $R_{\rm S}$ is the Schwarzschild radius of the mass $M_{\rm OV}$. It would thus be virtually indistinguishable from a black hole of the same mass, as the closest stable orbit around a black hole has a radius of 3 $R_{\rm S}$ anyway.

Near the lower end of the observed mass range is the compact dark object located at the Galactic center [10] with a mass of $M_c \simeq 2.6 \times 10^6 M_\odot$. Interpreting this object as a degenerate fermion ball consisting of $m \simeq 15$ keV and $g = 2$ fermions, the radius is $R_c \simeq 21$ light-days $\simeq 7 \times 10^4 R_{\rm S}$ [2], $R_{\rm S}$ being the Schwarzschild radius of the mass M_c. Such a nonrelativistic object is far from being a black

†Permanent address: Rudjer Bošković Institute, P.O. Box 180, 10002 Zagreb, Croatia; Email: bilic@thphys.irb.hr
‡Email: viollier@physci.uct.ac.za

PII: S0146-6410(02)00136-9

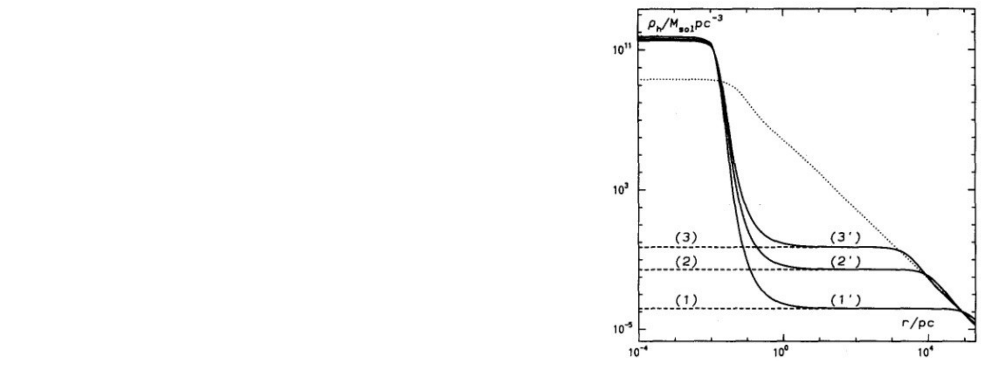

Figure 5: The density profile of the halo for $\eta_0 = 0$ (dotted line) and for the six η_0-values discussed in the text. Configurations with negative η_0 ((1)-(3)) are depicted by the dashed and those with positive η_0 ((1')-(3')) by the solid line.

For fixed N, there is a range of α where the Thomas-Fermi equation has multiple solutions. For example, for $N = 2\times10^{12}$ and $\alpha = 4\times10^{6}$ we find six solutions, which we denote by (1), (2), (3), (3'), (2'), and (1') corresponding to the values η_0 = -30.53, -25.35, -22.39, 29.28, 33.38, and 40.48, respectively. In Fig. 5 we plot the density profiles. For negative central value η_0, for which the degeneracy parameter is negative everywhere, the system behaves basically as a Maxwell-Boltzmann isothermal sphere. Positive values of the central degeneracy parameter η_0 are characterized by a pronounced central core of mass of about $2.5 \times 10^{6} M_\odot$ within a radius of about 20 mpc. The presence of the core is obviously due to the degeneracy pressure. A similar structure was obtained in collisionless stellar systems modeled as a nonrelativistic Fermi gas [23].

Fig. 5 shows two important features. First, a galactic halo at a given temperature may or may not have a central core depending whether the central degeneracy papameter η_0 is positive or negative. Second, the closer to zero η_0 is, the smaller the radius at which the r^{-2} asymptotic behavior of the density begins. The flattening of the Galactic rotation curve begins in the range $1 \lesssim r/\mathrm{kpc} \lesssim 10$, hence the solution (3') most likely describes the Galactic halo. This may be verified by calculating the rotation curves in our model. We know already from our estimate (4) that our model yields the correct asymptotic circular velocity of 220 km/s. In order to make a more realistic comparison with the observed Galactic rotation curve, we must include two additional matter components: the bulge and the disk. The bulge is modeled as a spherically symmetric matter distribution of the form [25]

$$\rho_b(s) = \frac{e^{-hs}}{2s^3}\int_0^\infty du \frac{e^{-hsu}}{[(u+1)^8 - 1]^{1/2}}, \tag{12}$$

where $s = (r/r_0)^1/4$, r_0 is the effective radius of the bulge and h is a parameter. We adopt $r_0 = 2.67$ kpc and h yielding a bulge mass $M_b = 1.5 \times 10^{10} M_\odot$ [26]. In Fig. 6 the mass of halo and bulge enclosed within a given radius is plotted for various η_0. The data points, indicated by squares, are the mass

Monthly Notices of the ROYAL ASTRONOMICAL SOCIETY

MNRAS **451,** 622–628 (2015) doi:10.1093/mnras/stv1016

On the core-halo distribution of dark matter in galaxies

R. Ruffini,[1,2]★ C. R. Argüelles[2]★ and J. A. Rueda[1,2]★

[1]*Dipartimento di Fisica and ICRA, Sapienza Università di Roma, Piazzale Aldo Moro 5, I-00185 Rome, Italy*
[2]*ICRANet, Piazza della Repubblica 10, I-65122 Pescara, Italy*

Accepted 2015 May 4. Received 2015 April 30; in original form 2015 March 31

ABSTRACT

We investigate the distribution of dark matter in galaxies by solving the equations of equilibrium of a self-gravitating system of massive fermions ('inos') at selected temperatures and degeneracy parameters within general relativity. Our most general solutions show, as a function of the radius, a segregation of three physical regimes: (1) an inner core of almost constant density governed by degenerate quantum statistics; (2) an intermediate region with a sharply decreasing density distribution followed by an extended plateau, implying quantum corrections; (3) an asymptotic, $\rho \propto r^{-2}$ classical Boltzmann regime fulfilling, as an eigenvalue problem, a fixed value of the flat rotation curves. This eigenvalue problem determines, for each value of the central degeneracy parameter, the mass of the ino as well as the radius and mass of the inner quantum core. Consequences of this alternative approach to the central and halo regions of galaxies, ranging from dwarf to big spirals, for SgrA*, as well as for the existing estimates of the ino mass, are outlined.

Key words: methods: numerical – galaxies: haloes – galaxies: nuclei – galaxies: structure – dark matter.

1 INTRODUCTION

The problem of identifying the masses and the fundamental interactions of the dark matter particles is currently one of the most fundamental issues in physics and astrophysics. The first astrophysical and cosmological constraints on the mass of the dark matter particle appeared in Cowsik & McClelland (1972), Weinberg (1972), Gott et al. (1974), Lee & Weinberg (1977), and Tremaine & Gunn (1979). As we will show, some inferences on the dark matter particle mass can be derived from general considerations based solely on quantum statistics and gravitational interactions on galaxy scales.

An important open issue in astrophysics is the description of the dark matter in terms of collisionless massive particles. Attempts have been presented to put constraints on its phase-space density by knowing its evolution from the cosmological decoupling until the approximate time of virialization of a dark matter halo. Phenomenological attempts have been proposed in the past in terms of Maxwellian-like, Fermi–Dirac-like or Bose–Einstein-like distribution functions. Since the 80's all the way up to the present, the problem of modelling the distribution of dark matter in terms of self-gravitating quantum particles has been extensively studied and contrasted against galactic observables. In Ruffini & Stella (1983), Viollier, Trautmann & Tupper (1993), Chavanis & Sommeria (1998), Bilic et al. (2002), Chavanis (2002a), Boyanovsky, de Vega & Sanchez (2008), Argüelles et al. (2013), Ruffini et al. (2013), Destri, de Vega & Sanchez (2013), Argüelles & Ruffini (2014), Argüelles et al. (2014), de Vega, Salucci & Sanchez (2014), Siutsou, Argüelles & Ruffini (2015), and references therein, this problem was studied by considering Fermi–Dirac statistics in different regimes, from the fully degenerate to the dilute one, and for different fermion masses going from few eV to keV. Instead, in Sin (1994), Hu, Barkana & Gruzinov (2000), Böhmer & Harko (2007), Boyanovsky et al. (2008), Spivey, Musielak & Fry (2013), and Harko (2014) the same problem was analysed in terms of Bose–Einstein condensates with particle masses from 10^{-25} eV up to few eV.

Attempts of studying galactic structures in terms of fundamental physical principles such as thermodynamics and statistical physics, has been long considered (e.g. Binney & Tremaine 2008) since galaxies present many quasi-universal self-organized properties such as: the constant mean surface density at one-halo scalelength for luminous and dark matter (Gentile et al. 2009); the Fundamental Plane of galaxies (Djorgovski & Davis 1987; Jorgensen, Franx & Kjaergaard 1996); or the fact that dark matter haloes can be well fitted by many different but similar profiles that resemble isothermal equilibrium spheres (e.g. de Blok et al. 2008; Chemin, de Blok & Mamon 2011; de Vega et al. 2014). Within the statistical and thermodynamical approach, the most subtle problem is the one of understanding the complex processes of relaxation which take place before a galactic halo enters in the steady states we observe. In the context of this paper, we will deal only with the (quasi) relaxed states of galaxies, and do not worry about the previous relaxation

★E-mail: ruffini@icra.it (RR); carlos.arguelles@icranet.org (CRA); jorge.rueda@icra.it (JAR)

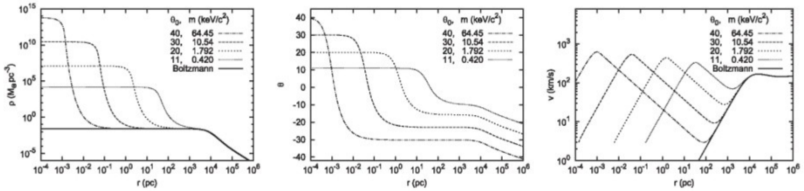

Figure 1. Mass density (left-hand panel), degeneracy parameter (central panel), and rotation velocity curves (right-hand panel) for specific ino masses m and central degeneracies θ_0 fulfilling the observational constraints (8). The density solutions are contrasted with a Boltzmannian isothermal sphere with the same halo properties. All the configurations, for any value of θ_0 and corresponding m, converge for $r \gtrsim r_h$ to the classical Boltzmannian isothermal distribution. It is clear how the Boltzmann distribution, is as it should be, independent of m. Interestingly, when the value $M_c(r \lesssim 10^{-2}$ pc) $\sim 10^6$ M$_\odot$ (i.e. $m \sim 10$ keV/c^2) is chosen as the one of more astrophysical interest, the onset of the classical Boltzmann regime takes place at distances of $r \gtrsim$ few 10^2 pc, in consistency with the observed cored nature of the innermost resolved regions in spiral galaxies as analysed in (de Blok et al. 2008).

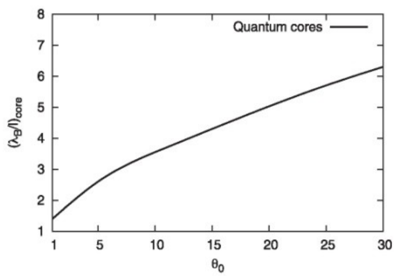

Figure 2. The less degenerate quantum cores in agreement with the halo observables (8) corresponds to $\theta_0 \approx 10$ ($\lambda_B \sim 3l_c$). These cores are the ones which achieve the largest sizes, of order $\sim 10^1$ pc, and implying the lowest ino masses in the sub-keV region.

Table 1. Core properties for different equilibrium configurations fulfilling the halo parameters (8) of spiral galaxies.

θ_0	m (keV/c^2)	r_c (pc)	M_c(M$_\odot$)	v_c (km s^{-1})	θ_c
11	0.420	3.3×10^1	8.5×10^8	3.3×10^2	2.1
25	4.323	2.5×10^{-1}	1.4×10^7	4.9×10^2	5.5
30	10.540	4.0×10^{-2}	2.7×10^6	5.4×10^2	6.7
40	64.450	1.0×10^{-3}	8.9×10^4	6.2×10^2	8.9
58.4	2.0×10^3	9.3×10^{-7}	1.2×10^2	7.5×10^2	14.4
98.5	3.2×10^6	3.2×10^{-13}	7.2×10^{-5}	9.8×10^2	21.4

as well as the numerical implications of β_0 and θ_0, they are given at the end of this section.

We define the core mass, the circular velocity at r_c, and the core degeneracy as $M_c = M(r_c)$, $v_c = v(r_c)$ and $\theta_c = \theta(r_c)$, respectively. In Table 1, we show the core properties of the equilibrium configurations in spiral galaxies, for a wide range of (θ_0, m). For any selected value of θ_0, we obtain the correspondent ino mass m to fulfil the halo properties (8), after the above eigenvalue problem of β_0 is solved.

It is clear from Table 1 and Fig. 1 that the mass of the core M_c is strongly dependent on the ino mass, and that the maximum space-density in the core is considerably larger than the maximum value considered in (Tremaine & Gunn 1979) for a Maxwellian distribution. Interestingly, as can be seen from Fig. 1, the less degenerate quantum cores in agreement with the halo observables (8), are the ones with the largest sizes, of the order of halo-distance-scales. In this limit, the fermion mass acquires a sub-keV minimum value which is larger, but comparable, than the corresponding sub-keV bound in (Tremaine & Gunn 1979), for the same halo observables. Indeed, their formula gives a lower limit $m \approx 0.05$ keV/c^2 when using the proper value for the King radius, $r_K \simeq 8.5$ kpc, as obtained from $\sigma = \sqrt{2/5}v_h$ and $\rho_0 = 2.5 \times 10^{-2}$ M$_\odot$ pc^{-3}, which are the associated values to the Boltzmannian density profile of Fig. 1. This small difference is formally understood by the following fact: while their conclusions are reached by adopting the maximum phase-space density, $Q^{h}_{max} \sim \rho^h_0 m^{-4}\sigma_h^{-3}$, at the centre of a halo described by a Maxwellian distribution; in our model the maximum phase-space density is reached at the centre of the dense quantum core described by Fermi–Dirac statistics, $Q^{c}_{max} \sim \rho^c_0 m^{-4}\sigma_c^{-3}$ (where lower and upper index c reads for the central core). An entire new family of solutions exists for larger values of central phase-space occupation numbers, always in agreement with the halo observables (see Fig. 1). Now, since these phase-space values, by the Liouville's theorem, can never exceed the maximum primordial phase-space density at decoupling, Q^{d}_{max}, we have $Q^{h,c}_{max} < Q^{d}_{max}$. Then, considering that all our quantum solutions satisfy $Q^{c}_{max} > Q^{h}_{max}$, it directly implies larger values of our ino mass with respect to the Tremaine and Gunn limit. Nevertheless, as we have quantitatively shown above, e.g. for the case of typical spiral galaxies, the two limits become comparable for our less degenerate ($\theta_0 \approx 10$) quantum cores in agreement with the used halo observables (8).

In the case of a typical spiral galaxy, for an ino mass of $m \sim 10$ keV/c^2, and a temperature parameter $\beta_0 \sim 10^{-7}$, obtained from the observed halo rotation velocity v_h, the de Broglie wavelength λ_B is higher than the interparticle mean-distance in the core l_c, see Fig. 2, safely justifying the quantum-statistical treatment applied here.

If we turn to the issue of an alternative interpretation to the black hole on SgrA*, we conclude that a compact degenerate core mass $M_c \sim 4 \times 10^6$ M$_\odot$ is definitely possible corresponding to an ino of $m \sim 10$ keV/c^2 (see Table 1). However, the core radius of our configuration is larger by a factor of $\sim 10^2$ than the one obtained with the closest observed star to Sgr A*, i.e. the S2 star (Gillessen et al. 2009). Nevertheless, for an ino mass of $m \sim 10$ keV/c^2 ($\theta_0 = 30$), the very low temperature of the dense quantum core is already a small fraction of the Fermi energy (i.e. $\lambda_B > l$), where additional

Bertrand's theorem

There are only two central potentials where all bounded orbits are closed and elliptical (L&L, Mechanics; Arnold, 1989)

$U_{OH}(r) = a\, r^2\ (a>0)$ (harmonic oscillator potential)

and

$U_N(r) = -\,k/r$ (Newtonian potential)

Graduate Texts in Mathematics

V. I. Arnold

Mathematical Methods of Classical Mechanics

Second Edition

Springer-Verlag

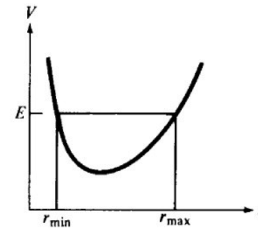

Figure 31 Graph of the effective potential energy

i.e., $\dot{r} = 0$. Therefore, the velocity of the moving point, in general, is not equal to zero since $\dot{\varphi} \neq 0$ for $M \neq 0$.

The inequality $V(r) \leq E$ gives one or several annular regions in the plane:

$$0 \leq r_{min} \leq r \leq r_{max} \leq \infty.$$

If $0 \leq r_{min} < r_{max} < \infty$, then the motion is bounded and takes place inside the ring between the circles of radius r_{min} and r_{max}.

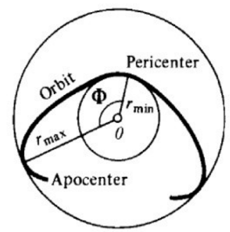

Figure 32 Orbit of a point in a central field

The shape of an orbit is shown in Figure 32. The angle φ varies monotonically while r oscillates periodically between r_{min} and r_{max}. The points where $r = r_{min}$ are called *pericentral*, and where $r = r_{max}$, *apocentral* (if the center is the earth—perigee and apogee; if it is the sun—perihelion and aphelion; if it is the moon—perilune and apolune).

Each of the rays leading from the center to the apocenter or to the pericenter is an axis of symmetry of the orbit.

In general, the orbit is not closed: the angle between the successive pericenters and apocenters is given by the integral

$$\Phi = \int_{r_{min}}^{r_{max}} \frac{M/r^2\, dr}{\sqrt{2(E - V(r))}}.$$

The angle between two successive pericenters is twice as big.

The smallest angle between apocenter and pericenter

$\Phi_{HO}=\pi/2$

$\Phi_N=\pi$

If astronomers monitor quasi-elliptical trajectories of stars with high eccentricities it is very easy to distinguish $U_{HO}(r)$ and $U_N(r)$ potentials since in the case of the RAR potential stars centers of ellipses should coincide with the Galactic Center while in the case of the Newtonian potential stars foci of the ellipses coincide with the Center.

Orbital periods of stars moving in the harmonic oscillator potential are constant and they do not depend on semi-major axis. Even in the case if the Galactic Center position is not accurately known in respect to quasi-elliptical trajectories, a set of trajectories with high eccentricity clearly showed that the Newtonian potential is preferable and stars are moving around a common focus but not around a common center (Zakharov, arXiv:2108.09709, MNRAS Letters, 2022)

Monthly Notices of the ROYAL ASTRONOMICAL SOCIETY

MNRAS 513, L6–L9 (2022)
Advance Access publication 2021 October 12

https://doi.org/10.1093/mnrasl/slab111

Testing the Galactic Centre potential with S-stars

Alexander F. Zakharov[1,2]★

[1]*Bogoliubov Laboratory for Theoretical Physics, JINR, Dubna 141980, Russia*
[2]*MEPhI (Moscow Engineering Physics Institute), National Research Nuclear University , Kashirskoe highway 31, Moscow 115409, Russia*

Accepted 2021 October 1. Received 2021 September 30; in original form 2021 August 27

ABSTRACT

Two groups of astronomers used the large telescopes Keck and VLT for decades to observe trajectories of bright stars near the Galactic Centre. Based on results of their observations, the astronomers concluded that trajectories of the stars are roughly elliptical and foci of the orbits are approximately coincide with the Galactic Centre position. In a last few years, a self-gravitating dark matter core–halo distribution was suggested by Ruffini, Argüelles, Rueda (RAR) and this model was actively used in consequent studies. In particular, recently it has been claimed that the RAR-model provides a better fit of trajectories of bright stars in comparison to the conventional model with a supermassive black hole. The dark matter distribution with a dense core having a constant density as it was suggested in the RAR-model leaves trajectories of stars elliptical like in Kepler's two-body problem. However, in this case not the foci of the ellipses coincide with the Galactic Centre but their centres while the orbital periods do not depend on semi-major axes. These properties are not consistent with the observational data for trajectories of bright stars.

Key words: Cosmology: dark matter – Black hole physics – Galaxy:centre – Galaxy:halo – Galaxies: quasars: supermassive black holes.

1 INTRODUCTION

For decades, astronomers observed bright stars which are moving very closely to the Galactic Centre. Analysing trajectories of these stars, one can deduce the functional form of the gravitational potential there. Observations of Keck and GRAVITY (VLT) groups showed that in the first approximation, the stars are moving along elliptical orbits and foci of these orbits are roughly coinciding with the Galactic Centre (Ghez et al. 2003, 2005, 2008; Gillessen et al. 2009a; Genzel, Eisenhauer & Gillessen 2010; Ciurlo et al. 2020). If we apply the simplest approach based on laws of classical mechanics, we could follow the Newton's derivation of the gravitational potential from the Kepler's laws (Kopeikin, Efroimsky & Kaplan 2011). In the last year, Gravity Collaboration et al. (2020) reported a discovery of relativistic (Schwarzschild) precession for S2 star orbit.

If there is a supermassive black hole along with a bulk distribution of ordinary matter forming a stellar cluster and a dark matter inside the orbits of bright stars, the bulk distribution of matter causes precession of the stellar orbits in the direction which is opposite to that caused by relativistic effects of the black hole (Rubilar et al. 2001; Nucita, De Paolis, Ingrosso et al. 2007; Zakharov et al. 2007).

Observational data for trajectories of bright stars can be used to test predictions of general relativity and to constrain parameters of alternative theories of gravity such as $f(R)$ (Borka et al. 2012), Yukawa potential (Borka et al. 2013), theories with massive graviton (Zakharov et al. 2016, 2018; Hees et al. 2017), black holes with a tidal

Trajectories of test bodies in the harmonic oscillator potential

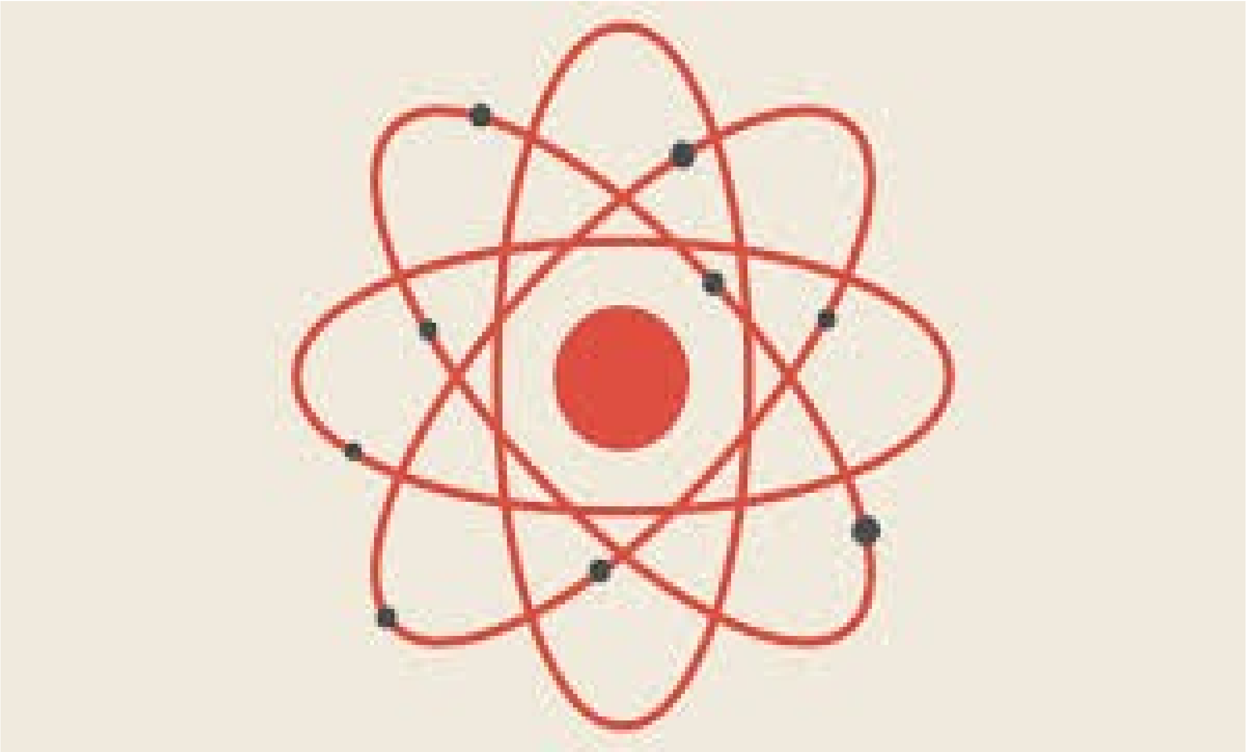

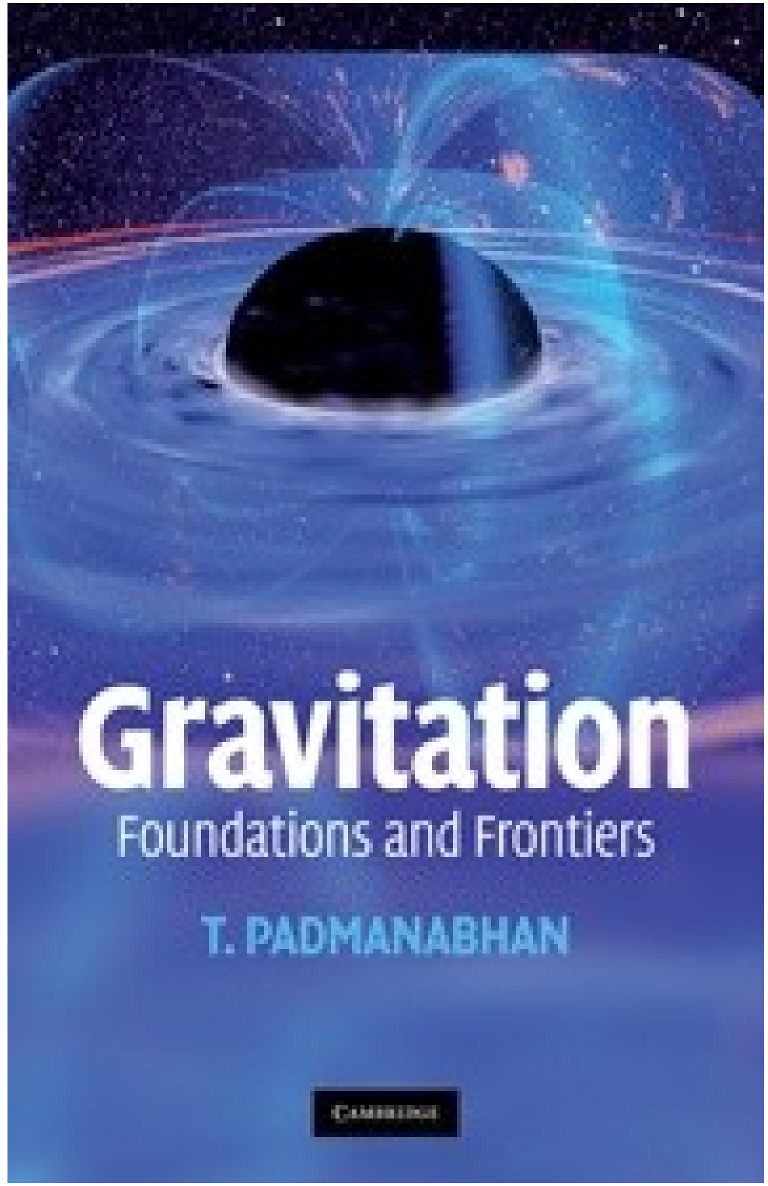
Gravitation
Foundations and Frontiers
T. PADMANABHAN
CAMBRIDGE

EXPLORING BLACK HOLES

Introduction to General Relativity

EDWIN F. TAYLOR
JOHN ARCHIBALD WHEELER
EDMUND BERTSCHINGER

SECOND EDITION

The Event Horizon Telescope Picture

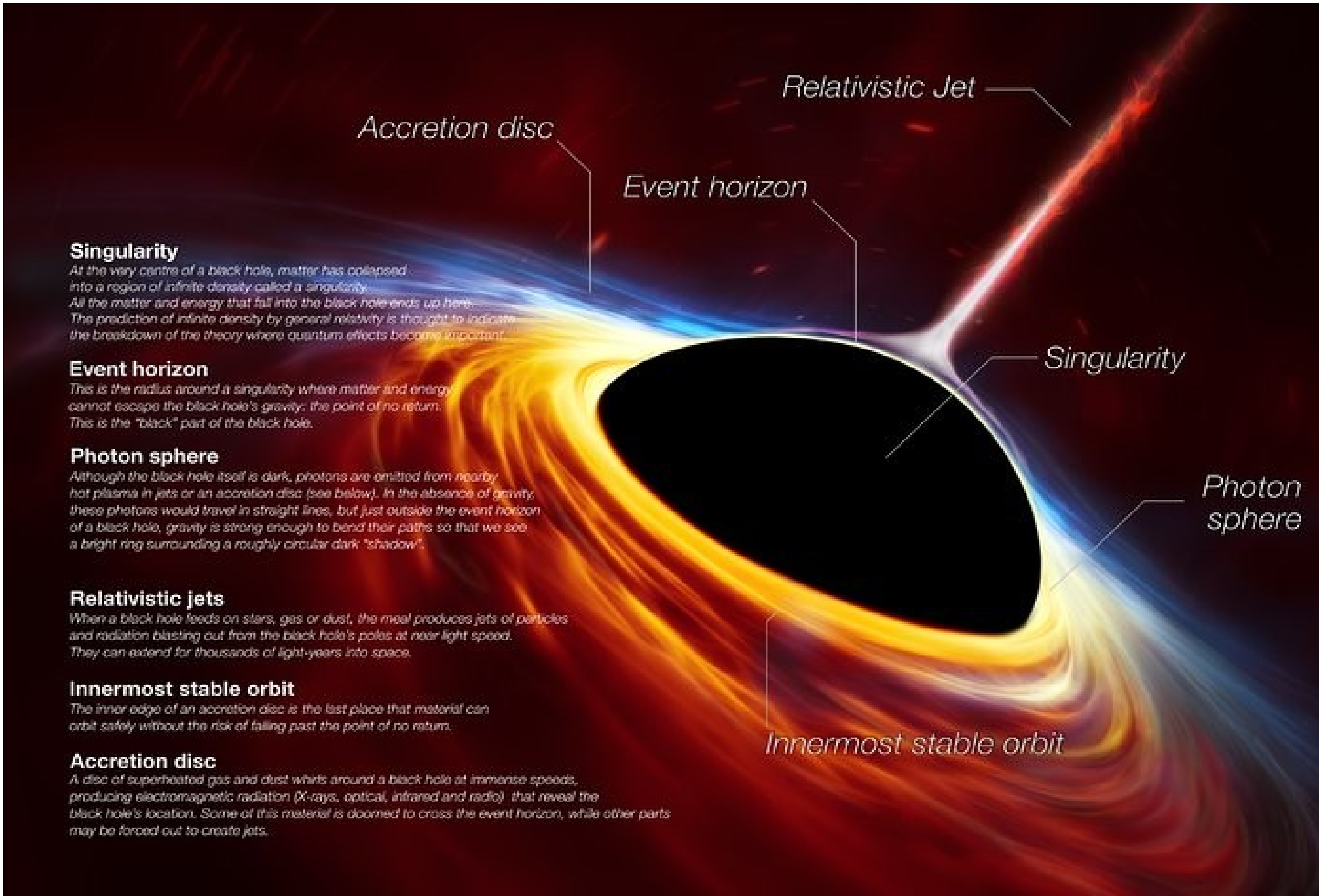

'A majestic story'
Financial Times

MICHIO KAKU

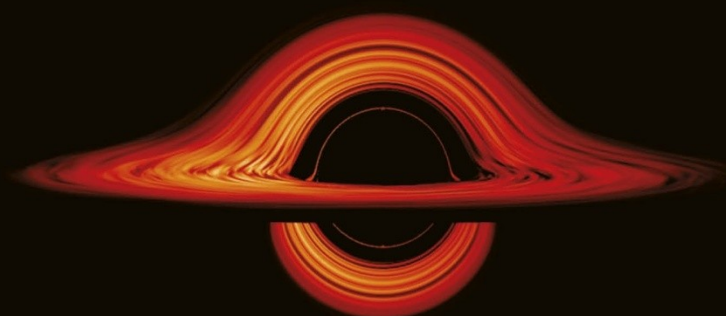

THE GOD EQUATION

The Quest for a Theory of Everything

Circular photon orbits and shadows

Canonical (Kerr – Newman) BHs: Existence of photon rings means Shadow Existence.

NS: It is possible an existence of photon rings without an existence of shadows.

For BH mimickers, “generalizations” of BHs and compact objects without event horizons relations between circular photon rings and shadows must be carefully analysed.

BHs, Naked Singularities (NSs), WHs

Canonical (Kerr – Newman) BHs: Existence of photon rings means Shadow Existence.

NS: It is possible an existence of photon rings without an existence of shadows.

WHs: For photons emitted only from Universe 1 shadows could exist, while if they are emitted from Universe 2 shadows are disappeared.

Conclusion

As we predicted the shadow concept has been transformed from a purely theoretical category into an observable quantity which may be reconstructed from astronomical observations.

Therefore, VLBI observations and image reconstructions for M87* and Sgr A* are in a remarkable agreement with an existence of supermassive black holes in centers of these galaxies.

Thanks for your kind attention!

Figure 13. Inset: paint-swatch accretion disk with inner and outer radii $r = 9.26M$ and $r = 18.70M$ before being placed around a black hole. Body: this paint-swatch disk, now in the equatorial plane around a black hole with $a/M = 0.999$, as viewed by a camera at $r_c = 74.1M$ and $\theta_c = 1.511$ (86.56°), ignoring frequency shifts, associated colour and brightness changes, and lens flare. (Figure from *The Science of Interstellar* [40], used by permission of W. W. Norton & Company, Inc, and created by our Double Negative team, TM & © Warner Bros. Entertainment Inc. (s15)). This image may be used under the terms of the Creative Commons Attribution-NonCommercial-NoDerivs 3.0 (CC BY-NC-ND 3.0) license. Any further distribution of these images must maintain attribution to the author(s) and the title of the work, journal citation and DOI. You may not use the images for commercial purposes and if you remix, transform or build upon the images, you may not distribute the modified images.

itself. This entire image comes from light rays emitted by the disk's bottom face: the wide bottom portion of the image, from rays that originate behind the hole, and travel under the hole and back upward to the camera; the narrow top portion, from rays that originate on the disk's front underside and travel under the hole, upward on its back side, over its top, and down to the camera—making one full loop around the hole.

There is a third disk image whose bottom portion is barely visible near the shadow's edge. That third image consists of light emitted from the disk's top face, that travels around the hole once for the visible bottom part of the image, and one and a half times for the unresolved top part of the image.

In the remainder of this section 4 we deal with a moderately realistic accretion disk—but a disk created for *Interstellar* by Double Negative artists rather than created by solving astrophysical equations such as [32]. In appendix A.6 we give some details of how this and other Double Negative accretion disk images were created. This artists' *Interstellar* disk was chosen to be very anemic compared to the disks that astronomers see around black holes and that astrophysicists model—so the humans who travel near it will not get fried by x-rays and gamma-rays. It is physically thin and marginally optically thick and lies in the black hole's equatorial plane. It is not currently accreting onto the black hole, and it has cooled to a position-independent temperature $T = 4500$ K, at which it emits a black-body spectrum.

Figure 14 shows an image of this artists' disk, generated with a gravitational lensing geometry and computational procedure identical to those for our paint-swatch disk, figure 13

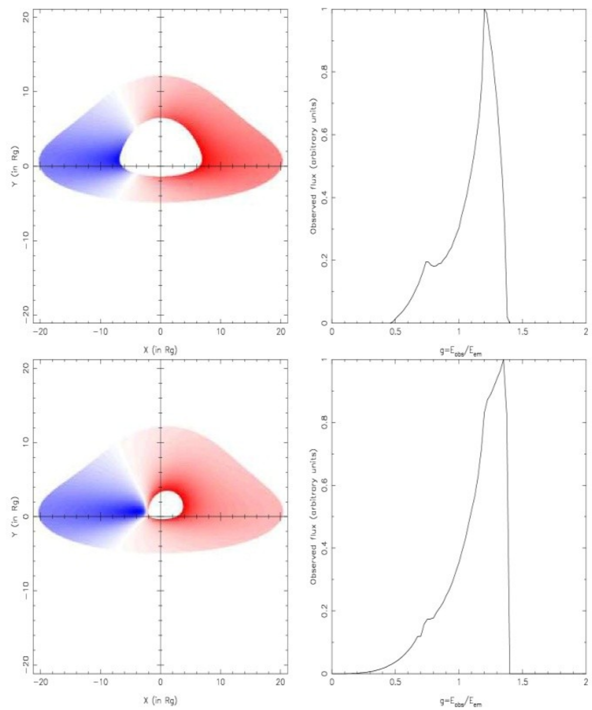

Fig. 2 (online colour at: www.fp-journal.org) The same as in Fig. 1 but for a highly inclined disk with $i = 75^\circ$.

asymmetric (see Fig. 3). If the line emission is originating at larger distances from the BH, the red peak of the line becomes brighter and line profile narrower and more symmetric. In majority of AGN, where the broad Fe Kα line is observed[1], its profile is more similar to the modeled profile as obtained under assumption that the line emitters are located close to the central BH. Therefore, comparisons between the observed and modeled Fe Kα line profiles can bring us some essential information about strong gravitational field in vicinity of central supermassive BH of AGN.

[1] Note here that in some AGN only the narrow Fe Kα line is observed, but it is supposed to be emitted in the disk corona that is located farther from the disk, and therefore, these relativistic effects cannot be detected in the line profile

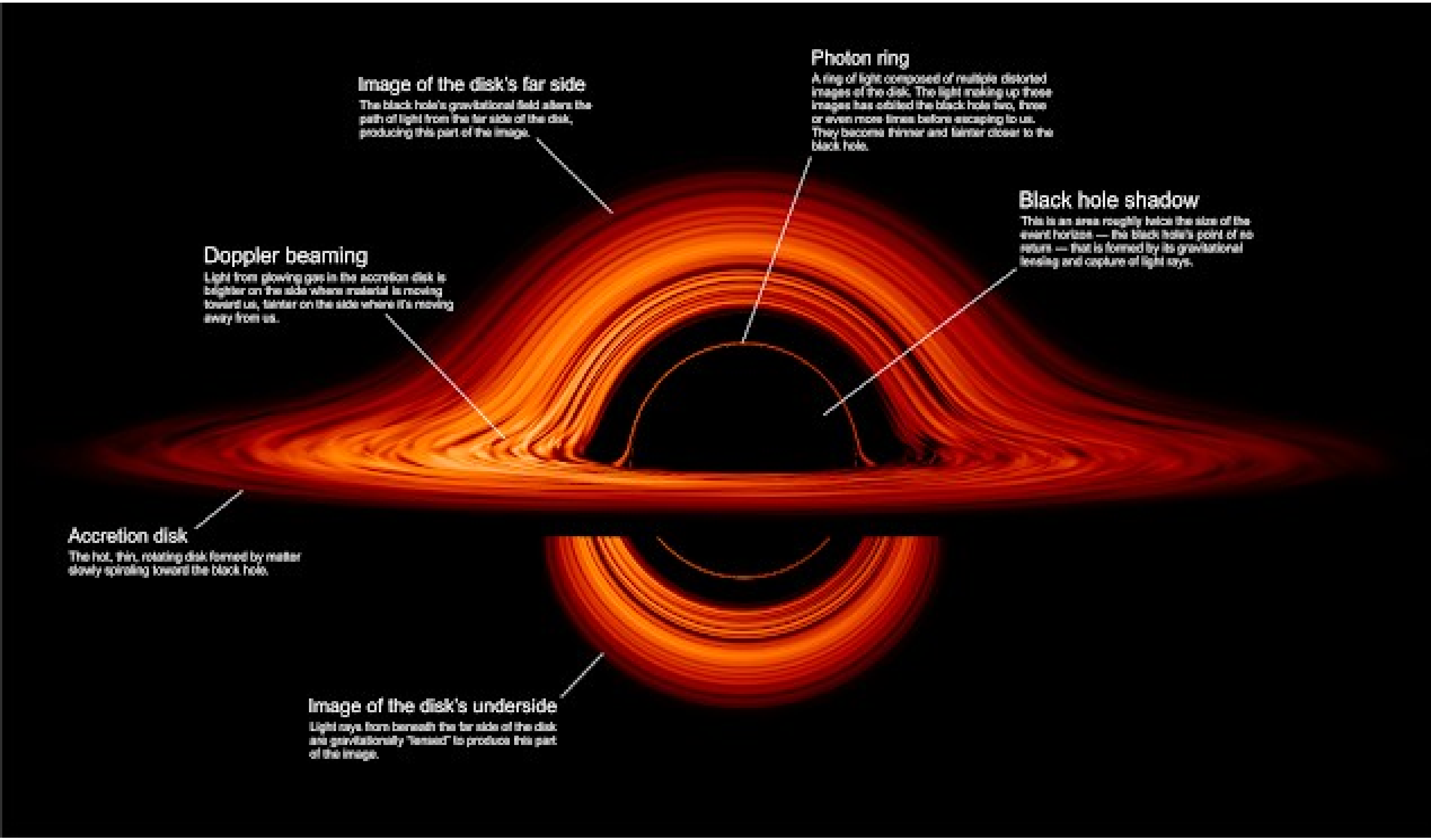
Image of the disk's far side
The black hole's gravitational field alters the path of light from the far side of the disk, producing this part of the image.
Photon ring
A ring of light composed of multiple distorted images of the disk. The light making up these images has orbited the black hole two, three or even more times before escaping to us. They become thinner and fainter closer to the black hole.
Black hole shadow
This is an area roughly twice the size of the event horizon — the black hole's point of no return — that is formed by its gravitational lensing and capture of light rays.
Doppler beaming
Light from glowing gas in the accretion disk is brighter on the side where material is moving toward us, fainter on the side where it's moving away from us.
Accretion disk
The hot, thin, rotating disk formed by matter slowly spiraling toward the black hole.
Image of the disk's underside
Light rays from beneath the far side of the disk are gravitationally "lensed" to produce this part of the image.

1. Fig. From Alexeyev et al. (2024) with a proper attribution was presented in talk by Alexeyev in conference https://indico.jinr.ru/event/4174/

and in talks by Zenin at conference https://indico.quarks.ru/event/2024/timetable/#all.detailed
and

.